UNIVERSITY OF CALIFORNIA,
IRVINE

Environmental infectious disease dynamics in relation to climate and climate change

DISSERTATION

submitted in partial satisfaction of the requirements
for the degree of

DOCTOR OF PHILOSOPHY

in Earth System Science

by

Morgan Elizabeth Gorris

Dissertation Committee:
Professor James T. Randerson, Co-Chair
Professor Charles S. Zender, Co-Chair
Professor Kathleen K. Treseder

2019

DEDICATION

To those whose livelihoods have been challenged as a result of their health,
in hope that a better scientific understanding of the relationships between climate,
climate change, and human health may help mitigate some future health burden.

TABLE OF CONTENTS

LIST OF FIGURES

LIST OF TABLES

ACKNOWLEDGMENTS

My work was supported by a Department of Defense (DoD) National Defense Science and Engineering Graduate Fellowship (32 CFR 168a), which allowed me to pursue my personal research interests. I gratefully acknowledge support from the Borrego Valley Endowment Fund. Thank you to the Jenkins Family for your contributions to UCI Earth System Science. I thank Wiley for allowing me to reproduce my published research in *GeoHealth* under the terms of the Creative Commons Attribution Non-Commercial No Derivatives License CC BY-NC-ND.

I was most fortunate to have been co-advised throughout my PhD by two brilliant and good-hearted individuals, who were constant advocates for my success. Jim Randerson has been an inspirational mentor. I strive to achieve his same positive energy towards science and his ability to conjure endless scientific ideas. Jim is selfless and puts his students first; many times he gave me great scientific ideas, along with all the credit for them (which never hurt the grad student ego). I thank Jim for his constant encouragement and praise; I left our meetings remembering why I love science.

Charlie Zender has been an honest, patient, and grounding advisor. He recognizes his students as individuals and celebrates their strengths, which translates into his research group being a strong scientific team. I admire Charlie's breadth of expertise across multiple fields in Earth System Science and hope to achieve the same. I thank Charlie for emphasizing a healthy work-life balance and being tuned in with both my personal and professional goals.

I am privileged to have had Kathleen Treseder as my committee member. Kathleen has been an exemplary female role model not only as a scientist, but also as an advocate for students. She is a leader on campus and I thank Kathleen for being a voice for many unheard individuals. I am honored to have been a sit-in member of the Treseder Lab group, where we focused on both science and our personal growth as scientists.

I am grateful for the collaborations, encouragement, and support from my colleagues within the Coccidioidomycosis Study Group, Washington State Department of Health, Los Alamos National Laboratory, and many GeoHealth affiliates. I was blessed with a brilliant cohort of ESS graduate students who were selfless in helping others, as well as present and past members of the Randerson, Zender, and Treseder Labs. Thank you to the zotCAMS board members for somehow letting me talk you into starting a student AMS chapter, and then taking it so far beyond my expectations—it was an honor to work with such brilliant scientists and leaders. Thank you to the many members of Anomalous SpikESS for letting me be your Captain Morgan and humoring me as I took intermural volleyball way too seriously. A special thanks to Mindy and Zack for being exceptionally inspirational colleagues and friends.

In addition to those at UCI, I have had several mentors during internships and research experiences that fully supported my endeavors, despite the fact that I now recognize taking

me on as an undergraduate student fell more along the lines of community service: a sincere thank you especially to William Chan, Richard DeLaura, Jim Hansen, and Gretchen Keppel-Aleks. I'd also like to thank teachers and professors who continued to spark my interest in science, weather, and climate, some of which probably don't realize what a positive impact they've had on the life of a student, including Derek Posselt, Christopher Weiss, Mark Flanner, Frank Marsik, Mike Liemohn, Jennifer Courey, and Russ Stowers.

What truly drove me forward throughout my PhD was the unconditional love and support from my family and friends. My parents, Dawn and Joe, continually put me and my siblings first so that we may pursue our dreams; thank you for being so selfless. Thank you to my family for learning what a PhD is along with me, including my siblings Matt and Mason, and Carissa; it has been fun to connect with Dr. Matt Gorris, MD about my newfound interests in infectious diseases and medicine. Thank you to Grandma Ronnie and Grama Jean for being inspirational women, watching my recorded scientific presentations, and constantly bragging about me. I owe many thanks to my late Grandpa Gorris, who helped instill my sense of awe in the outdoors and the physical world. Jessica Wang provided pivotal support throughout and I deeply cherish our newfound friendship. As always and forever, the ripest love from and to my bananas: Stacey, Naomi, Lexi, and Kalie. Thank you, Sander Cohen, for everything.

Lastly, my biggest supporter was my soulmate and love of my life, Jeremiah. Without fail, he always listened to me ramble on about my research. His own work ethic and logical thinking has been inspirational. I am grateful for him beyond measure.

CURRICULUM VITAE

MORGAN E. GORRIS

EDUCATION

Ph.D. **Earth System Science, University of California, Irvine** Aug 2019
Dissertation: Environmental infectious disease dynamics in relation to climate and climate change
Thesis co-advisors: Dr. James Randerson, Dr. Charles Zender
Committee members: Dr. Kathleen Treseder

M.S. **Earth System Science, University of California, Irvine** Dec 2016

B.S.E. **Earth System Science and Engineering, University of Michigan** May 2014
Concentration in Meteorology, Minor in Mathematics

PROFESSIONAL EXPERIENCE

Subcontractor for Industrial Economics, Incorporated Irvine, CA
Environmental Protection Agency Contract EP-D-14-031 Apr 2019 – Sep 2019

Los Alamos National Laboratory – Visiting Scientist Los Alamos, NM
Theoretical Biology and Biophysics Jun 2018 – Aug 2018
Advisors: Dr. Carrie Manore, Dr. Chonggang Xu

The University of California, Irvine – Teaching Assistant in Earth System Science Irvine, CA
Earth System Science Laboratory and Field Methods Mar 2016 – Jun 2016
Professor: Dr. Alex Guenther

Advanced Data Modeling Jan 2016 – Mar 2016
Professor: Dr. James Randerson

Introduction to Earth System Science Sep 2015 – Dec 2015
Lecturer: Dr. Julie Ferguson

Naval Research Laboratory – Research Intern Monterey, CA
Marine Meteorology Division Jun 2014 – Aug 2014
Advisor: Dr. James Hansen

University of Michigan – Undergraduate Research Ann Arbor, MI
Northern ecosystems and trends in the seasonal cycle of CO_2 Oct 2013 – May 2014
Advisor: Dr. Gretchen Keppel-Aleks

MIT Lincoln Laboratory – Research Intern Lexington, MA
Air Traffic Management Group Jun 2013 – Aug 2013
Advisor: Richard DeLaura

Texas Tech University – Undergraduate Field Study Lubbock, TX
Tornado Radar Research May 2013
Advisors: Dr. Christopher Weiss, Dr. Derek Posselt

NASA Ames Research Center – Research Intern Moffett Field, CA
Aviation Weather Systems Division Jun 2012 – Aug 2012
Advisor: William Chan

Geophysical Flows in the Atmosphere and Ocean Ann Arbor, MI
Undergraduate Research Opportunities Program *Sep 2011 – Apr 2012*
Advisor: Dr. John Boyd

PEER REVIEWED PUBLICATIONS

PUBLISHED

Gorris, M. E., Treseder, K. K., Zender, C. S., & Randerson, J. T. (2019), Expansion of coccidioidomycosis endemic regions in response to climate change in the United States, *GeoHealth.* In press.

Cat, L. A., **Gorris, M. E.**, Randerson, J. T., Riquelme, M., & Treseder, K. K. (2019), Crossing the Line: Human Disease and Climate Change Across Borders, *Journal of Environmental Health*, 81(8), 14-22.

Aburto-Oropeza, O., Johnson, A. F., Agha, M., Allen, E. B., Allen, M. F., **et al.** (2018), Harnessing cross-border resources to confront climate change, *Environmental Science and Policy*, 87, 128-132, https://doi.org/10.1016/j.envsci.2018.01.001

Gorris, M. E., Cat, L. A., Zender, C. S., Treseder, K. K., & Randerson, J. T. (2018), Coccidioidomycosis dynamics in relation to climate in the southwestern United States, *GeoHealth*, 2(1), 6-24, https://doi.org/10.1002/2017GH000095.

IN REVIEW

Cat, L. A, **Gorris, M. E.**, J. Randerson, J. T., & Treseder, K. K. (In Review, 2019), Dispersal of pathogenic fungi in soil and air across the US Southwestern region. *Fungal Ecology*.

Gorris, M. E., Cat, L. A., Matlock, M., Ogunseitan, O. A., Treseder, K. K., Randerson, J. T., & Zender, C. S. (In Review, 2019), Coccidioidomycosis (Valley fever) case data for the southwestern United States, *Open Health Data*.

FIRST AUTHOR PRESENTATIONS

Gorris, M. E., Zender, C. S., Randerson, J. T., Cat, L. A., & Treseder, K. K. (2019), *Using climate and environmental data to understand Valley fever disease dynamics*, Invited department seminar in Environmental Sciences at University of California, Riverside. Riverside, CA. May 17.

Gorris, M. E., Salamone, A., Clifford, W., Zender, C. S., Treseder, K. K., & Randerson, J. T. (2019), *Environmental niche modeling of Coccidioides ssp. in Washington State*, oral presentation at the 63rd Coccidioidomycosis Study Group Meeting, Sacramento, CA. Apr 5.

Gorris, M. E., Treseder, K. K., Zender, C. S., Clifford, W., Salamone, A., Oltean, H. N., & Randerson, J. T. (2019), *Coccidioidomycosis Climate Niche Model for Predicting Current and Future Endemic Regions in the United States through the 21st Century and Applications to Environmental Soil*

Sampling, oral presentation at the American Meteorological Society 99th Annual Meeting. Phoenix, AZ. Jan 9.

***Gorris, M. E.,** Zender, C. S., Randerson, J. T., Goodsman, D. W., Xu, C., & Manore, C. A. (2018), *Expanding a seasonal forecast of US West Nile virus for 21st century disease projections*, oral presentation at the American Geophysical Union Fall Meeting. Washington, DC. Dec 10.
***Recipient of Outstanding Student Presentation Award: American Geophysical Union**

Gorris, M. E., Zender, C. S., Randerson, J. T., Goodsman, D. W., Xu, C., & Manore, C. A. (2018), *Expanding a seasonal forecast of US West Nile virus for 21st century disease projections*, poster presentation at the 75th Los Alamos National Laboratory Student Symposium. Los Alamos, NM. Aug 1.

Gorris, M. E., Treseder, K. K., Zender, C. S., & Randerson, J. T. (2018), *The effects of climate change on coccidioidomycosis endemic regions in the United States*, oral presentation at the 62nd Annual Coccidioidomycosis Study Group Meeting, Northern Arizona University. Flagstaff, AZ. Apr 14.

Gorris, M. E. & Zender, C. S. (2018), *Evaluating Particulate Matter Air Quality in Borrego Springs. Year 2: An overview and cases studies of particulate matter air quality in Borrego Springs*, Borrego Springs, CA. Feb 18.

Gorris, M. E., Hoffman, F. M., Treseder, K. K., Zender, C. S., & Randerson, J. T. (2017), *The Influence of Current and Future Climate on the Spatial Distribution of Coccidioidomycosis in the Southwestern United States*, oral presentation at the American Geophysical Union Fall Meeting, New Orleans, LA. Dec 12.

***Gorris, M. E.,** Cat, L. A., Zender, C. S., Treseder, K. K., & Randerson, J. T. (2017), *The Effects of Climate on Valley Fever Incidence in the Southwestern United States*, poster presentation at the 7th International Coccidioidomycosis Symposium, Stanford University, Stanford, CA. Aug 11.
***Recipient of Best Student Oral Presentation: American Meteorological Society**

Gorris, M. E. (2017), *Valley Fever: More than just Dust in the Wind*, oral presentation at Associated Graduate Student Symposium, UC Irvine, Irvine, CA. Apr 21.

Gorris, M. E., Parajuli S. P., & Zender, C. S. (2017), *Evaluating Particulate Matter Air Quality in Borrego Springs. Year 1: Characterization and evaluation of historical air quality*, Borrego Springs, CA. Feb 26.

Gorris, M. E., Cat, L. A., Treseder, K. K., Zender, C. S., & Randerson, J. T. (2017), *The Spatiotemporal Relationship between Climate and Valley Fever in the Southwestern United States*, oral presentation at the American Meteorological Society 97th Annual Meeting, Seattle, WA. Jan 23.

Gorris, M. E. & Cat, L. A. (2016), *Disease in the Desert: Ecology, Epidemiology and Environmental Modeling of Valley Fever*, invited talk at the 2016 Colorado Desert Natural History Research Symposium, Nov 4.

Gorris, M. E., Cat, L. A., Randerson, J. T., Zender, C. S., & Treseder, K. K. (2016), *Climate Drivers and Coccidioidomycosis Incidence at the Regional Scale*, poster presentation at the 60th Annual Coccidioidomycosis Study Group Meeting, UCSF Fresno. Fresno, CA. Apr 9.

Gorris, M. E. & Cat, L. A. (2015), *Out of the Valley: A multi-disciplinary approach to forecasting valley fever dispersal in the U.S. Southwest*, invited talk and poster presentation at University of California, Irvine's 1st Annual Data Science Initiative Summer Symposium. Irvine, CA. Sept 17.

Gorris, M. E. (2014), *Analysis of Convective Weather Impact Prediction on Arrival Routes in the New York Airspace*, Abstract S30, poster presentation at the American Meteorological Society 13th Annual Student Conference, Atlanta, GA, Feb 2–6.

***Gorris, M. E**. & Boyd J. P. (2012), *Geophysical Flows in the Atmosphere and Ocean*, poster presentation at the University of Michigan Undergraduate Research Opportunities Program Spring Symposium. Ann Arbor, MI. Apr 18.
***Recipient of Best Student Poster award**

AWARDS AND HONORS

Los Alamos National Laboratory Center for Nonlinear Studies July 2019
Postdoctoral Fellowship

National Defense Science and Engineering Graduate Fellowship Sep 2016 – Sep 2019
American Society of Engineering Education

UC Irvine Earth System Science Faculty Endowed Fellowship Jun 2019

Borrego Valley Endowment Fund Support Feb 2016 – Feb 2019

Outstanding Student Presentation Award: American Geophysical Union Jan 2019
GeoHealth Conference

Best Student Oral Presentation: American Meteorological Society Feb 2017
7th Conference on Environment and Health

UC Irvine Physical Sciences Travel Grant ($250; $300) Dec 2016; Mar 2019

Coccidioidomycosis Study Group Travel Grant ($500) Apr 2016

Data Science Initiative Fellowship Jun 2015 – Sept 2015

Jenkins Family Graduate Fellowship Oct 2014 – Dec 2014

Outstanding Poster Award: Apr 2012
University of Michigan Undergraduate Research Opportunities Program Spring Symposium

Naval Weather Service Association Scholarship Sep 2010

PROFESSIONAL AFFILIATIONS

American Meteorological Society Dec 2011 – Current
President and Co-founder of zotCAMS: Student Chapter of AMS at UC Irvine (Apr 2017 – Aug 2019)
Aviation, Range, and Aerospace Meteorology Committee, Student Member (Jan 2015 – Jan 2019)

American Geophysical Union Jul 2017 – Current
Early Career Scientist Co-chair for GeoHealth Meetings Committee (Jan 2019 – Current*)*
Fall Meeting Session chair: "Climate Influences on Infectious Disease Dynamics and the Potential for Transnational Outbreaks: Posters" (Dec 2018)

POPULAR PRESS

Baer, S. K. (Oct. 2018), *An Incurable Disease Is On The Rise In California, And Scientists Say Climate Change Could Cause It To Spread To Much Of The Western US*. BuzzFeed News. Available at https://www.buzzfeednews.com/article/skbaer/valley-fever-fungal-infection-spreading-climate-change

EXTRA CURRICULAR ACTIVITIES

Journal Referee: *Ecohealth (2018)*

zotCAMS *Apr 2017 – Aug 2019*
Student Chapter of the American Meteorological Society at UC Irvine
President (Apr 2017 – Jun 2019) and Co-founder
UC Irvine Anteater Awards Best New Student Organization (2017 – 2018)
AMS Student Chapter of the Year Honor Roll (2017 – 2018; 2018 – 2019)
AMS Annual Meeting Best Local Student Chapter Poster (Jan 2019)
UC Irvine Student Organization of the Month (Apr 2018)

Undergraduate Students
Patrick Mara, UC Irvine, BS Earth System Science Feb 2018 – Jun 2019

CLEAN (Climate, Literacy Empowerment And iNquiry) Oct 2014 – Jun 2019
Elementary School Outreach – Student Member

UC Irvine Physical Sciences Student Mentor Oct 2016 – Jun 2019

Southern California Science Olympiad exam writer Spring 2017, 2018, 2019

ABSTRACT OF THE DISSERTATION

Environmental infectious disease dynamics in relation to climate and climate change

By

Morgan Elizabeth Gorris

Doctor of Philosophy in Earth System Science

University of California, Irvine, 2019

Professors James T. Randerson and Charles S. Zender

Climate change poses multiple threats to human health, including changes in the burden of infectious diseases. Rising temperatures and shifts in precipitation patterns may reshape the geographical distributions of pathogenic organisms and disease vectors, potentially placing new communities at risk. Projections of environmental infectious diseases in response to climate change will help public health officials create disease surveillance programs and mitigation strategies. A precursor to modeling these projections is a basic understanding of the relationships between each infectious disease and the environment.

My dissertation examined how climate conditions influence two different environmental infectious diseases in the United States: coccidioidomycosis (Valley fever) and West Nile virus. In my first study, I examined the climate and environmental conditions that structure the spatiotemporal dynamics of Valley fever incidence. To do so, I compiled a Valley fever case dataset for the southwestern U.S. From this study, I found areas endemic to Valley fever are described by hot and dry climate thresholds. In my second study, I used

these climate thresholds to create a predictive model of the area currently endemic to Valley fever. Then, I used climate projections to create the first maps of future Valley fever endemicity. In my third chapter, I used machine learning to explore which climate conditions structure West Nile virus incidence throughout the U.S. I found the highest disease incidence in the northern Great Plains, which is categorized by dry and cold winters. This predictive model of disease incidence may be used for future projections of West Nile virus risk in response to climate change.

The collective results of my dissertation help us understand how climate conditions influence two of the most important environmental infectious diseases in the U.S. and how climate change may affect the future burden of each disease. I am now sharing the results from my dissertation with the U.S. Environmental Protection Agency, state health agencies and epidemiologists, and physicians in hopes to alleviate the future burden of disease.

Chapter 1

Introduction

1.1 Climate change and environmental infectious diseases

Climate change will continue to cause a variety of threats to human health and will challenge the status of human welfare and national security. Already, the health of US citizens is suffering from the direct and indirect effects of climate change, including exposure to extreme weather events such as heat waves, floods, and droughts; changing air, food, and water quality; added stresses to mental health; and emerging and spreading vector-, food- and waterborne infectious diseases (Ebi et al., 2018; Balbus et al., 2016; Smith et al., 2014). Environmental infectious diseases may be affected by climate change if warming temperatures and changing precipitation patterns (Hayhoe et al., 2018) alter the abundance of pathogenic organisms and disease vectors or their geographical distribution, influencing which communities are at risk (Beard et al., 2016). However, whether climate change will cause a net positive increase in the burden of environmental infectious diseases, shift the regions susceptible to these diseases, or both, is a matter of debate (Epstein, 2010; Lafferty, 2009, 2010; Lafferty & Mordecai, 2016).

To assess the future burden of environmental infectious diseases, it is important to consider the multiple pathways climate can influence these diseases. First, climate conditions generally define species ranges, thus controlling the spatial extent of environmental infectious diseases. Most likely, climate change will cause an expansion of the geographical range of most diseases when physiological temperature limitations are lifted as the climate warms, which is happening disproportionately faster towards the geographic poles (Epstein, 2001). As temperatures warm, tropical and subtropical

pathogens may be able to migrate poleward and inhabit areas once too cold to survive, exposing new communities to the disease. This could lead to the emergence or reemergence of diseases in the U.S., as exemplified by the recent outbreaks of dengue and chikungunya virus in Florida (Beard et al., 2016; CDC, 2019a; Radke et al., 2009). However, climate change could diminish the geographical range of other diseases if temperatures become too hot for species survival or water resources become limited (Lafferty & Mordecai, 2016). This could alleviate the associated health burden and free healthcare resources, allowing those resources to be reallocated appropriately.

Climate change may also affect the biological processes that control the number of disease cases, including the lifecycle of the pathogenic organism or disease vector. For example, warmer temperatures may increase the reproduction rate, and therefore biting rate, of mosquitos (e.g., Kilpatrick et al., 2008). In another example, water stress from drought may cause mortality of free-living ticks since maintaining adequate body-water levels is one of the most important determinants of off-host survival (Needham & Teel, 1991). Yet another pathway is through increased climate variability and extreme weather events driven by climate change, which may produce more climatic and environmental conditions conducive to disease outbreaks (Chretien et al., 2015; Gage et al., 2008; Gubler et al., 2001). For example, in 2012 there was an outbreak of West Nile virus cases in Texas following a mild winter and earlier spring (CDC, 2012). In September 2013, central Colorado experienced record rainfall which resulted in widespread flooding throughout the Denver-Boulder region; excess water mixed with organic matter created conditions for an outbreak of a relatively rare fungal disease called mucormycosis (Benedict & Park, 2014; Davies et al., 2017; Neblett Fanfair et al., 2012).

Projections of environmental infectious diseases in response to climate change will help public health officials create disease surveillance programs and mitigation strategies to appropriately adapt to these changing health risks. A precursor to modeling these projections is a basic understanding of the relationships between each infectious disease and the environment. Studying both the case counts and incidence (cases normalized by population) of each disease may provide further insight on the probable roles of environmental or non-environmental controls on the disease. For instance, large case counts are usually recorded in highly populated regions; deviations from this norm may be indicative of important biological controls supporting a disease hotspot. Moreover, climate conditions likely influence both the geographical distribution and the interannual variability in cases of each disease. Sometimes, these relationships may be based on different biological processes and warrant separate analyses.

The goal of my dissertation was to create frameworks for analyzing how climate change may affect the spatial distribution of two important environmental infectious diseases in the U.S.: coccidioidomycosis, an infectious fungal disease, and West Nile virus. Coccidioidomycosis, otherwise known as Valley fever, has gained attention in the US due to a recent increase in cases (CDC, 2018a). The lifecycle of the soil-dwelling fungi that cause Valley fever, *Coccidioides* spp., is sensitive to environmental conditions: wet periods allow the fungi to grow and subsequent dry periods cause the formation of fungal spores that can become airborne and inhaled by a host (Pappagianis, 1994). Valley fever has been recognized in the U.S. since the 1930s (Hirschmann, 2007). In contrast, West Nile virus was introduced to the U.S. in New York in 1999, most likely by an infected mosquito or bird, but there is no clear evidence how (Kilpatrick, 2011). Since then, West Nile virus incidence

levels have stabilized in many regions, allowing for analysis of climate conditions that shape the spatial structure of the mosquitos and bird populations integral to the West Nile virus transmission cycle.

1.2 Organization of research

In Chapter 2, I examined the climate and environmental conditions that structure the spatiotemporal dynamics of Valley fever incidence. To do so, I combined county-level case records from state health agencies to create the first Valley fever database for the southwestern U.S., including Arizona, California, Nevada, New Mexico, and Utah. I found that Valley fever incidence was greater in areas with warmer air temperatures and drier soils. Counties with higher levels of incidence generally had greater proportions of land designated for crops and higher surface dust concentrations. The mean annual cycle of incidence varied throughout the southwestern U.S. and peaked following periods of low precipitation and soil moisture. Spatially, the areas of higher Valley fever incidence could be described by meeting hot and dry climate thresholds. This analysis provided a framework for interpreting the influence of climate change on Valley fever incidence dynamics. This research was published in GeoHealth as:

"Gorris, M. E., Cat, L. A., Zender, C. S., Treseder, K. K., & Randerson, J. T. (2018). Coccidioidomycosis dynamics in relation to climate in the southwestern United States. GeoHealth, 2(1), 6–24. https://doi.org/10.1002/2017GH000095"

In Chapter 3, I used the statistical relationships I found in Chapter 2 between Valley fever incidence, mean annual temperature, and mean annual precipitation to create a climate constrained niche model of the areas currently endemic to Valley fever. Then, I used our model with projections of climate from Earth system models to assess how

endemic areas will change during the 21st century. This was the first quantitative estimate of how climate change may influence Valley fever in the U.S. Our predictive model of Valley fever endemicity may provide guidance to public health officials to establish disease surveillance programs and design mitigation efforts to limit the impacts of this disease. This research was accepted for publication in GeoHealth as:

"Gorris, M. E., Treseder, K. K., Zender, C. S., & Randerson, J. T. (2019). Expansion of coccidioidomycosis endemic regions in the United States in response to climate change. GeoHealth. In press."

In Chapter 4, I identified which seasonal climate variables influence the spatial extent and magnitude of West Nile virus incidence in humans. To do so, I created predictive models of present day mean annual West Nile virus incidence using county-level CDC case reports from 2005-2017, monthly-mean climate variables from PRISM, and random forest and multiple linear regression algorithms. Both the random forest and linear regression models accurately captured a v-shaped area of higher West Nile virus incidence that extends south from states on the Canadian border through the middle of the Great Plains. The highest levels of West Nile virus incidence were in regions with dry and cold winters, mild summers, and dry falls. I then explored which aspects of the West Nile virus transmission cycle these climate conditions may benefit the most, thus creating the highest levels of WNV incidence in the U.S. A next important step for this research is to use these statistical models to project changes in West Nile virus risk in response to climate change.

The collective results of my dissertation help us understand how climate conditions influence two of the most important environmental infectious diseases in the U.S. and how climate change may affect each disease. Warming temperatures may allow the area

endemic to Valley fever to expand throughout much of the western U.S. In contrast, if cold temperatures are an important control on the highest levels of West Nile virus incidence, warming temperature may cause the highest levels of incidence to move northward out of the U.S. The results of my dissertation are being actively shared with the U.S. Environmental Protection Agency, state health agencies and epidemiologists, and physicians in hopes to alleviate the future burden of environmental infectious diseases.

Chapter 2

Coccidioidomycosis dynamics in relation to climate in the southwestern United States

Adapted from:

Gorris, M. E., Cat, L. A., Zender, C. S., Treseder, K. K., & Randerson, J. T. (2018). Coccidioidomycosis dynamics in relation to climate in the southwestern United States. *GeoHealth*, 2, 6–24. https://doi.org/10.1002/2017GH000095

2.1 Introduction

Coccidioidomycosis, also known as Valley fever, is an infectious disease that has gained attention from a recent increase in cases. Fluctuations in cases are likely driven by changes in climate and environmental conditions, which impact the lifecycle of the disease agent. The agent for Valley fever is *Coccidioides* spp., which are saprotrophic fungi that grow in the soils of the southwestern United States (Smith et al., 1946a). When water-stressed, *Coccidioides* spp. autolyze into spores comparable in size to dust aerosols (Huppert et al., 1967). Soil disturbance can aerosolize these spores, which if inhaled, cause Valley fever in roughly 40% of hosts (Smith et al., 1946a). No Valley fever cases have been reported from human transmission, so cases are likely a direct consequence of environmental exposure to *Coccidioides* spp.

Valley fever symptoms range from short term, flu-like illness, to long term, disseminated disease (Tsang et al., 2010; Thompson, 2011). Moreover, human populations differ in their disease risk. Immuno-compromised persons are more susceptible to Valley fever (Woods et al., 2000; Blair & Logan, 2001; Rosenstein et al., 2001; Bercovitch et al., 2011). In addition, disseminated cases are more frequent in non-white races (Durry et al., 1997; Rosenstein et al., 2001; Crum et al., 2004).

The amount of *Coccidioides* spp. in the soil and air may be modulated by both abiotic and biotic factors (Nguyen et al., 2013), therefore influencing Valley fever incidence (Figure 2.1). Important environmental factors include air temperature, water availability, biological competition, and anthropogenic and natural dust emissions (Nguyen et al., 2013). Previous studies examining the relationship between climate and Valley fever incidence analyzed time series from a few, highly endemic counties (Kolivras & Comrie, 2003; Komatsu et al., 2003; Comrie, 2005; Park et al., 2005; Zender & Talamantes, 2006; Talamantes et al., 2007; Tamerius & Comrie, 2011; Coopersmith et al., 2017; Tong et al., 2017). Climate controls on the spatial structure of Valley fever incidence have not been systematically explored across the suspected endemic region of the southwestern U.S. due to the lack of an integrated Valley fever incidence database.

Figure 2.1. Climate, environmental, and human factors may modulate the abundance of *Coccidioides* spp. in the soil and air, and therefore influence the temporal and spatial patterns of valley fever incidence.

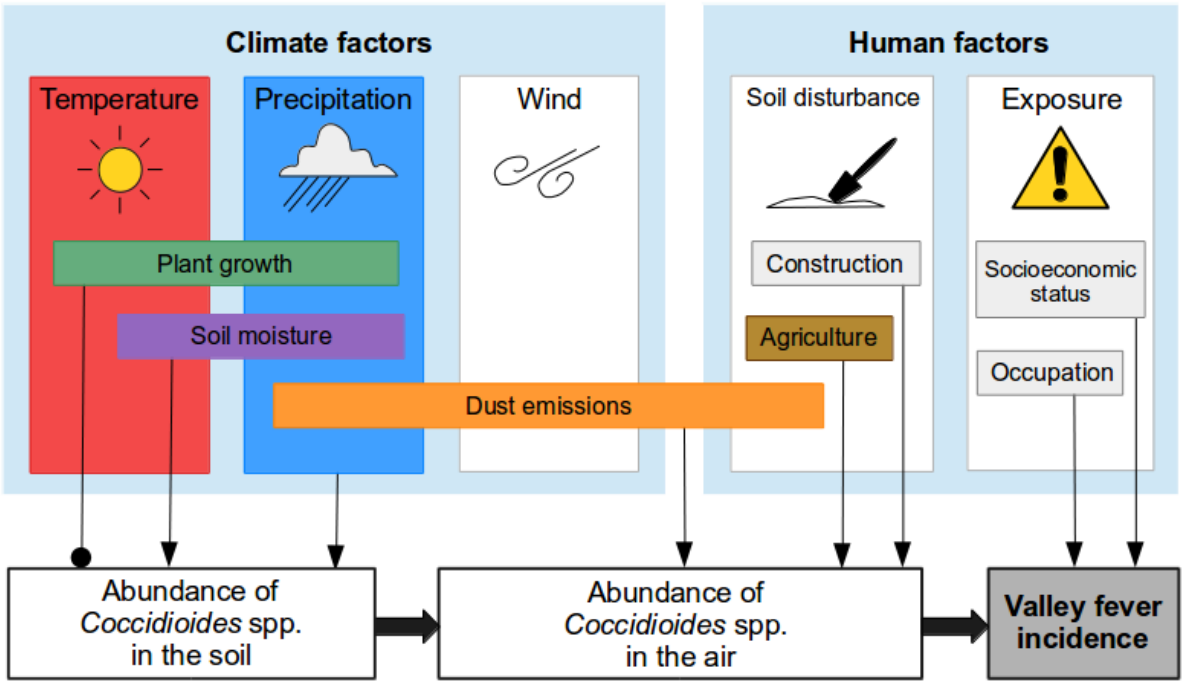

The temperature range of habitats favorable for *Coccidioides* spp. remains poorly constrained. One study found *Coccidioides* spp. spores survived for six months at temperatures ranging from -15°C to 37°C and for over a week at 50°C (Friedman et al., 1956). This temperature adaptability is the basis for the soil sterilization hypothesis, which suggests high temperature extremes limit the growth of many fungi, but *Coccidioides* spp. may survive by retreating to deeper soils (Maddy, 1965). Then, upon the return of rain, *Coccidioides* spp. grow towards the soil surface and proliferate with little competition. Two independent studies in Pima and Maricopa Counties in Arizona found significant positive relationships between temperature in the preceding season and Valley fever incidence, which supports the soil sterilization hypothesis (Kolivras & Comrie, 2003; Park et al., 2005). This hypothesis may help explain how *Coccidioides* spp. can flourish at the same location for many years (Greene et al., 2000; Barker et al., 2012), even though lab experiments suggest they are poor competitors relative to other fungi (Swatek & Omioczynski, 1970; Greene et al., 2000; Barker et al., 2012).

The most established relationship between precursor climate conditions and fluctuations in Valley fever incidence is that a wet period followed by a dry period causes increased incidence (Smith et al., 1946b; Pappagianis, 1994). This pattern first provides water availability, a critical factor for *Coccidioides* spp. growth in arid desert soils (Maddy, 1957; Swatek, 1975; Fisher et al., 2007). Then, when soils dry, the fungi may autolyze into spores that are small, and easily dispersed by winds (Huppert et al., 1967). Previous studies provide support for this hypothesis on both seasonal and inter-annual time scales in a few, highly endemic counties in Arizona (Kolivras & Comrie, 2003; Komatsu et al., 2003; Comrie, 2005; Park et al., 2005; Tamerius & Comrie, 2011, Coopersmith et al., 2017),

but support for this hypothesis is mixed in California (Zender & Talamantes, 2006; Talamantes et al., 2007; Coopersmith et al., 2017).

Since precipitation is subject to runoff and evaporation, soil moisture may be a more precise measurement of water availability for *Coccidioides* spp. In several Arizona and California counties, decreases in soil moisture preceded increased Valley fever incidence (Coopersmith et al., 2017). Other work focusing on Maricopa, Pima, and Pinal Counties in Arizona used normalized difference vegetation index (NDVI), a measure of green plant cover, as a proxy for soil moisture (Stacy et al., 2012). The authors found no correlation with Valley fever incidence on an inter-annual time scale, but identified a bimodal mean annual cycle in NDVI that was negatively correlated with a bimodal seasonality of Valley fever incidence (Stacy et al., 2012). Use of NDVI as a proxy for water availability may have further implications to environmental conditions, because changes in plant cover may also influence near surface winds and thus the dispersal of spores from the soil surface (e.g., Zender & Talamantes, 2006).

Human activity can exacerbate dust emissions from natural and managed ecosystems, thus increasing the probability of aerosolizing *Coccidioides* spp. spores. Population in the southwestern U.S. is increasing faster than many other parts of the nation (U.S. Census Bureau, 2011b). To meet the demands of a rising population, increased soil disturbance from construction and agriculture may aerosolize more *Coccidioides* spp. spores. Individuals directly disturbing the soil have a high risk of contracting Valley fever. Soil disturbance from construction sites (California Department of Public Health, 2013; Wilken et al., 2015), military training (Smith et al., 1946b), archaeological digs (Werner & Pappagianis, 1973; Perera et al., 2002; Petersen et al., 2004), and film shoots (Wilken et al.,

2014) have been associated with Valley fever outbreaks. Dust storms have also been correlated with increased incidence in a few, highly endemic Arizona counties (Tong et al., 2017) and have caused localized outbreaks of Valley fever in California (Williams et al., 1979). Human soil disturbance may exacerbate these natural events, leading to increased exposure to *Coccidioides* spp.

The goal of our study was to identify spatial and temporal relationships between environmental factors and Valley fever incidence throughout the southwestern U.S., drawing upon a new regional Valley fever incidence database that we assembled. In our analysis, we assessed how surface air temperature, precipitation, soil moisture in the top 10 cm, surface dust concentration, normalized difference vegetation index, and cropland area influence Valley fever incidence. We hypothesized that Valley fever incidence will be higher in counties with warmer and drier conditions, and where human land use and natural processes increase dust concentrations. We tested our hypothesis using linear and non-linear regression models to quantify climate and environmental controls on the spatial pattern of incidence in 152 counties across 5 states. In addition, we assessed the influence of climate on seasonal and annual variability as well as the spatial structure of long-term trends in Valley fever incidence. Improving our understanding of the spatial extent of Valley fever incidence and the relationships between climate and incidence may help mitigate both immediate and future health impacts of this disease. This information can help to predict how climate change may modify the vulnerability of different communities to Valley fever outbreaks over the next several decades.

2.2 Methods

2.2.1 Valley fever database

We compiled county-level Valley fever case data from Arizona, California, Nevada, New Mexico, and Utah using state-level data records to create a regional Valley fever incidence database (Table 2.1). We selected this domain because *Coccidioides* spp. is known to be endemic to the desert soils of the southwestern U.S. Our analysis spanned the period from January 2000 through December 2015, when month-level data was available for each county. During this period, each of the five state health agencies identified Valley fever as a reportable disease, meaning immediate disease control was necessary and reporting cases to state health agencies was mandatory (CDC, 2015). Over the 16 years and 152 counties in

Table 2.1. County-level data gathered from state health agencies used to create the Valley fever database.

State	Year Made Reportable	Data Availability	Reference
Arizona	1997	1990 – 2015	Arizona Department of Health Services 150 N 18th Ave, Ste 140 Phoenix, AZ 85007
California	1995	2000 – 2015	California Department of Public Health PO Box 997377, MS 0500 Sacramento, CA 95899
Nevada	1992	1991 – 2015	Nevada Department of Health and Human Services 4126 Technology Way Carson City, NV 89706
New Mexico	1988	1993 – 2015	New Mexico Department of Health 1190 St. Francis Drive, Runnels N1361 Santa Fe, New Mexico 87502
Utah	1995	1998 – 2015	Utah Department of Health PO Box 142104 Salt Lake City, Utah 84114

our analysis, our database consisted of 149,286 individual Valley fever cases. County-level cases was the finest spatial scale for which curated Valley fever data was available.

Each Valley fever case has a date corresponding to the month and year when the diagnosing health institution submitted the official case report. However, there is an incubation time between environmental exposure to *Coccidioides* spp. and the onset of symptoms from one to three weeks (Smith et al., 1946b) and a further lag between the onset of symptoms, subsequent Valley fever diagnosis, and submission of the official case report. The time lag between onset of symptoms and submission of the official Valley fever case report is estimated to be between 1 and 1.5 months (Comrie, 2005, Tsang et al., 2010). It is important to consider this lag when interpreting temporal relationships between climate and Valley fever incidence. In addition, the location of infection may have not occurred in the county which filed the case report, if for example, an individual was exposed to *Coccidioides* spp. during travel.

We estimated county-level Valley fever incidence by dividing the number of monthly reported cases by annual county-level population. We obtained county-level population data for 2000 to 2015 using intercensal population estimates from the U.S. Census Bureau (U.S. Census Bureau, 2011a, 2015).

We compared our dataset of incidence with the endemicity map from the U.S. Centers for Disease Control and Prevention (CDC). The CDC endemicity map is derived from about 49,000 skin tests administered from 1945-1951, with 80% of participants being 17 to 21 year old, Caucasian male, Navy personnel (Edwards & Palmer, 1957; CDC, 2017a). The map was modified to include Valley fever outbreaks in northern California (Werner & Pappagianis, 1973), northeastern Utah (Petersen et al., 2004), and southeastern

Washington State (Marsden-Huag et al., 2012). When interpreting differences between our mean annual Valley fever maps and that used by the CDC, it's important to recognize that Caucasian males and people 17 to 21 years old are not recognized as a highly susceptible population to Valley fever, and there have been considerable changes in population and land use in the southwestern U.S. over the past half century.

2.2.2 Climate and environmental data

We collected monthly climate and environmental data from 2000 to 2015 (Table 2.2). The gridded data were spatially averaged to the county-level using county cartographic boundary shapefiles from the U.S. Census Bureau at 1:500,000 scale in the Quantum Geographic Information System (QGIS, http://www.qgis.org/en/site/).

Table 2.2. Climate and environmental variables analyzed against the Valley fever database

Variable	Data Product	Resolution	Time Span	Reference
Surface precipitation	PRISM Climate Group - AN81m	4 km2	2000 – 2015	Daly et al., 1994, 2008
Surface air temperature	PRISM Climate Group - AN81m	4 km2	2000 – 2015	Daly et al., 1994, 2008
Average soil moisture 0-10 cm	NASA Global Land Data Assimilation System, Noah land surface model L4, Version 2.1	0.25 × 0.25º	2000 – 2015	Rodell et al., 2004; Rodell & Beaudoing, 2007
Surface dust concentration	MERRA2 Monthly mean, time averaged, aerosol diagnostics, Version 5.12.4	0.5 × 0.625º	2000 – 2015	Rienecker et al., 2011; Bosilovich et al., 2015; Molod et al., 2015
Normalized difference vegetation index	NASA Terra MODIS L3, Version 6, MOD13C2	0.05 × 0.05º	02-2000 – 2015	Huete et al., 2002, 2010; Didan, 2015
Cropland area	USDA, NASS, Cultivated Layer based upon the NASS Cropland Data Layers	30 m	2015	Boryan et al., 2011, 2012

For surface air temperature and precipitation, we used 4 km gridded products from the Precipitation-elevation Regressions on Independent Slopes Model (PRISM)(Daly et al., 1994, 2008). PRISM is a climate interpolation model for the conterminous U.S. that assimilates surface station data using topographic variables and other information. It is recognized as the official spatial climate dataset of the U.S. Department of Agriculture. For soil moisture, we used the 0-10 cm layer product at a 0.25° spatial resolution from NASA's Global Land Data Assimilation System (GLDAS)(Rodell et al., 2004; Rodell & Beaudoing, 2007). GLDAS is a land surface model that assimilates precipitation and solar radiation observations and other land surface driving variables from reanalysis. For dust loading, we used the 0.5° x 0.625° surface dust concentration from the second Modern-Era Retrospective Analysis for Research and Applications (MERRA-2) atmospheric reanalysis data (Rienecker et al., 2011; Bosilovich et al., 2015; Molod et al., 2015). For NDVI, we used the Moderate Resolution Imaging Spectroradiometer (MODIS) collection 6 product (MOD13C2)(Huete et al., 2002, 2010; Didan, 2015). NDVI values range from -1 to 1; barren rock and sand often have values between 0.1 and 0.2, grasslands or other ecosystems with sparse leaf area have values between 0.2 and 0.4, and high leaf area ecosystems, including closed canopy forests, often have values between 0.6 and 0.8 (Huete et al., 2010). As a measure of agricultural activity, we used an estimate of the cropland area per county from the 2015, 30 m cultivated land layer developed by the U.S. Department of Agriculture (USDA) National Agricultural Statistics Service (NASS)(Boryan et al., 2011, 2012). The area of cropland is estimated by taking the sum of the individual NASS Cropland Data Layers within each county. Cultivated land includes any land area prepared for crop cultivation, fallow land, or idle crop land (Boryan et al., 2012).

2.2.3 Statistical analysis

We constructed mean annual Valley fever case and incidence maps for the 2000 to 2015 period using the Valley fever database and population data. We used month-level climate and environmental data to construct mean annual maps over the same period, allowing for a direct comparison between these variables and mean annual Valley fever incidence.

For cropland area, we used the 2015 map because of a lack of cropland data for other years. We used the total area of cropland per county, instead of fractional cover, to better represent the impact of agriculture in large heterogeneous counties that also encompass large regions with mountain or desert ecosystems.

We focused our time series analyses on two Valley fever endemic sub-regions: the San Joaquin Valley of California and south-central Arizona. We selected these regions because the large number of cases in these areas allowed us to quantitatively examine environmental controls on seasonal and inter-annual timescales. The San Joaquin Valley of California consisted of Fresno, Kern, Kings, Madera, Merced, San Joaquin, Stanislaus, and Tulare Counties and included the cities of Fresno, Bakersfield, and Stockton. South-central Arizona consisted of Maricopa, Pima, and Pinal Counties and included the cities and metropolitan areas of Phoenix and Tucson.

We used linear and non-linear regression to examine the relationships between climate and Valley fever incidence. For each variable, we first calculated county-level means. For the San Joaquin Valley and south-central Arizona, we calculated regional means as an area-weighted average of the individual counties. We calculated the mean annual cycles of both climate variables and Valley fever incidence by computing the long-term

mean for each month from 2000-2015 (or when data were available, see Table 2.2). We then subtracted this mean annual cycle from the climate and incidence data to examine climate controls on monthly incidence anomalies.

2.3 Results

2.3.1 Spatial extent and climate controls on Valley fever incidence

We constructed mean annual maps of Valley fever cases and incidence per county by averaging annual case and incidence data from 2000 to 2015 (Figure 2.2). These maps highlighted regions endemic to Valley fever. Valley fever incidence (Figure 2.2b) was greatest in the San Joaquin Valley of California and south-central Arizona. Within California, Valley fever incidence was almost non-existent in northern coastal counties, at low to intermediate levels in the coastal and desert counties of southern California, and at very high levels in the San Joaquin Valley and along the south-central coast. In Arizona, the highest levels of incidence occurred in the Basin and Range regions.

Figure 2.2. The mean annual maps of valley fever (a) cases and (b) incidence per county from 2000 to 2015 demonstrate that the extent of valley fever differs in some areas than depicted by the CDC, shown in panel (c) (CDC, 2017), including the northern San Joaquin valley and south-central coast of California. Units are (a) mean annual cases from 2000 to 2015 and (b) mean annual incidence from 2000 to 2015. Counties considered endemic by the CDC are outlined in green in the top panels (a, b).

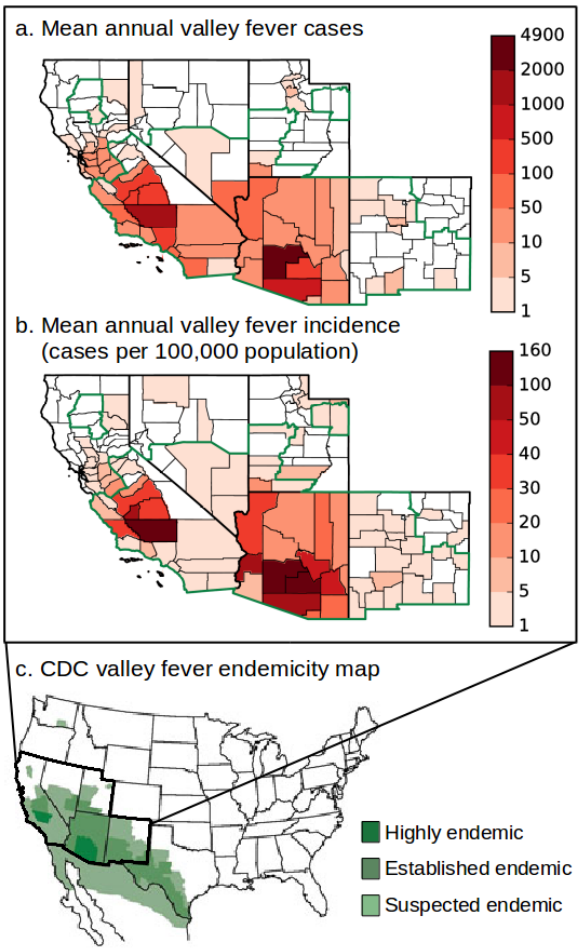

Our map provided evidence that Valley fever incidence may extend beyond the suspected endemic regions identified by the CDC in several areas (CDC, 2017a). In California, Valley fever incidence extended further north in the San Joaquin Valley, into Merced, Stanislaus, and San Joaquin Counties. Combined, these three counties reported 1,622 cases from 2000 to 2015. In contrast, a neighboring CDC suspected endemic region of similar area to the east, including Amador, Calaveras, Tuolumne, and Mariposa Counties, reported only 64 cases. Incidence throughout northern California, Nevada, New Mexico, and Utah was low, but more widespread and extended further north than depicted by the CDC. We also note that our dataset did not detect Valley fever incidence in several counties that the CDC reported as endemic. These differences may have been caused by the interpolation approach used by the CDC, small sample sizes in sparsely populated counties in our incidence dataset, or changes in *Coccidioides* spp. abundance over time.

We compared our mean annual map of Valley fever incidence with the maps of the climate and environmental drivers and found Valley fever incidence was higher in hotter, drier, and dustier regions, and often where there were large areas of cropland (Figure 2.3, Table 2.3). Mean annual surface air temperature was a significant, positive non-linear driver of Valley fever incidence ($p<0.001$, Figure 2.4a). No county with a mean annual temperature lower than 10ºC had incidence higher than 6 cases per 100,000 population, whereas the 6 counties in Arizona and California with the highest incidence (greater than 70 cases per 100,000 population) all had mean annual temperatures exceeding 16ºC. The two measures of ecosystem moisture had significant, negative non-linear relationships with Valley fever incidence (precipitation: $p<0.001$, soil moisture: $p<0.001$). No county with mean annual precipitation greater than 600 mm/yr had Valley fever incidence

Figure 2.3. The mean annual maps of climate and environmental drivers from 2000 to 2015 (except cropland area, which include 2015 data only). (a) Surface air temperature, (b) annual precipitation, (c) average soil moisture in the top 10 cm, (d) surface dust concentration, (e) NDVI, and (f) cropland area.

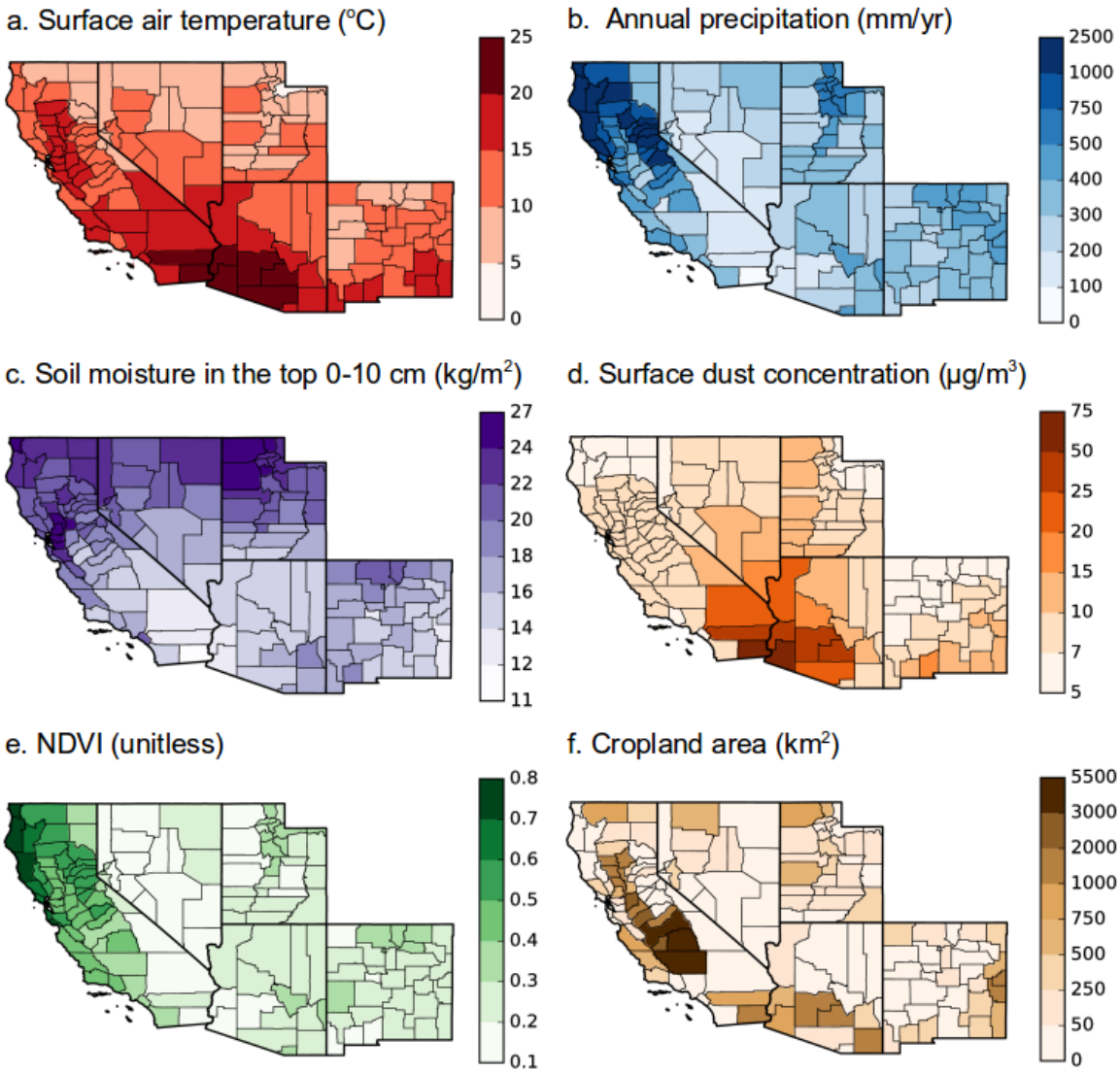

exceeding 4 cases per 100,000 population (Figure 2.4b). Thus, northern coastal counties of California had very low levels of Valley fever incidence. Similarly, counties with the greatest soil moisture had almost no Valley fever incidence (Figure 2.4c). Surface dust concentrations had a weak, positive linear relationship with Valley fever incidence ($p<0.001$, Figure 2.4d). NDVI did not have a significant linear or non-linear relationship with Valley fever incidence, although counties with over 10 cases per 100,000 population

Table 2.3. The statistical relationships between mean annual valley fever incidence and climate and environmental variables. Data were averaged across the time spans indicated

Variable	Time span	Best fit	r	Threshold (Counties greater than 10 cases/100,000 population, n=22)
Temperature	2000 – 2015	Exponential	0.48**	>11°C
Precipitation	2000 – 2015	Exponential	-0.29**	<600 mm/yr
Soil Moisture	2000 – 2015	Exponential	-0.43**	<19 kg/m2
Surface Dust Concentration	2000 – 2015	Linear	0.30**	
NDVI	02-2000 – 2015	Not Significant		0.16 – 0.45
Cropland Area	2015 only	Linear	0.56**	

** Values are significant at $p<0.05$

spanned a range of NDVI values between 0.16 and 0.45, indicating that Valley fever incidence was elevated in areas with intermediate levels of vegetation cover (Figure 2.4e). Valley fever incidence was less than or equal to 1 case per 100,000 in counties with NDVI values greater than 0.55, suggesting dense vegetation and tree cover may decrease human exposure to *Coccidioides* spp.

The amount of cropland area per county in 2015 had a significant, positive linear relationship with Valley fever incidence ($p<0.001$, Figure 2.4f). Counties with higher levels of cropland area were more likely to have elevated levels of Valley fever incidence. This relationship was weaker ($r=0.20$), but still significant ($p=0.01$), when we analyzed the fraction of county area with cropland (data not shown). Valley fever incidence was particularly high in the Central Valley of California, a major area of agricultural activity. Over 250 different crops are grown and approximately one-quarter of U.S. food production occurs in that region (U.S. Geological Survey, 2017). There were also large areas of

agriculture in southeastern Arizona, which overlapped with higher incidence counties in south-central Arizona.

Figure 2.4. The spatial relationships between mean annual valley fever incidence and (a) surface air temperature, (b) annual precipitation, (c) average soil moisture in the top 10 cm, (d) surface dust concentration, (e) NDVI, and (f) cropland area. Statistically significant non-linear relationships for surface air temperature ($p<0.001$), annual precipitation ($p<0.001$), soil moisture ($p<0.001$) and statistically significant linear relationships for surface dust concentration ($p<0.001$) and cropland area ($p<0.001$) are plotted in black lines. All variables except cropland area are averaged from 2000 to 2015; cropland area is 2015 data only.

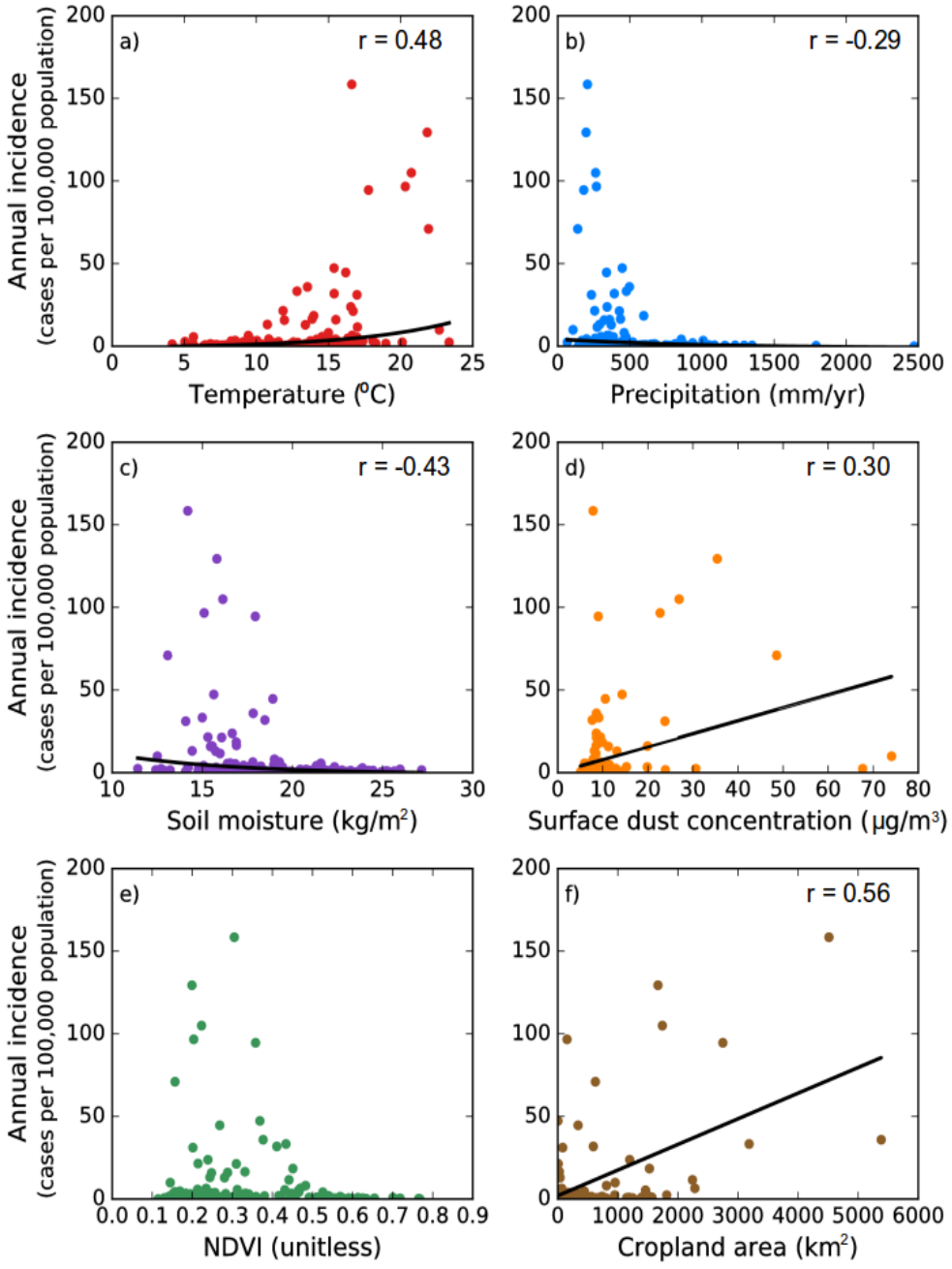

2.3.2 Seasonal dynamics of climate and Valley fever incidence

Valley fever incidence had a different mean annual cycle in the San Joaquin Valley of California compared to south-central Arizona (Figure 2.5). Maximum Valley fever incidence in the San Joaquin Valley occurred in October, at a level (6.2 cases per 100,000 population) about double the minimum incidence observed in April (3.2 cases per 100,000 population). In contrast, Valley fever incidence in south-central Arizona was less variable across seasons (averaging 10.1 cases per 100,000 population), and had a bimodal distribution with small peaks in both summer (10.3 cases per 100,000 population) and winter (13.3 cases per 100,000 population).

In the San Joaquin Valley of California, the October peak in incidence occurred approximately 3 months after the maximum in surface air temperature and 2 months after the summer minimum in precipitation and soil moisture (Figure 2.5b-d, Table 2.4). Surface dust concentrations were lower in the San Joaquin Valley compared to south-central Arizona. We observed a small peak in dust concentration in the San Joaquin Valley during late autumn and winter months (Oct-Dec). The dust peak had a long lead time relative to the seasonal maximum in Valley fever incidence (Figure 2.5e). NDVI was at a minimum in October, during the same month as peak incidence (Figure 2.5f). Low level of plant cover during late summer and fall may allow for greater exposure of bare soils that increase surface wind speeds and loft *Coccidioides* spp. spores into the air (Zender & Talamantes, 2006). Combined, the monthly patterns of climate and incidence in the San Joaquin Valley suggested that dispersal was greater during hot and dry periods following wet conditions optimal for *Coccidioides* spp. growth, supporting previous work (Smith et al., 1946b; Pappagianis, 1994). In south-central Arizona, peaks of Valley fever incidence during

Figure 2.5. Mean annual cycles of valley fever incidence and climate variables in the San Joaquin Valley of California and south-central Arizona. (a) Monthly valley fever incidence, (b) surface air temperature, (c) monthly precipitation, (d) average soil moisture in the top 10 cm, (e) surface dust concentration, and (f) NDVI. Valley fever incidence reaches seasonal maximums following periods of low environmental moisture. Error bars are the standard deviation of the monthly averages between counties in each sub-region.

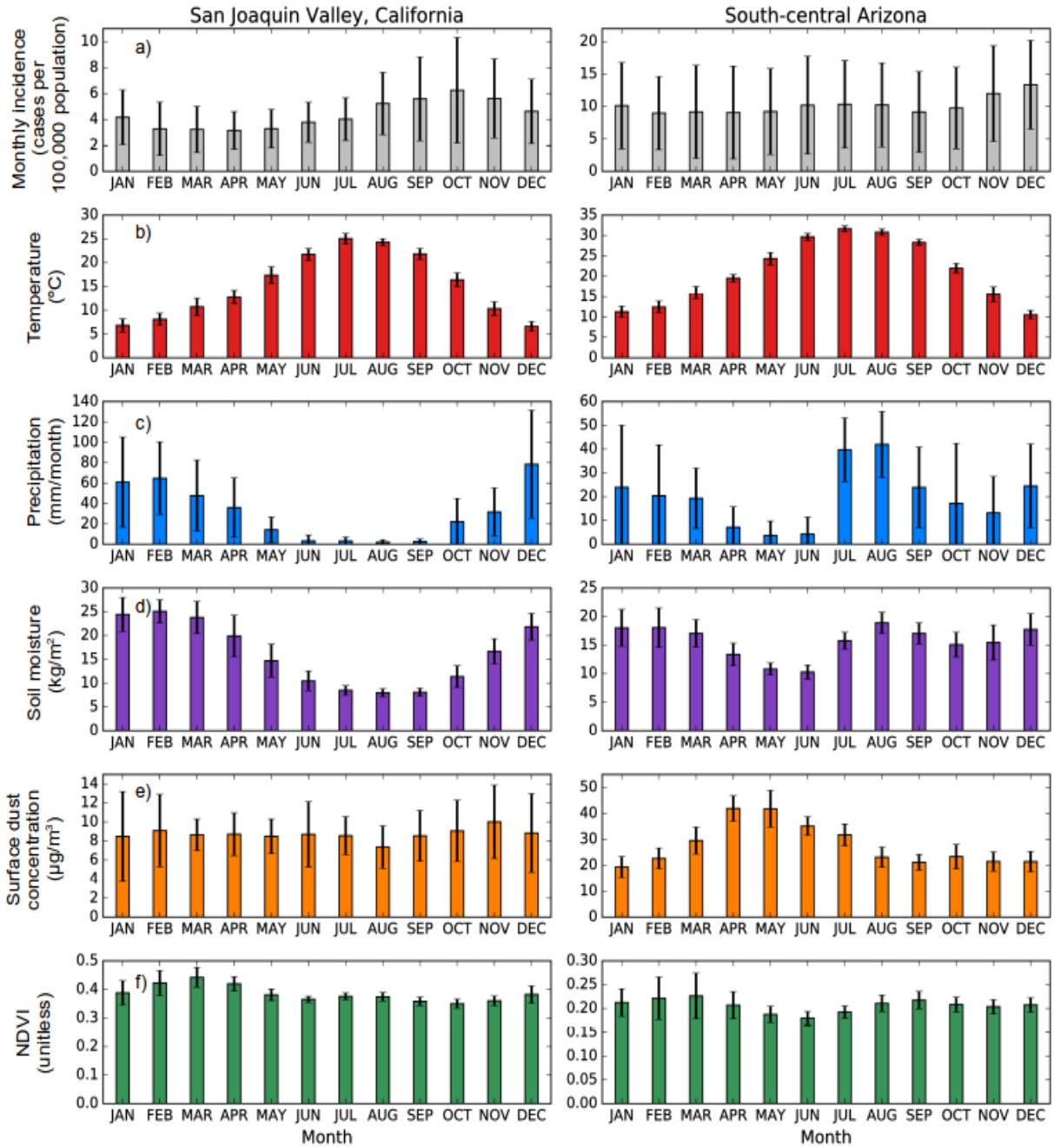

Table 2.4. The statistical relationships between Valley fever incidence and climate variables at each time scale.

	Seasonal Cycle				Monthly Anomalies				Long Term Annual			
	San Joaquin Valley of California		South-Central Arizona		San Joaquin Valley of California		South-Central Arizona		San Joaquin Valley of California		South-Central Arizona	
Variable	r	Lag (months) [0-11]	r	Lag (months) [0-11]	r	Lag (months) [0-11]	r	Lag (months) [0-11]	r	Lag (years) [0-2]	r	Lag (years) [0-2]
Temperature	0.95**	3	0.59**	4	-0.32**	6	-0.11	11	-0.59**	0	-0.37	1
Precipitation	0.92**	8	0.72**	4	0.26**	9	-0.17**	2	0.57**	1	-0.26	0
Soil Moisture	0.98**	8	-0.74**	6	0.42**	7	-0.19**	1	0.55**	1	-0.23	0
Surface Dust Concentration	0.51*	11	0.71**	7	0.17**	3	0.23**	1	0.33	0	0.35	0
NDVI	0.90**	7	-0.76**	6	0.48**	9	-0.28**	0	0.66**	1	-0.30	0

* Values are significant at $p<0.10$
** Values are significant at $p<0.05$
Note. Lag times refer to the delay in valley fever incidence relative to each environmental variable.

summer and winter months follow minima in precipitation during spring and autumn (Figure 2.5). Soil moisture was less seasonally variable in south-central Arizona than in the San Joaquin Valley, which may have contributed to the more homogenous seasonal dynamics of Valley fever incidence. Surface dust concentrations had a lead time of 7 months relative to the peak of Valley fever incidence in winter; however, dust concentrations did not follow a bimodal seasonal pattern like environmental moisture, plant growth, and Valley fever incidence.

To further explore the role of precipitation in structuring Valley fever incidence, we created a seasonality index by calculating the fraction of mean annual precipitation and incidence that occurred during each three-month season (Figure 2.6). Areas surrounding and including the San Joaquin Valley of California had a more pronounced seasonality of Valley fever incidence than areas surrounding and including south-central Arizona. Near the San Joaquin Valley, high winter precipitation preceded low levels of Valley fever incidence in spring, while low summer precipitation preceded a peak of incidence in autumn. This annual cycle changed to the east. Across Arizona and New Mexico, counties experienced increased precipitation from the North American monsoon during summer and autumn. The regional differences in precipitation timing may be one of the factors contributing to differences in the seasonality of Valley fever incidence observed across the southwestern U.S.

2.3.3 Monthly climate and Valley fever incidence anomalies

We calculated monthly climate and Valley fever incidence anomalies by removing the mean annual cycle from the original time series for each variable (Figure 2.7). In the San Joaquin Valley of California, monthly air temperature anomalies were negatively

Figure 2.6. A seasonality index showing the fraction of annual precipitation and annual valley fever incidence that occurred during each three-month period. (a) Winter (DJF), (b) spring (MAM), (c) summer (JJA), and (d) autumn (SON) intervals. Counties that averaged less than 1 valley fever case per 1,000,000 population per year from 2000 to 2015 were masked to reduce the noise associated with small sample sizes.

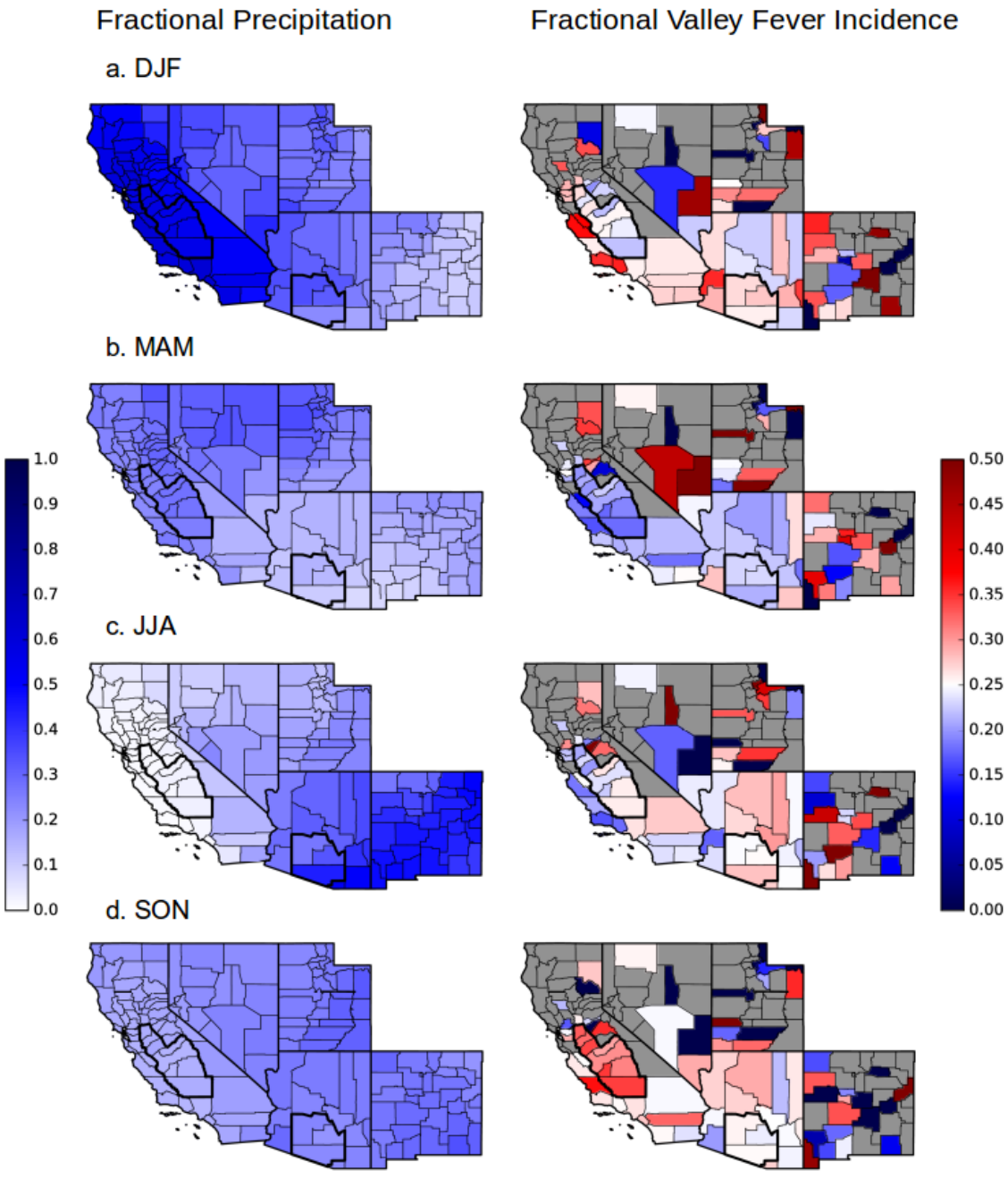

Figure 2.7. Monthly climate and valley fever incidence anomalies after removing the mean annual cycle from the original time series for each variable. (a) Valley fever incidence anomalies, (b) surface air temperature anomalies, (c) monthly precipitation anomalies, (d) soil moisture in the top 10 cm anomalies, (e) surface dust concentration anomalies, and (f) NDVI anomalies.

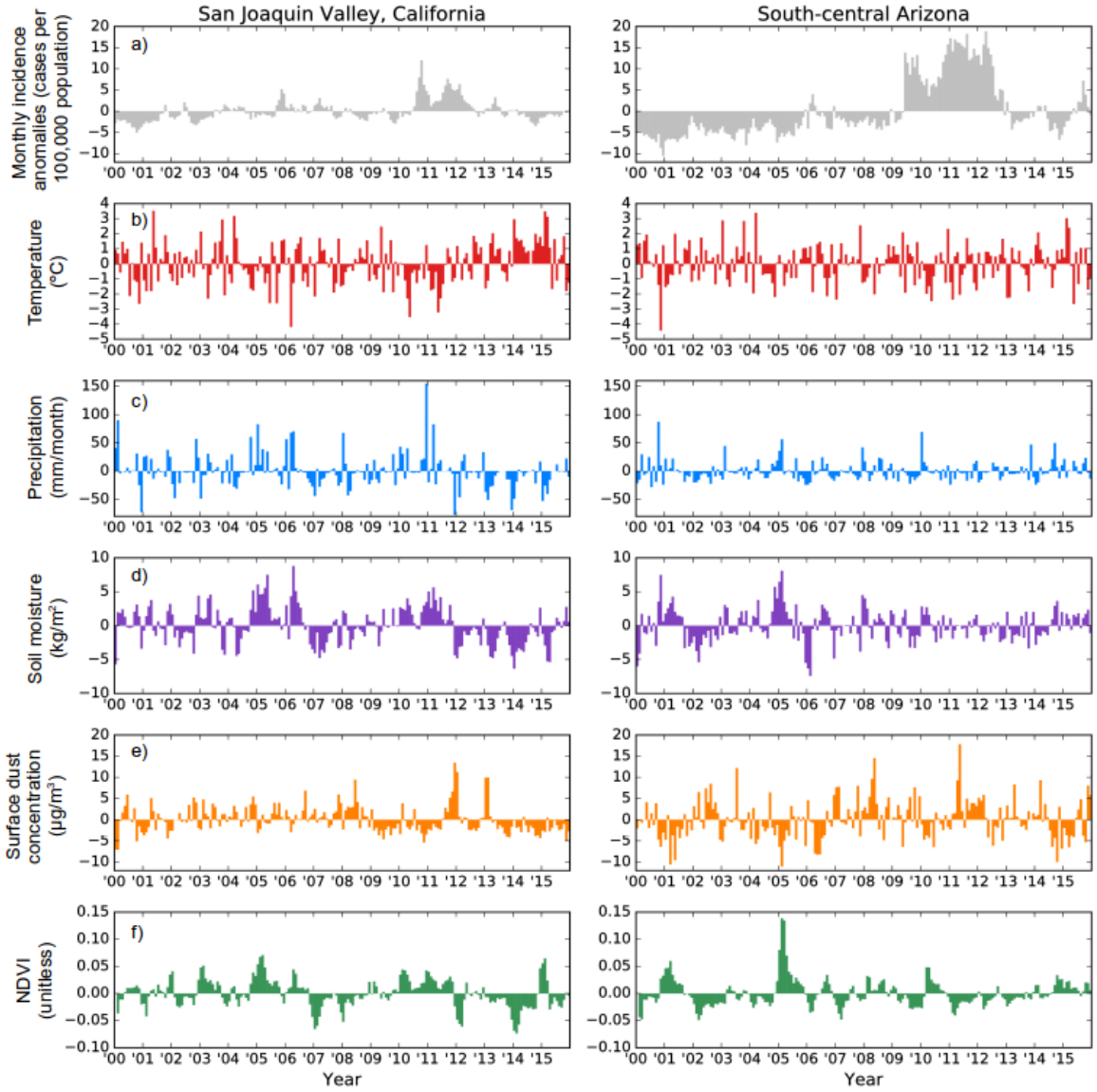

correlated with Valley fever incidence anomalies 6 months later (Figure 2.7b, Table 2.4). Precipitation, soil moisture, and NDVI anomalies all had significant, positive correlations with Valley fever incidence anomalies 7-9 months later (Figure 2.7c,d,f, Table 2.4). Taken together, these results provide preliminary evidence for higher autumn Valley fever incidence in years with cool, wet, and productive spring growing seasons.

In south-central Arizona, we found no significant relationship between air temperature anomalies and Valley fever incidence anomalies (Figure 2.7b). Incidence anomalies were negatively correlated with precipitation and soil moisture anomalies over the previous 1-2 months, positively correlated with surface dust in the previous month, and negatively correlated with NDVI anomalies in the same month (Figure 2.7c,d,e,f, Table 2.4). The shorter lag times of incidence following climate and dust anomalies suggested that in south-central Arizona, climate variability within a single season can modify the risk of contracting Valley fever. The dual influence of both Pacific storms and the North American monsoon likely contributes to both the bimodal seasonality of Valley fever incidence and shorter time delays observed between climate and incidence anomalies.

2.3.4 Long term trends in Valley fever incidence

Trends in annual Valley fever cases and incidence across the southwestern U.S. followed similar patterns between states, especially in Arizona and California (Figure 2.8a). Cases in Arizona and California had a minor peak in 2006 and a longer duration peak from 2009 through 2012, which was followed by a moderate decrease from 2013 to 2015. The majority of cases within Arizona and California occurred in the two sub-regions with high Valley fever incidence; the San Joaquin Valley of California accounted for over 57% of cases in California each year and south-central Arizona accounted for over 94% of cases in

Figure 2.8. Long term trends of valley fever from 2000 to 2015, with relative peaks in 2006 and 2011. (a) Annual cases in California and Arizona are dominated by two sub-regions of high valley fever cases: the San Joaquin Valley of California and south-central Arizona, (b) annual incidence in Arizona becomes greater than in California by 2015, and (c) significant changes in annual valley fever incidence occurred throughout the entire state of Arizona and portions of the San Joaquin Valley and south-central coast of California. Striped counties indicate trends that were not significant at $p<0.10$. The units are the change in annual incidence per year.

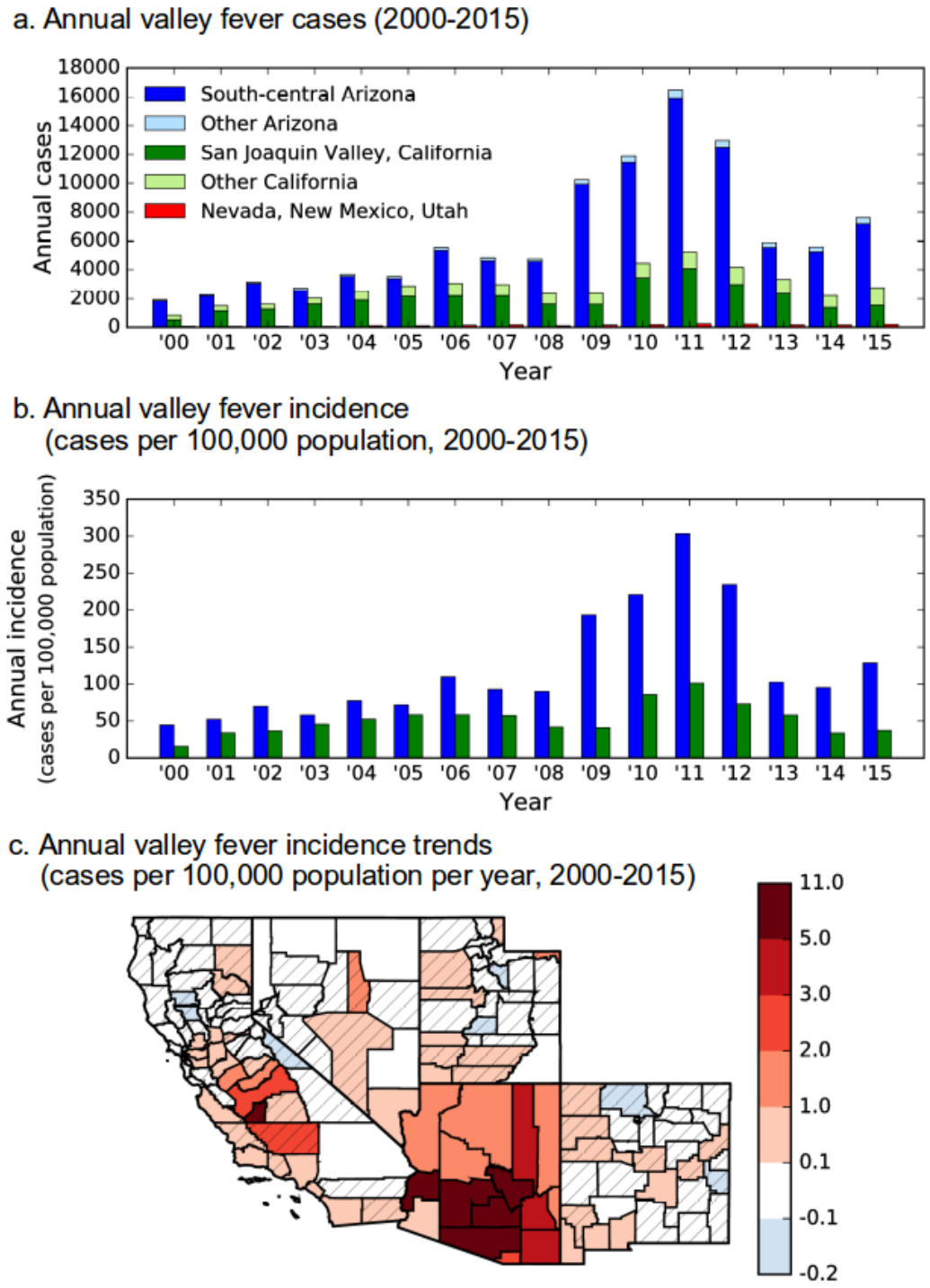

Arizona each year (Figure 2.8a). The combined set of cases from Nevada, New Mexico, and Utah was small compared to the totals from Arizona and California.

Valley fever incidence in the San Joaquin Valley and south-central Arizona was similar at the beginning of our time series from 2000 to 2008 (Figure 2.8b). However, from 2009 to 2012, south-central Arizona experienced a rapid increase in incidence, with levels more than doubling during this 4 year interval. Incidence in both sub-regions declined after 2012, but incidence in south-central Arizona remained over two and a half times the annual incidence in the San Joaquin Valley. Overall, the long term trend in annual Valley fever incidence in south-central Arizona significantly increased on average by 9.3 cases per 100,000 population per year from 2000 to 2015 ($p<0.05$), whereas the San Joaquin Valley had no significant trend. At the state level, Arizona ($p<0.05$), California ($p<0.05$), Nevada ($p<0.001$), New Mexico ($p<0.01$), and Utah ($p<0.05$) all had significant positive long-term trends in annual Valley fever incidence.

A map of long-term trends in Valley fever incidence (Figure 2.8c) highlighted significant ($p<0.1$) increases in annual Valley fever incidence throughout the entire state of Arizona. Annual incidence in the northern part of the San Joaquin Valley of California increased significantly, but this was balanced by areas in the southern part of the Valley that did not significantly change. Small increases in annual incidence also occurred along the south-central and southern coast of California, including Monterey, Santa Barbara, Los Angeles, Orange, and San Diego Counties. Of the 152 counties of the southwestern U.S., 38 (25%) had a positive, significant increase in annual incidence over 0.01 cases per 100,000 population per year ($p<0.1$) and no county had a significant decrease in incidence. These

trends provide evidence that south-central Arizona is the current, main endemic area to Valley fever.

We examined relationships between annual climate and Valley fever incidence, examining 0, 1, and 2 year lags in incidence (Table 2.4). In the San Joaquin Valley of California, temperature was negatively correlated with Valley fever incidence in the same year, which is consistent with the negative relationship we found between monthly anomalous temperature and incidence. Precipitation, soil moisture, and NDVI were all positively correlated with incidence in the following year. Since the Pacific storm tracks are the main source of precipitation in the San Joaquin Valley, October through December precipitation in in the previous year may be important for the growth of *Coccidioides* spp. and subsequent spore formation during the following autumn. In south-central Arizona, we found no significant correlations between annual climate and Valley fever incidence. There were no significant correlations between annual dust concentrations and incidence in either sub-region.

2.4 Discussion

2.4.1 The spatial extent of Valley fever incidence and need for enhanced Valley fever surveillance

Our mean annual map of Valley fever incidence suggested that regions of Valley fever endemicity may extend beyond the current boundaries depicted by the CDC, most notably extending further north. This highlights the need for systematic monitoring in counties with lower Valley fever incidence and states outside the suspected endemic zone.

Texas was not included in our study since the state does not declare Valley fever as a reportable disease. However, the CDC estimates Texas is an established endemic region

(CDC, 2017a) and cases in Texas date back to the 1930s (Caldwell, 1932, Maddy, 1965). A few county-level health departments in Texas initiated local Valley fever surveillance programs and reported non-zero amounts of cases (i.e., El Paso County: 12 cases in 2015, or 1.4 cases per 100,000 population)(City of El Paso Department of Public Health, 2015).

States outside of the southwestern U.S. have also reported increases in Valley fever. Several cases of Valley fever in Washington State led to an investigation that detected *Coccidioides* spp. in Washington State soils (Litvintseva et al., 2014). Cases in Missouri are increasing, largely in part to people traveling to endemic areas (Turabelidze et al., 2015). Humans may unintentionally aid spore dispersal and cause new communities to be at risk for Valley fever, especially since population and domestic travel are increasing (Bureau of Transportation Statistics, 2016]. Defining Valley fever as a reportable disease outside the endemic zone would strengthen our ability to quantify climate and environmental drivers that structure the spatial and temporal trends of Valley fever.

More broadly, international collaboration on Valley fever surveillance would improve disease management, especially in countries with cases or where *Coccidioides* spp. has been detected; this includes countries in North, Central, and South America (Campins, 1961; Eulálio et al., 2001; de Macêdo et al., 2011; Baptista-Rosas et al., 2012]. For example, *Coccidioides* spp. has been detected in Mexico at multiple locations over 70 years (Sotomayor et al., 1960; Baptista-Rosas et al., 2012]. An environmental niche model of *Coccidioides* spp. highlighted substantial portions of Mexico as suitable habitat (Baptista-Rosas et al., 2007]. Information on disease trends in Mexico could help define the main drivers of disease trend, especially since there are large similarities in climate and land-use

patterns between the southwestern U.S. and northern Mexico, yet differences in demographics and healthcare infrastructure.

2.4.2 The role of climate and environmental variables in structuring the spatial pattern of Valley fever incidence

Comparing the mean annual map of Valley fever incidence with climate and environmental variables does not suggest that regions of high Valley fever incidence are structured by a single driver, but rather a combination of climate factors. Hot, dry, and dusty conditions appeared to create the optimal conditions for elevated disease incidence. Collectively, the relationships between Valley fever incidence and climate variables begin to define a climate envelope for increased Valley fever incidence, and by proxy, the geographical range of *Coccidioides* spp. Air temperature, precipitation, soil moisture, surface dust concentration, NDVI, and cropland area may all be useful for developing a predictive model of Valley fever incidence, and thus a means to analyze scenarios of future environmental change.

Local to regional-scale patterns of high Valley fever incidence are likely structured by a broad suite of mechanisms influencing soil disturbance. In this context, it would be beneficial to further examine human activities that contribute to dust emission. Land-use change and some agricultural practices are known to enhance the wind erosion of soils (Liu et al., 2007; McConnell et al., 2007; Neff et al., 2008). In combination with reduced water availability for irrigation, these factors may increase the number of dust storms, which are known to carry large numbers of fungal spores (Griffin, 2007). Dust storm activity in the U.S. increased in recent decades and has been linked to changes in Valley fever incidence (Williams et al., 1979; Tong et al., 2017). Other short-lived natural dust events, including a

landslide triggered by an earthquake, have also been related to Valley fever outbreaks (Harp & Jibson, 1996). Since our study was limited to the monthly time scale, the impact of dust contributions on the daily or weekly time scales were not well resolved. New, high resolution observations and reanalysis of surface dust, including the contributions from dust storms, is needed to further explore controls on Valley fever incidence.

Soil characteristics may also play a role in structuring the spatial extent of Valley fever. However, the low number of soil samples that have detected *Coccidioides* spp. make it difficult to identify key soil characteristics that influence abundance (Elconin et al., 1957; Maddy, 1958; Swatek et al., 1967; Swatek & Omieczynski, 1970; Lacy & Swatek, 1974; Greene et al., 2000; Barker et al., 2012; Lauer et al., 2012). Alkalinity, salinity, soil porosity, and soil texture may be important factors; however, more systematic soil sampling campaigns across the southwestern U.S. are needed to better constrain these soil characteristics.

In addition to local environmental conditions, human demographics may contribute to the observed patterns of Valley fever incidence. Race, gender, and local population age may play a role, especially in disseminated disease (Louie et al., 1999; Rosenstein et al., 2001; Hector et al., 2011; Odio et al., 2017). Occupation, especially in agriculture, may also be a compounding factor that influences dust exposure and subsequent Valley fever incidence.

2.4.3 Seasonal and inter-annual dynamics of Valley fever incidence in relation to climate

Our study found support that a wet season, which allows the fungi to grow, followed by a dry period, which allows the generation of dust and dispersal of spores (Smith et al.,

1946b; Pappagianis, 1994), regulates the seasonal timing of Valley fever incidence. Our analysis builds upon this paradigm by showing that incidence seasonality varied across the southwestern U.S. and was linked to different precipitation regimes, including Pacific storm systems and the North American monsoon. In California, the October peak in incidence occurred near the end of a hot and dry Mediterranean summer climate. In contrast, smaller bimodal peaks in incidence in south-central Arizona occurred during summer and early winter after dry intervals in late spring and autumn.

The differences we observed in seasonal Valley fever dynamics between California and Arizona were consistent with previous studies, but differed slightly in timing. In the San Joaquin Valley of California, the singular peak of Valley fever incidence we observed during autumn is consistent with individual studies in Kern County. However, our study indicated an October maximum of Valley fever incidence, while earlier studies broadly identified that the maximum occurred in summer to autumn (Smith et al., 1946b), or in October to January (Zender and Talamantes, 2006). In south-central Arizona, the bimodal peak of Valley fever incidence is similar to previous temporal patterns identified for Pima County (Hugenholtz, 1957). Our results indicated a secondary peak in incidence occurs in December, whereas prior analyses reported this peak to occur earlier, between October and November (Hugenholtz, 1957; Kerrick et al., 1985; Comrie, 2005).

The sensitivity of Valley fever incidence to wetting and drying cycles appeared to impact inter-annual anomalous incidence. In the San Joaquin Valley of California, cool, wet, and productive springs appeared to increase Valley fever incidence the following autumn. In south-central Arizona, no significant pattern was observed on this timescale, possibly from dual forcing from Pacific storms and the North American monsoon damping out

seasonal precipitation variability. However, a recent study used aggregated soil moisture and Valley fever incidence data over varying, inter-annual monthly time intervals and found evidence for this relationship in both California and Arizona (Coopersmith et al., 2017).

Our study lacked strong evidence supporting dust as a driver of seasonal Valley fever incidence. There was significant, but weak, support for this relationship on the inter-annual time scale. In both the San Joaquin Valley and south-central Arizona, dust concentrations in the preceding 1-3 months were positively correlated with Valley fever incidence. This may suggest that localized dust emissions that are not captured in atmospheric reanalysis models may be an important mechanism for the dispersion of *Coccidioides* spp. spores. Moreover, isolated short-lived dust storms may be an important mechanism for widespread exposure to *Coccidioides* spp., especially storms that impact large populations (Tong et al., 2017). Recent work found that the frequency of dust storms was a better indicator of increased Valley fever incidence than surface dust measurements (Tong et al., 2017). However, this finding was only significant for two highly endemic counties: Maricopa and Pima Counties (Tong et al., 2017). Dust storms may have caused anomalous monthly surface dust concentrations in our analysis if the signal was strong enough. Otherwise, the signal from these short-lived events may be lost by analyzing monthly averaged data.

2.4.4 Long term trends in Valley fever incidence

Our study highlighted a shift from 2000 to 2015 in the location of the highest Valley fever incidence from the San Joaquin Valley of California to south-central Arizona. Levels of Valley fever incidence between the San Joaquin Valley and south-central Arizona in the

beginning of our time series analysis were similar. However, incidence in south-central Arizona has been significantly increasing since 2000 and is now more than double the incidence rate in the San Joaquin Valley. Significant increases in incidence in counties surrounding the south-central Arizona hotspot may suggest that the major endemic region is also expanding spatially.

It is unclear whether the extended peak in Valley fever incidence from 2009-2011 is a result of precursor climate conditions or other factors related to demographics and health management. Peaks in annual Valley fever incidence were suggested to be the result of changes in Valley fever diagnosis protocol and reporting, especially the 2009 peak in Arizona (Arizona Department of Health Services, 2012). However, Valley fever hospitalization rates in both Arizona and California also peaked in 2006 and from 2009 to 2011 (Arizona Department of Health Services, 2013; Sondermeyer et al., 2013; Koski et al., 2016). Simultaneous increases in both Valley fever incidence and hospitalization rates suggest that these peaks may not be the result of changes in diagnosis alone.

2.4.5 The potential effects of climate change on Valley fever incidence dynamics

Climate change may have varying effects on the suitable habitat, abundance, and dispersion of *Coccidioides* spp. Temperatures in the southwestern U.S. are expected to increase by at least 2oC by 2100, with the greatest increase expected during summer and autumn (Garfin et al., 2014). Given the temperature threshold for higher Valley fever incidence identified in our analysis (Table 2.3), this warming may shift Valley fever endemic regions further north as *Coccidioides* spp. inhabits locations previously unsuitable for survival.

Projections of precipitation are more uncertain for the southwestern U.S. (Cayan et al., 2013; Kunkel et al., 2013; Garfin et al., 2014). Winter and spring precipitation is projected to decrease for the southern part of the region, but not significantly change in the north. Less water availability and increases in evaporative demand in the southwestern U.S. may limit the growth of *Coccidioides* spp. However, periods of drought throughout the southwestern U.S. are expected to intensify (Cayan et al., 2013), which could increase dust concentrations and *Coccidioides* spp. dispersal.

Considering changes in precipitation and temperatures together, the effects of climate change in the southwestern U.S. may favor both the enhanced growth and prolonged emission of *Coccidioides* spp. spores. Previous work identified populations in Tulare, Madera, and Kern Counties in California and in Pinal, Pima, and Maricopa Counties in south-central Arizona as particularly vulnerable to increased Valley fever incidence (Shriber et al., 2017). These counties already have some of the highest Valley fever incidence and climate change may further increase the disease burden. The potential effects of climate change warrant enhanced surveillance of this disease and more wok to understand the relationship between climate and Valley fever incidence.

2.5 Conclusions

We assessed environmental controls on the spatial extent, seasonal dynamics, and long term trends of Valley fever incidence using a new regional Valley fever database. Our analysis drew upon over 149,000 case reports from 152 counties in the southwestern U.S. We found that surface air temperature, precipitation, soil moisture, surface dust concentrations, NDVI, and cropland area all provided information regulating spatial and temporal patterns of Valley fever incidence. Incidence was higher in regions with warm

surface air temperatures and drier soils, with elevated levels of incidence in counties with a mean annual temperature above 11°C. The seasonal pattern of Valley fever incidence differed across the southwestern U.S. and appeared to be linked to precipitation drivers, including the influence of Pacific storm systems and the North American monsoon. Two hotspots of Valley fever in the San Joaquin Valley of California and in south-central Arizona had maximum seasonal Valley fever incidence following dry periods, supporting previous work showing that a wet season followed by a dry season increases incidence (Smith et al., 1946b; Pappagianis, 1994).

Our results suggested there are several northern regions where Valley fever is endemic that are outside the current domain identified by the CDC. To improve our ability to map endemic regions of Valley fever, surveillance programs should be implemented to enhance disease management and reporting, especially in areas where *Coccidioides* spp. is hypothesized or proven to be present. Improving our ability to link the current magnitude and extent of Valley fever with climate observations at a regional scale may help us to predict future changes in disease impact. Changes may occur in both the timing and levels of Valley fever incidence, as climate change alters regional temperatures and precipitation. The relationships between climate and incidence defined in our study can be incorporated into future forecast models that estimate the risk of contracting Valley fever.

Acknowledgements

M. E. Gorris is supported by a Department of Defense (DoD), National Defense Science & Engineering Graduate Fellowship (32 CFR 168a). L. A. Cat and K. K. Treseder acknowledge the UC Mexico Initiative and K. K. Treseder was supported by NSF DEB-

1457160. C. S. Zender acknowledges support from the Borrego Valley Endowment Fund. J. T. Randerson received support from the Gordon and Betty Moore Foundation (GBMF#3269), NASA Soil Moisture and Interdisciplinary Science Programs, and the U.S. Dept. of Energy Office of Science RUBISCO Science Focus Area. We thank Shane Brady from the Arizona Department of Health Services, Colleen McLellan from the California Department of Public Health, Joseph Bareta from the New Mexico Department of Health, Jennifer Thompson from the Nevada Department of Health and Human Services, and Randon Gruninger from the Utah Department of Health for providing us with Valley fever case data from their respective state health agencies. Valley fever data may be obtained from the affiliated state health agencies. The authors declare no competing financial interests.

Chapter 3

Expansion of coccidioidomycosis endemic regions in the United States in response to climate change

Adapted from:

Gorris, M. E., Treseder, K. K., Zender, C. S., & Randerson, J. T. (2019). Expansion of coccidioidomycosis endemic regions in the United States in response to climate change. *GeoHealth*. In press.

Supporting information located in Appendix A

3.1 Introduction

Coccidioidomycosis, commonly known as Valley fever, is an infectious fungal disease that has gained attention in the United States due to a recent increase in cases (CDC, 2018a). Humans contract Valley fever when they inhale *Coccidioides* spp. fungal spores. At onset, symptoms of Valley fever closely resemble the flu, which may delay diagnosis (CDC, 2018b). If left untreated, debilitating symptoms may occur, and on rare occasion may cause death. Valley fever is not a communicable disease, so cases are a result of human exposure to *Coccidioides* spp. in the environment.

Coccidioides spp., and therefore Valley fever, is endemic to the southwestern United States and parts of Central and South America (CDC, 2017b). Currently, there are two known species of *Coccidioides*, both of which cause Valley fever: *C. immitis* and *C. posadasii* (Lauer, 2017). *C. immitis* is thought to be the primary species present in California, while *C. posadasii* has a broader geographic distribution and is more commonly found in the highly endemic areas of Arizona (Barker et al., 2019; Lauer, 2017). The fungi grow as hyphae within desert soils (Stewart & Meyer, 1932). As such, *Coccidioides* spp. growth and abundance are influenced by environmental conditions (Maddy, 1957). The fungi

proliferate during wet periods. When water becomes limiting, *Coccidioides* spp. hyphae then break apart into spore-containing fragments, small enough for humans to inhale (Maddy, 1957). Any type of soil disturbance, like high winds or digging in dry soils, can cause *Coccidioides* spp. spores to become airborne and potentially inhaled by humans. Many details about the *Coccidioides* spp. life cycle and the microecosystem characteristics that structure its presence in soils are unknown. As a consequence, environmental surveillance for the fungi has yielded relatively few soil samples that have tested positive for *Coccidioides* spp.

Because the fungi have not been systematically mapped across the hypothesized endemic region, much of our understanding of the relationships between environmental factors and *Coccidioides* spp. comes from studying epidemiological data. On a regional scale, weather and climate are known to influence the seasonal and interannual variability of disease incidence. Previous studies support a pattern of wet, then dry conditions preceding increased Valley fever incidence across the southwestern U.S. (Comrie, 2005; Coopersmith et al., 2017; Gorris et al., 2018; Kolivras & Comrie, 2003; Komatsu et al., 2003; Park et al., 2005; Talamantes et al., 2007; Tamerius & Comrie, 2011; Zender & Talamantes, 2006). These dual controls first increase fungal growth during periods of higher than normal moisture. Then, they increase spore production and effective dispersal when hot temperatures and low rainfall desiccate soils and enhance the production of dust. Time delays between drying and elevated levels of incidence are observed in the two highly endemic regions, the San Joaquin Valley of California and south-central Arizona, despite regional differences in the timing of precipitation (Gorris et al., 2018). On finer temporal and spatial scales, processes such as soil disturbance, dust storms, and agricultural activity

can also influence Valley fever incidence (Tong et al., 2017; Williams et al., 1979; Wilken et al., 2015).

These connections between climatic conditions and disease dynamics suggest on regional scales, climate may also structure the environmental range of the fungi, and therefore the spatial extent of Valley fever endemicity (Baptista-Rosas et al., 2007; Fisher et al., 2007). Two main climate conditions that regulate the occurrence of *Coccidioides* spp. in the environment are temperature and precipitation (Baptista-Rosas et al., 2007; Fisher et al., 2007; Gorris et al., 2018). County-level Valley fever case reports from 2000-2015 across 5 states in the southwestern U.S. revealed the spatial pattern of incidence has a non-linear positive relationship with mean annual temperature and non-linear inverse relationship with mean annual precipitation (Gorris et al., 2018). Ultimately, these two climate conditions structure the presence of deserts: the biome in which *Coccidioides* spp. thrives (Fisher et al., 2007; Maddy, 1957). High temperatures may limit the growth of many microbial competitors, allowing *Coccidioides* spp. to more effectively compete for soil resources (Barker et al., 2012; Greene et al., 2000). Low levels of precipitation in deserts may also limit microbial competitors; however, occasional periods of high moisture availability are important for *Coccidioides* spp. fungal growth and reproduction (Fisher et al., 2007; Maddy, 1957). In contrast, wet soils in regions with high mean annual precipitation may limit dust production, spore dispersal, and thus human exposure to *Coccidioides* spp. (Gorris et al., 2018).

There is also preliminary evidence from the few soil samples positive for *Coccidioides* ssp. that temperature and precipitation may be important for structuring the spatial pattern of Valley fever endemicity. Most soil samples positive for *Coccidioides* ssp.

were collected from the Central Valley of California (Colson et al., 2017; Lauer et al., 2012; 2014), south-central Arizona (Barker et al., 2012), and Baja Mexico (Baptista-Rosas et al., 2012; Catalán-Dibene et al., 2014; Vargas-Gastelum et al., 2015)—all areas that are hot and dry. Nineteen soil samples positive for *Coccidioides* ssp. and measures of both temperature and precipitation along with a large suite of other bioclimatic variables were used in the first known statistical environmental niche model of *Coccidioides* ssp. in northwestern Mexico and parts of the southwestern U.S. (Baptista-Rosas et al., 2007). This model identified the most likely habitat for *Coccidioides* spp. as the Lower Sonoran Desert habitat and successfully highlighted epidemiological hotspots of Valley fever in the Central Valley of California and south-central Arizona. However, the niche model derived from this set of observations cannot fully explain the current spatial pattern of Valley fever cases (CDC, 2018b). This may be a consequence of the relatively small number of soil samples used to initialize the model. Until soils are systematically sampled across the western U.S., epidemiological data may provide a more robust way of delineating the effects of temperature and precipitation on the regions endemic for Valley fever.

Climate change is increasing temperatures and shifting precipitation patterns throughout the U.S. These changes could alter the regions endemic to Valley fever, as well as the number of Valley fever cases. Temperatures in the contiguous U.S. are expected to increase by 1.6–6.6°C by 2100 (relative to 1986–2015) under a high greenhouse gas emissions scenario, representative concentration pathway 8.5 (RCP8.5; Hayhoe et al., 2018; Swain et al., 2018). This warming may allow *Coccidioides* spp. to expand its geographical range farther north, in areas previously unsuitable for the species to survive. Precipitation projections are more uncertain for the western U.S., and changes will likely vary by region

and season (Easterling et al., 2017; Hayhoe et al., 2018). Along the Pacific coast, especially in the Pacific Northwest, mean annual precipitation is projected to increase (Easterling et al., 2017; Hayhoe et al., 2018). In contrast, the southwestern U.S. will likely experience little to no change in precipitation, while the southern Great Plains may become drier. In dry areas, increasing temperatures will likely increase evaporative demand, which may contribute to desertification. The expansion of dryland ecosystems may increase the area suitable for the occurrence of *Coccidioides* spp., along with the production of dust and fungal spores.

To predict how climate change may influence the spatial pattern of Valley fever in the future, it is important to have an accurate map of the current endemic area. The basis of the U.S. Centers for Disease Control and Prevention (CDC) estimate of endemic areas is a historical skin test study of approximately 88,000 young men at a Naval Training Center in San Diego, CA from 1948–1950 that detected exposure to *Coccidioides* spp. (CDC, 2018b; Edwards & Palmer, 1957). Since the original study, the endemicity map has been modified to account for localized outbreaks of Valley fever (Marsden-Huag et al., 2012; Peterson et al., 2004; Werner & Pappagianis, 1973; Werner et al., 1972). One outbreak caused by *C. immitis* occurred in Washington State, well outside its normal geographical range in the Central Valley of California, and outside the hypothesized endemic region of Valley fever throughout the southwestern U.S. (Litvintseva et al., 2014; Marsden-Huag et al., 2012).

More recently, a county-level map of mean annual Valley fever incidence derived from sixteen years of epidemiological data collected from state health agencies provided an independent way to estimate endemic areas (Gorris et al., 2018). This incidence database has not been used with niche modeling to explore the spatial pattern of disease. Valley

fever case reports alone may be an underestimate of the actual burden of disease due to misdiagnosis, underreporting, or other host factors (Ampel, 2010; Chang et al., 2008; Jones et al., 2017). Despite this limitation, further analysis of epidemiological data may provide a means to better estimate where Valley fever is currently endemic. This could allow public health agencies to improve surveillance programs and help decrease the time to patient diagnosis. The incidence database also provides a starting point for predicting how climate change will modify the location and extent of endemic areas.

The goal of our work was to create a model that describes the area in the U.S. currently endemic to Valley fever and then to use this model to predict how the endemic area may shift in response to climate change. First, we used established relationships between climate and the spatial distribution of Valley fever incidence to create a climate-constrained niche model that predicts the contemporary pattern of Valley fever endemicity. Then, we used our niche model with climate projections from Earth system models to analyze where the climate limits are lifted in the future, potentially allowing the area to become endemic to Valley fever. A secondary goal of our work is to estimate future Valley fever incidence and the number of people who may contract this disease. We report future estimates of the endemic area and potential changes in incidence for the years 2035, 2065, and 2095 under both moderate and high climate warming scenarios. We also examine the compounding effect of climate change and increases in human population on the number of people living in the endemic region and number of potential Valley fever cases. This is the first quantitative projection for the U.S. of how climate change may affect Valley fever. Our predictive model of the endemic area to Valley fever and estimate of future disease burden

may provide guidance to public health officials as to where increased Valley fever surveillance and education may improve health outcomes.

3.2 Methods

3.2.1 Valley fever incidence data

To create our models of endemic area and incidence, we used a previously compiled dataset of Valley fever cases for the southwestern U.S. (Gorris et al., 2018). This dataset included monthly, county-level Valley fever cases from 2000–2015 from Arizona, California, Nevada, New Mexico, and Utah. We calculated Valley fever incidence for each county using 2000–2015 intercensal population estimates from the U.S. Census Bureau (U.S. Census Bureau, 2011a; 2016). We performed our analysis at the county-level, which was the highest resolution available from the state health agencies for the de-identified, aggregated case data.

3.2.2 Current and future projections of climate

We focused our analyses on two main climate drivers that influence the presence of *Coccidioides* ssp. in the environment: temperature and precipitation. We gathered surface air temperature and surface precipitation data for years 2000–2015 to compare directly with Valley fever incidence. For both climate variables, we used 4 km gridded products from the Precipitation-elevation Regressions on Independent Slopes Model (PRISM; Daly et al., 2008). To compare county-level Valley fever incidence data with climate data, we calculated county-level climate averages by spatially averaging the gridded PRISM climate data within each county using QGIS (https://www.qgis.org). We obtained county shapefiles from the U.S. Census Bureau (https://www.census.gov/geo/maps-data/data/tiger-line.html).

In previous work, we found a significant, positive nonlinear relationship between county-level mean annual temperature and Valley fever incidence, and a significant, nonlinear inverse relationship between mean annual precipitation and incidence throughout the southwestern U.S. (Figure 3.1a–b; Gorris et al., 2018). We previously analyzed a suite of climate variables and found that mean annual temperature, mean annual precipitation, mean annual soil moisture, surface dust concentration, and cropland area had significant relationships with the spatial distribution of Valley fever incidence in the southwestern U.S. (Gorris et al., 2018). We chose to use precipitation here instead of soil moisture for mapping the spatial extent of Valley fever because of large model-to-model differences in the representation of the processes regulating soil moisture content in Coupled Model Intercomparison Project Phase 5 (CMIP5) models. We did not include dust or cropland area because of the ineffectiveness of these variables in constraining Valley fever endemic areas at the continental scale of the conterminous U.S. (data not shown). Analysis of these data show that counties with higher levels of mean annual Valley fever incidence have a hot and dry contemporary climate (Figure 3.1c).

For future climate projections, we used output of monthly surface air temperature (variable 'tas') and surface precipitation (variable 'pr') from 30 Earth system models from the Bias-Corrected Spatially Downscaled (BCSD) CMIP5 Climate Projections archive (Table A.1; available at https://gdo-dcp.ucllnl.org/downscaled_cmip_projections/; Maurer et al., 2007; Reclamation, 2013). The CMIP5 model simulations were used extensively in the Intergovernmental Panel on Climate Change 5th Assessment Report (Stocker et al., 2013; Taylor et al., 2012). We analyzed data for representative concentration pathway 4.5 (RCP4.5), a moderate fossil fuel emissions and warming scenario in which emissions peak

Figure 3.1. Valley fever incidence for counties in the southwestern US (n = 152) as a function of mean annual temperature (a) and mean annual precipitation (b). All counties that have endemic levels of Valley fever incidence (defined as meeting or exceeding 10 or more cases per 100,000 population during 2000–2015; n = 23) have a mean annual temperature greater than or equal to 10.7°C and a mean annual precipitation level less than or equal to 600 mm/yr. Counties with higher levels of mean annual Valley fever incidence are concurrently hotter and drier (c). We adapted panels a and b of this figure from Gorris et al. (2018) and added the gray lines to indicate the position of the climate thresholds we used to build our climate-constrained niche model.

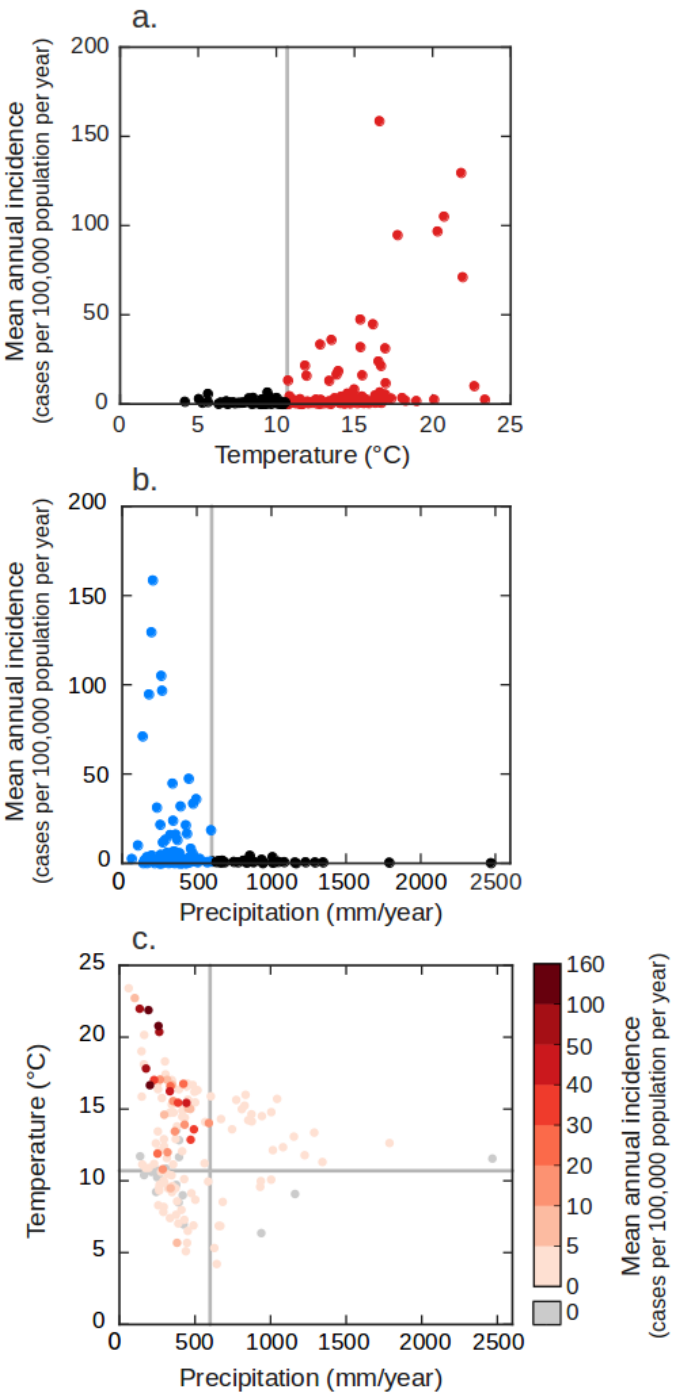

in the mid-21st century and decrease thereafter, and RCP8.5, a high fossil fuel emissions and warming scenario in which emissions increase continuously through the 21st century (Moss et al., 2010). We calculated a mean annual temperature for our analyses by averaging the raw, gridded monthly temperatures and we calculated a mean annual precipitation by taking the sum of monthly precipitation for each year, separately for each of the 30 models.

To estimate future climate, we combined information from the CMIP5 simulations with contemporary climate observations from PRISM. We first selected a baseline period of 2007 (averaging across the years 2000–2015) to match the period of available Valley fever case data. We averaged the raw, gridded CMIP5 output to calculate future mean annual temperature and precipitation for 2035 (the average of years 2030–2040), 2065 (the average of years 2060–2070), and 2095 (the average of years 2090–2100). We used 11-year averages to reduce (but not eliminate) the uncertainty associated with low-frequency internal variability that can make it difficult to detect or quantify trends from anthropogenic forcing (Deser et al., 2012). Next, we spatially averaged these climate projections to the county-level. We then calculated climate anomalies as the difference between each of these future time periods and our baseline period for each county, separately for each CMIP5 model. For mean annual temperature, we calculated the absolute difference between our baseline and each future time period. For mean annual precipitation, we calculated the percent change between the baseline and each future time period. We created climate projections by adding the CMIP5 climate anomalies to our 2007 baseline PRISM data. We averaged the climate anomalies from the 30 CMIP5 simulations to create a multi-model mean climate projection that we added to our 2007 baseline PRISM

data; we used this multi-model mean to create our main projections of Valley fever endemicity.

To provide an estimate of the uncertainty in our multi-model mean, we calculated the standard deviation across the 30 CMIP5 simulations for each Valley fever statistic. As another measure of climate projection uncertainty, we report individual model projections of the number of counties endemic to Valley fever in 2095 for both RCP4.5 and RCP8.5 climate scenarios in Table A.1. We further used the individual CMIP5 simulations to quantify the level of agreement among models that each county will become endemic to Valley fever for both the RCP4.5 and RCP8.5 scenarios and report this uncertainty metric in map form.

Our climate projections show the highest warming in the north-central contiguous U.S. and relatively high levels of warming throughout the northern U.S. and Rocky Mountains (Figure 3.2a–c; Figure A.1). Mean annual temperatures are predicted to increase for the RCP8.5 climate scenario by 3.1°C to 6.0°C by the end of the 21st century. Mean annual precipitation is predicted to increase across the Pacific Northwest and in the eastern U.S., but decrease in the south-central and southwestern U.S. (Figure 3.2d–f; Figure A.2). Both the increase in temperature and changes in precipitation are larger for the RCP8.5 climate scenario than for the RCP4.5 climate scenario (Figure A.1; Figure A.2).

3.2.3 Climate niche modeling of current and future Valley fever endemic regions

We used the observed relationships between mean annual Valley fever incidence and both mean annual temperature and precipitation to map regions endemic to Valley fever. First, we selected a minimum level of mean annual Valley fever incidence (averaged from 2000–2015) to designate that a county was endemic by comparing our Valley fever

Figure 3.2. RCP8.5 climate projections indicate warming throughout the contiguous US with the highest levels occurring in northern states (a–c). Changes in precipitation will vary by region. RCP8.5 projections indicate drying in the southwestern US and south-central Great Plains and wetting across the Pacific Northwest and eastern US (d–f). The difference panels (c, f) are the difference between the 2095 and 2007 maps for each climate variable.

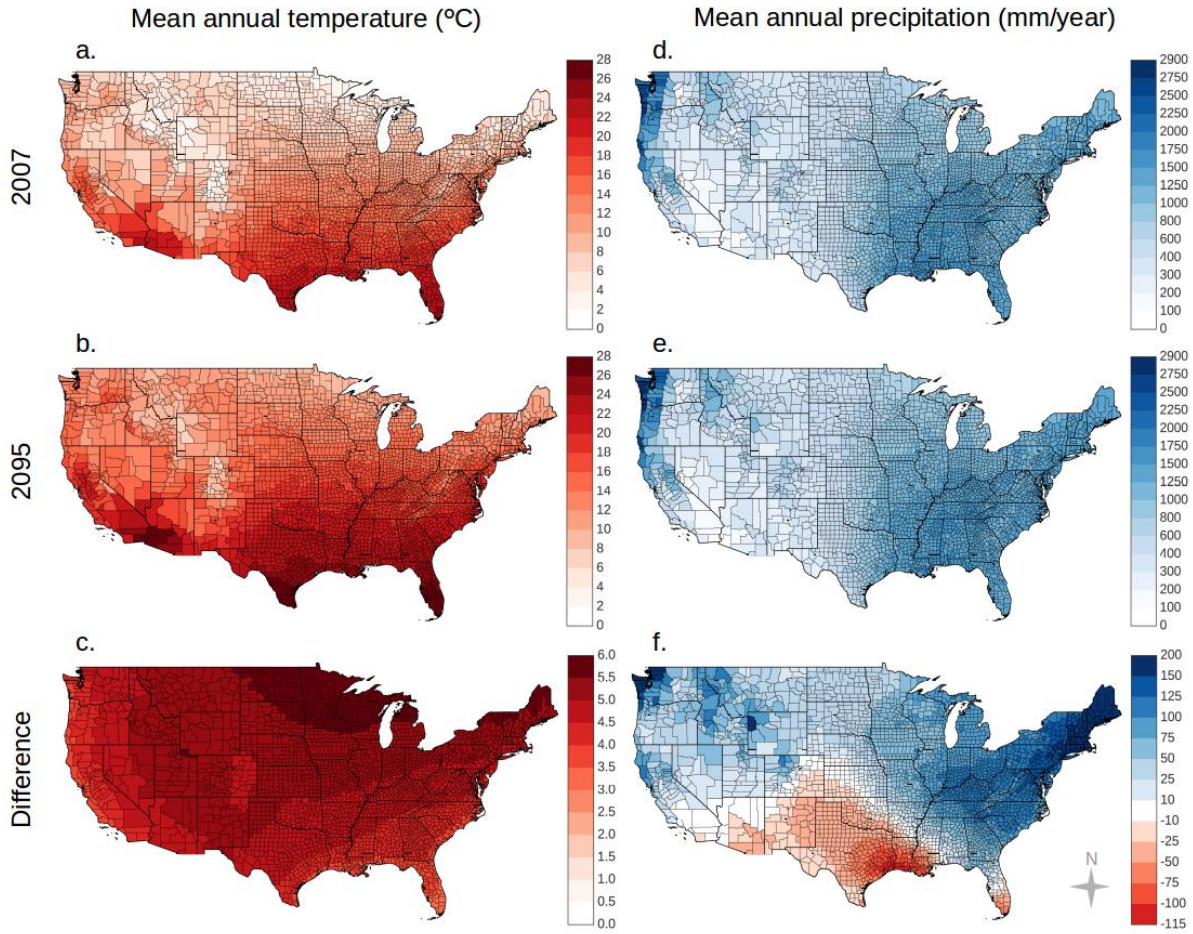

incidence data against the CDC endemicity map. We found there were large variations in the mean annual incidence between the three CDC definitions of endemicity: counties considered "highly" endemic by the CDC had mean annual Valley fever incidence between 21.3 and 158.4 cases per 100,000 population per year. Counties considered "established" endemic had between 0.7 and 94.5 cases per 100,000 population per year. Counties

considered “suspected” endemic had between 0.0 and 31.8 cases per 100,000 population per year.

Taking these large variations into account, we selected a conservative level of mean annual incidence to define a county as endemic, which we defined as meeting or exceeding 10 cases per 100,000 population per year. This definition included all the counties the CDC defined as “highly” endemic (5/5), over half the counties the CDC described as “established” endemic (16/28), and one county the CDC described as “suspected” endemic (1/44; San Luis Obispo, CA; mean annual incidence of 31.8 cases per 100,000 population).

Then, we examined the mean annual temperature and precipitation for the counties we defined as endemic. For temperature, all of the counties we defined as endemic have a mean annual temperature above 10.7°C (Figure 3.1). For precipitation, all of the counties we defined as endemic have mean annual precipitation less than 600 mm/yr. We used these two thresholds together to create a climate-constrained niche model which describe the climate necessary for Valley fever endemicity. Our niche model identifies a county as endemic if that county has both a mean annual temperature greater than of equal to 10.7°C and mean annual precipitation less than or equal to 600 mm/yr (Figure 3.1c).

We applied our climate-constrained niche model to the entire U.S. to estimate the areas which may currently be endemic to Valley fever. Then, we used our climate projections for both the RCP4.5 and RCP8.5 scenarios as input to estimate the areas that may become endemic to Valley fever in years 2035, 2065, and 2095.

We attempted different optimizations of our incidence and climate thresholds to improve the accuracy of our map in comparison to the CDC map. When we apply our climate-constrained niche model to the U.S., we acknowledge there may be differences

between the area we defined as endemic and the area the CDC defines as endemic since the basis for the CDC map is over 65 years old (Edwards & Palmer, 1957). Moreover, Valley fever incidence varies widely for counties within each of the three classes of endemicity defined by the CDC.

As a sensitivity analysis to complement our climate-constrained niche model, we ran the ecological niche model Maxent (R package 'dismo' version 1.1-4 and Maxent version 3.3.3k; Phillips et al., 2006). We trained our model by defining occurrence points as the counties that met our definition of endemicity (10 cases per 100,000 population per year; n = 23). All other counties were considered background points (n = 3085). We ran our models with default configurations, so all feature types were possible. We ran two scenarios with Maxent: one with the PRISM baseline mean annual temperature and mean annual precipitation as explanatory variables and a second with the PRISM mean January temperature, mean July temperature, and mean annual precipitation as explanatory variables. The output of Maxent is a relative environmental suitability measure, ranging from zero to one, where one describes an environment most similar to the training dataset. To identify a county-level endemicity threshold, we optimized the environmental suitability variable to attain the highest accuracy when compared to the CDC endemicity map (comprised of all three CDC endemicity classes; Table A.2). Counties at or above this suitability threshold were considered endemic. After this optimization, the two-variable Maxent model has an accuracy of 96.3% and the three-variable Maxent model has an accuracy of 96.8%. As described below, we compared the areas identified as endemic to Valley fever by our climate-constrained niche model to the more conservative predictions from the Maxent models as a sensitivity analysis and report the results in Table A.2.

3.2.4 Modeling of current and future mean annual Valley fever incidence

We estimated an upper bound of current and future Valley fever incidence for counties our climate-constrained niche model defined as endemic. To do so, we applied a multiple linear quantile regression using iterative reweighted least squares for the 90th percentile (Eq. 1) using the observed relationships between mean annual Valley fever incidence (VFI) and mean annual temperature (T) and precipitation (P) for the endemic counties (red and blue colored counties in Figure 3.1, n = 78).

$$VFI = \beta_1 T + \beta_2 P$$

$$VFI = (6.57)T + (-0.12)P$$

Our model had a pseudo r-square (not analogous to ordinary least squares r-square) value of 0.29 describing the local fit for our baseline period. We chose to report the 90th percentile estimate as an indicator of potential Valley fever incidence, recognizing there is a wide spread in the incidence among counties that met our climate-constrained niche model thresholds (Figure 3.1). Some of this spread may be caused by fine-scale variations in agriculture, dust storms, health care infrastructure, epidemiological reporting, and other natural and socioeconomical factors known to influence *Coccidioides* spp. abundance and disease incidence (Gorris et al., 2018; Louie et al., 1999; Tong et al., 2017; Williams et al., 1979). Following a similar approach to our endemicity analysis, we used the climate projections from CMIP5 to estimate future changes in potential Valley fever incidence.

3.2.5 Projections of human population

To isolate the effects that climate change alone may have on the number of people who contract Valley fever, in our main analysis we assumed an invariant human population in the U.S. However, U.S. population is projected to increase throughout the 21st century

(Hauer, 2019), which may expose more people to *Coccidioides* ssp. and lead to more Valley fever cases. To estimate the combined effect of both climate change and increasing population, we used future projections of human population from the Shared Socioeconomic Pathways (SSPs; Hauer, 2019) to calculate future population levels within the Valley fever endemic region. The county-level human population projections we used take into account age, sex, and race, and were specifically tailored for the U.S. (Hauer, 2019).

The SSPs describe how socioeconomic factors such as population, economic growth, and technological development evolve in the absence of climate change or climate policy (O'Neill et al., 2014). We used both SSP2, a scenario in which there is moderate population growth in the U.S. throughout the 21st century, and SSP5, a scenario in which there is large population growth (O'Neill et al., 2014). Our 2007 (mean of years 2000–2015) baseline U.S. population is 300 M (U.S. Census Bureau, 2011a; 2016). By 2095, SSP2 projects the total U.S. population to be 454 M and SSP5 projects it to be 690 M (Hauer, 2019). We examined each SSP population scenario in combination with the RCP4.5 and RCP8.5 climate scenarios.

3.3 Results

3.3.1 Estimating the current spatial extent of Valley fever endemicity

We used our climate-constrained niche model to map counties potentially endemic to Valley fever for the 2007 baseline period (mean of years 2000–2015; Figure 3.1a). Counties where mean annual temperature and mean annual precipitation are suitable for Valley fever endemicity are shown in magenta. Counties with suitable temperature but unsuitable precipitation are shown in red. Likewise, counties with suitable precipitation

but unsuitable temperature are shown in blue. Counties where both temperature and precipitation are unfavorable are shown in white. This analysis reveals that precipitation limits the area endemic to Valley fever to the north along the coast of the Pacific Northwest and to the east across eastern Texas, Oklahoma, and Kansas, whereas temperature limits the northern range of Valley fever endemicity in many interior western states.

Using our climate niche model, we estimate 217 counties may currently be endemic to Valley fever. These counties span 12 states–Arizona, California, Colorado, Idaho, Kansas, Nebraska, Nevada, New Mexico, Oklahoma, Texas, Utah, and Washington State. Using the 2007 baseline county population estimate, approximately 47.5 M people live within this endemic region (U.S. Census Bureau, 2016).

The niche model predicts a spatial pattern of endemicity that is broadly similar to the map produced by the CDC but with several notable differences (Figure 3.3b). Of the 170 counties identified by the CDC as endemic, the niche model classifies 110 counties as potentially endemic. Of the 60 counties not classified as endemic by our model but identified by the CDC, many are located in southwestern Utah, northwestern New Mexico, and southcentral Texas. Compared to the CDC map, our model also omits a few counties that previously experienced localized outbreaks of Valley fever. These outbreaks include cases contracted in Dinosaur National Monument and Duchesne County in Utah (Peterson et al., 2004), where *Coccidioides* spp. is thought to survive in isolated areas with high soil temperatures, and cases associated with archeological sites in northern California in Tehama and Butte Counties (Werner & Pappagianis, 1973; Werner et al., 1972).

Our niche model predicts 107 counties as endemic that the CDC model did not identify as endemic. The niche model predicts endemic areas extend farther north

Figure 3.3. Counties our climate-constrained niche model identify as endemic (with a mean annual temperature greater than or equal to 10.7°C and a mean annual precipitation level less than or equal to 600 mm/yr) are colored in magenta in panel a. There is reasonable agreement between this set of counties and the endemic region identified by the CDC shown in panel b. Counties shown in red in panel a have a mean annual temperature greater than or equal to 10.7°C but unsuitable mean annual precipitation (greater than 600 mm/yr). Counties shown in blue have a mean annual precipitation level less than or equal to 600 mm/yr but unsuitable mean annual temperature (less than 10.7°C). Counties in white our model defines as unsuitable according to both thresholds.

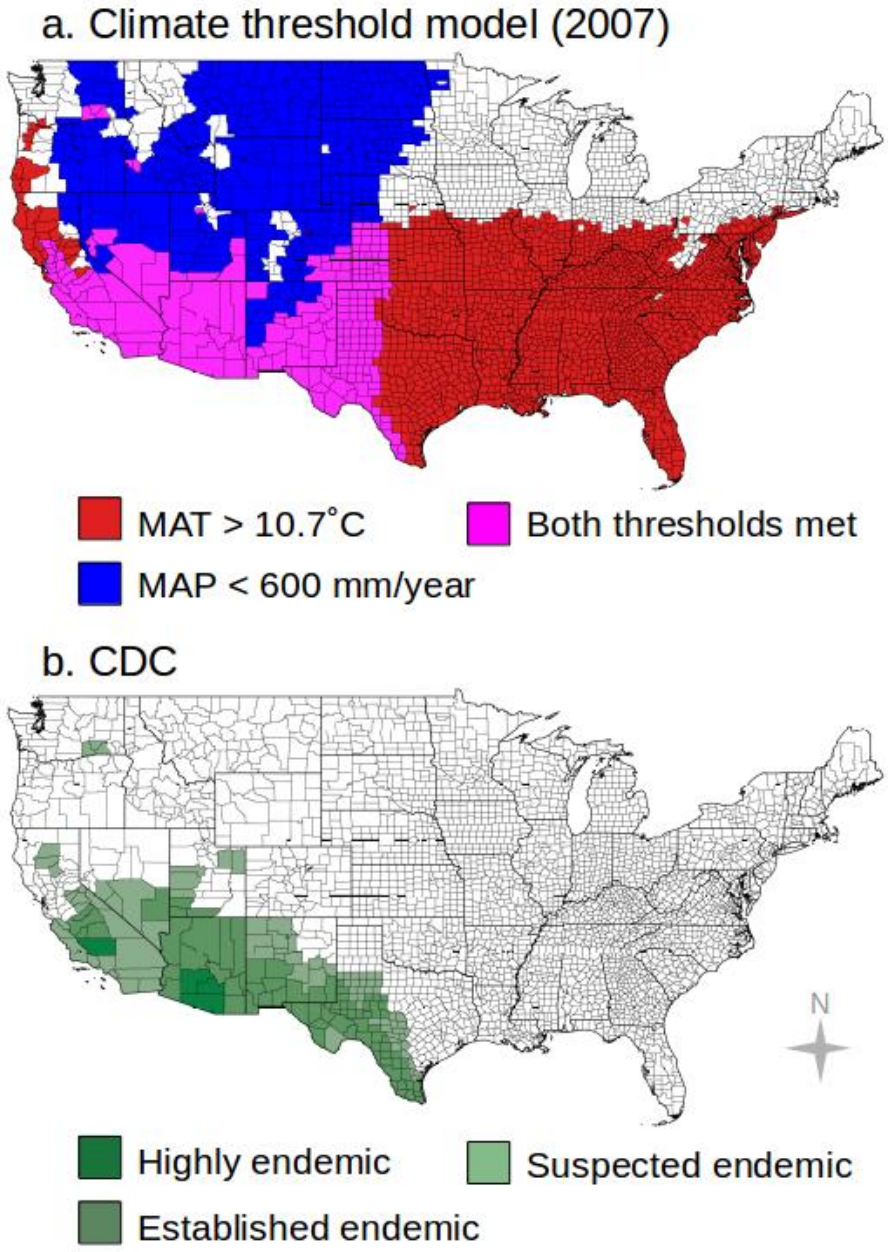

throughout the Great Plains and Central Valley of California. These areas include several states that are absent from the CDC map, including Colorado, Idaho, Kansas, Nebraska, and Oklahoma. The model identifies the two most populous counties in Idaho–Ada and Canyon County–as potentially endemic, including the city of Boise (U.S. Census Bureau, 2016).

One striking similarity between our model estimate and the CDC map is the identification of endemicity in three counties in southeastern Washington State, originally thought to be well outside the endemic region. These counties were recently added to the CDC map after an outbreak of Valley fever cases was reported in 2013 (Marsden-Haug et al., 2012). Since then, C. *immits* has been extracted from Washington State soils (Litvintseva et al., 2014).

Considering the CDC endemic map as truth, our model identifies 2831 counties in the U.S. as true negatives (TN; non-endemic), 110 counties as true positive (TP; endemic), 107 counties as false positives (FP), and 60 counties as false negatives (FN). This corresponds to a 94.6% accuracy rate ([TP+TN]/total) for predicting endemic counties in the U.S. (a 5.4% error rate) and a 64.7% recall rate (TP/[TP+FN]).

The Maxent ecological niche models that we ran as a sensitivity analysis produces similar, but more conservative patterns of contemporary endemicity when compared to our climate-constrained niche model. Both the two-variable and three-variable Maxent models have higher accuracy rates (96.3% and 96.8%, respectively; Table A.2). However, the two-variable Maxent model considerably underestimates the number of endemic counties compared to the CDC map, with a 37.6% recall rate; it yields more false negatives (106) and fewer true positives (64) when compared to the climate-constrained niche model. The relative contributions of the environmental variables in the two-variable

Maxent model are 80% for mean annual precipitation and 20% for mean annual temperature, highlighting the importance of precipitation in structuring contemporary areas of endemicity. The three-variable Maxent model performs better than the two-variable Maxent model, but again yields more false negatives (79) and fewer true positives (91) compared to the climate-constrained niche model. The relative contributions of variables in the three-variable model are 75% for mean annual precipitation, 25% for mean annual January temperature, and less than 0.1% for mean annual July temperature, which again demonstrates the importance of precipitation and suggests winter temperatures may be more important than summer temperatures in structuring the spatial pattern of endemicity.

Overall, our simple, two variable climate-constrained niche model provides a reasonable regional-scale depiction of the area endemic to Valley fever. Other factors such as soil characteristics and competition among microorganisms may further refine where *Coccidioides* spp. is present on finer spatial scales. Additionally, *Coccidioides* spp. may be able to adapt to different soil environments (Colson et al., 2017). Recognizing that many additional processes contribute to *Coccidioides* spp. abundance and disease dynamics at finer spatial scales, our model may enable preliminary exploration of climate change impacts on areas affected by Valley fever throughout the 21st century.

3.3.2 Estimating the future spatial extent of Valley fever endemic regions

We applied our climate-constrained niche model to identify counties that may become endemic to Valley fever in the future for the moderate (RCP4.5) and high (RCP8.5) climate warming scenarios. Over time, the area of climate-constrained endemicity is predicted to expand northward, most notably throughout the Great Plains and in the rain

Figure 3.4. For the RCP8.5 climate change scenario, areas where climate will permit Valley fever endemicity are shown for the years (a) 2035, (b) 2065, and (c) 2095. Areas where mean annual temperature will permit endemicity are shown in red, areas where mean annual precipitation will permit endemicity are shown in blue, and areas where both temperature and precipitation will permit endemicity are shown in magenta, following the color scheme used in Figure 3. The area endemic to Valley fever will extend farther north in future decades, especially in the rain shadows of the Sierra Nevada and Rocky Mountains Ranges. Precipitation will play a key role in determining which areas become endemic through time, as greater rainfall and moisture availability will limit the eastward extent of Valley fever as well as its presence in the Pacific Northwest and in western counties at higher elevations.

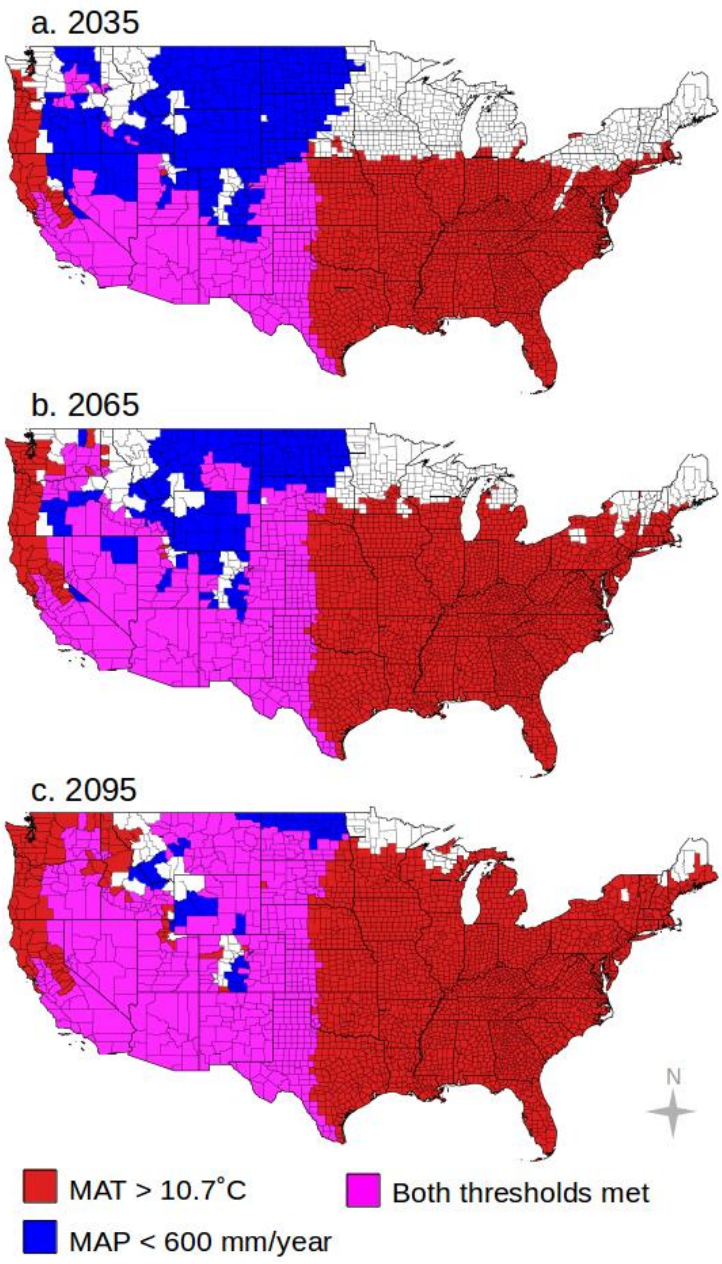

Figure 3.5. Time series of change in (a) the total area potentially endemic to Valley fever, (b) the number of endemic states, (c) the number of endemic counties, (d) the number of people living within endemic regions, and (e) the estimated number of annual cases from 2007 to 2095 for both RCP8.5 and RCP4.5 climate scenarios. The shaded areas are the standard deviation describing variation among the 30 CMIP5 Earth system models used in our analyses.

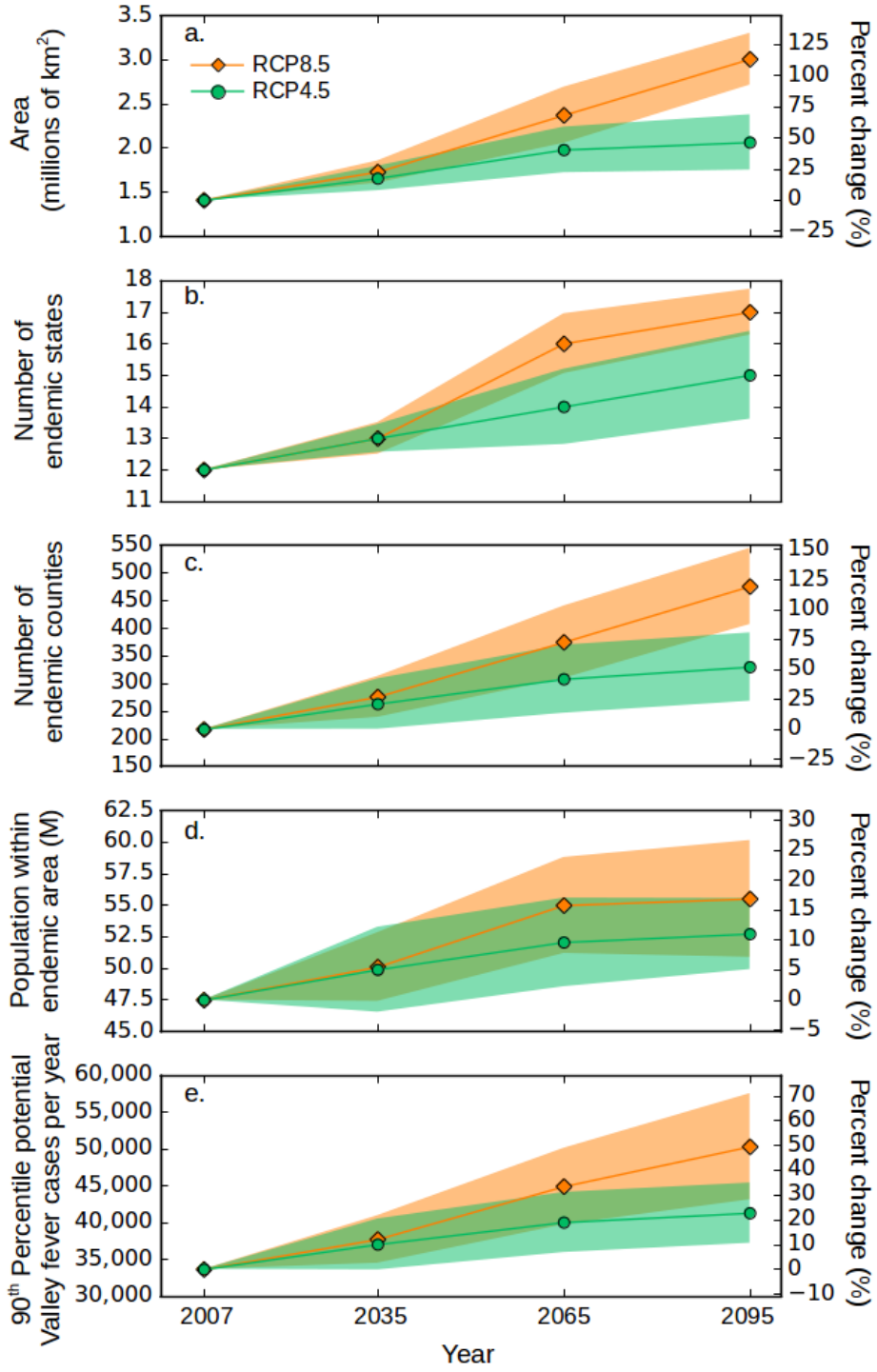

shadows of the Sierra Nevada and Rocky Mountain Ranges (Figure 3.4; Figure A.3). For the high climate warming scenario (RCP8.5), the model predicts by the end of the 21st century the area endemic to Valley fever will more than double (a 113% increase), the number of states with Valley fever endemicity will increase from 12 to 17, the number of counties with endemicity will increase from 217 to 476, and the number of people living within the endemic region will increase by 17% (Figure 3.5). The smaller relative change in human exposure compared to endemic area is caused by increases in endemicity in many western counties that have relatively low population (and follows our assumption here of an invariant population). For the moderate climate warming scenario (RCP4.5), the model predicts that by the end of the 21st century the expansion of Valley fever endemic area will be considerably smaller than for the RCP8.5 scenario, increasing by only about 46% (Figure A.3; Figure 3.5a). Other Valley fever disease metrics also change more slowly for RCP4.5 (Figure 3.5b-e). The contrast between the two scenarios highlights the importance of climate change mitigation as a means for limiting the health impacts of Valley fever, especially for more northern states (Table A.3).

By 2035 for RCP8.5, we predict the climate-constrained range of Valley fever will expand into northern Utah and eastern Colorado. By 2065, southern Idaho, Nebraska, southeastern Montana, and South Dakota will become endemic, and by 2095, Valley fever will enter North Dakota and move farther north in Montana. The Valley fever endemic region will expand northward in dry western states primarily as a consequence of warming that pushes mean annual temperatures above the temperature threshold required for disease establishment. From our baseline time period to 2095 for RCP8.5, 242 counties will become endemic to Valley fever because of warming above the temperature threshold, 20

counties will become endemic because of drying below the precipitation threshold, and 3 counties will become unsuitable for endemicity because of increases in precipitation.

Precipitation has a key role in determining whether a county becomes endemic in the future. By 2095 for RCP8.5, most of the western U.S. will have a climate that permits Valley fever endemicity, except for counties near the central and northern Pacific Coast and counties at higher elevations in mountain ranges. Northern California, western Oregon, and western Washington State will meet the mean annual temperature threshold yet will be shielded from becoming endemic because of high levels of precipitation. The eastward extent of the climate-constrained endemic range across the Great Plains is also limited for contemporary and future periods by precipitation, with a sustained north-south barrier occurring near the 100°W meridian. This axis corresponds to a zonal atmospheric water vapor gradient where dry, continental air from the southwestern U.S. meets moist, warm maritime air from the Gulf of Mexico, creating a sharp increase in moisture availability to the east (Lin, 2007).

We calculated the percent of the individual CMIP5 model simulations that are in agreement that each county will have a climate that permits Valley fever endemicity for the RCP4.5 and RCP8.5 scenarios. There is strong model agreement across the majority of the projected endemic region (Figure 3.6; Figure A.4). By 2095 for RCP8.5, some models predict Valley fever will be endemic farther east throughout the Central Plains, even into Minnesota. However, there is still a clear climate control on the eastern boundary of endemicity driven by the moisture gradient along the 100°W meridian. There is also strong agreement that several high elevation counties within the Rocky Mountains, as well as counties along the northern Pacific Coast, will remain outside the zone of endemicity.

Figure 3.6. There is strong model agreement throughout the majority of the area we estimate as endemic to Valley fever for the RCP8.5 climate scenario in years (a) 2035, (b) 2065, and (c) 2095. The model agreement shows a measure of uncertainty for the counties along the edge of the endemic area. Some models predict the endemic range in 2095 will expand into counties as far east as western Minnesota. Percent model agreement was calculated as the number of individual CMIP5 models that predict the county will have a climate that permits endemicity, divided by the total number of models (n = 30), as projected by the climate-constrained niche model.

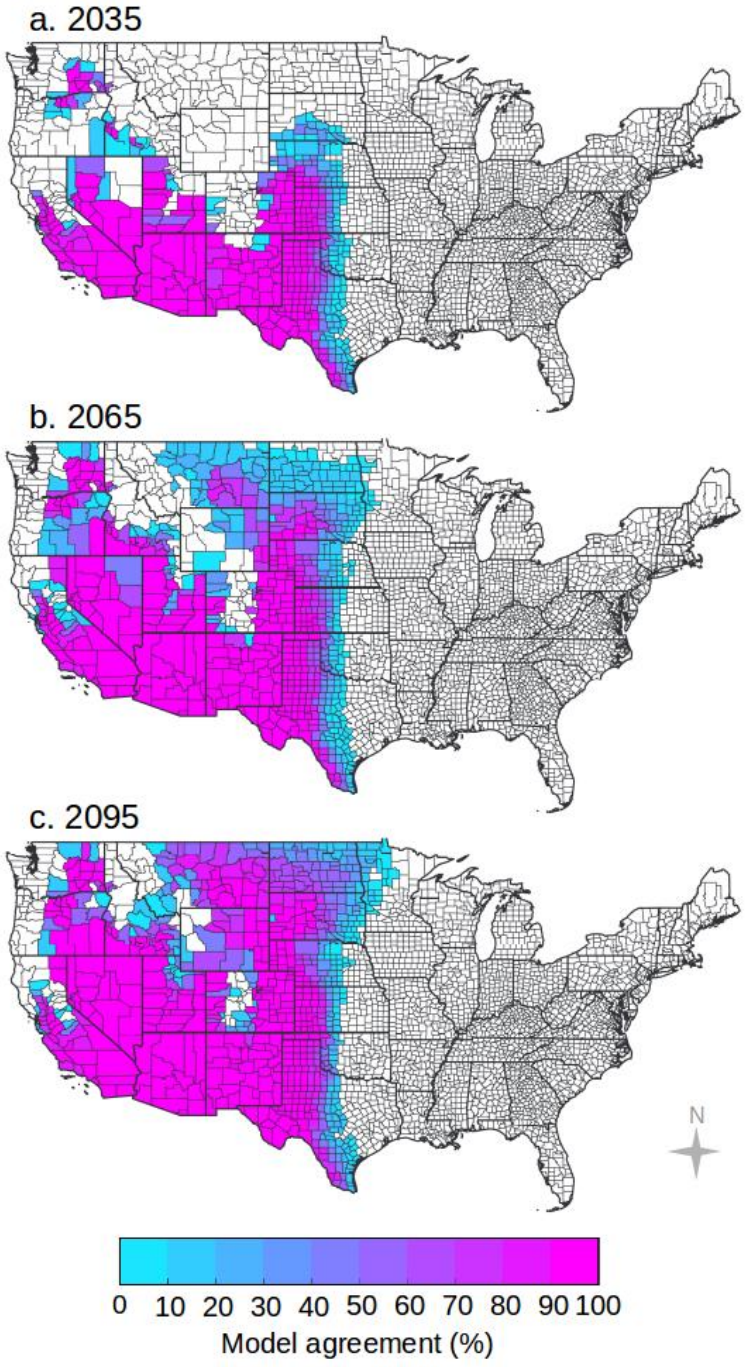

As a sensitivity analysis, we ran projections of our Maxent ecological niche models for RCP8.5. Both the two-variable and three-variable Maxent models also predict an expansion of areas endemic to Valley fever along the leeside of the Rocky Mountains and in the dry inland areas of the Pacific Northwest including southeastern Washington State. By 2095 for RCP8.5, the two-variable Maxent model identifies 15 states will have a climate that permits endemicity and the three-variable Maxent model identifies 14 states (Table A.2). We calculated the relative change in the population living within the Valley fever endemic area to compare across models, not considering changes in human population. Our climate-constrained threshold model predicts the population living within the Valley fever endemic area will increase by 6% in year 2035, by 16% in 2065, and by 17% in 2095. Similarly, the two-variable Maxent model predicts a 5% increase in 2035, a 12% increase in 2065, and an 18% increase by 2095. Projections using the three-variable Maxent model show similar changes and yield a 16% increase in the population living within the Valley fever endemic area by 2095. Although the Maxent models are more conservative in estimating the area endemic to Valley fever for the contemporary period, the projected pattern of Valley fever expansion is broadly consistent across all three models. The three-variable Maxent model that includes both January and July mean annual temperatures as explanatory variables allows us to better represent biological limits on the fitness of *Coccidioides* spp. to inhabit regions that experience exceptionally cold winters or hot summers. This more complex model still yields a pattern of future expansion that is similar to the simpler models that use mean annual climate variables.

3.3.3 Estimating current and future mean annual Valley fever incidence

We estimated an upper bound of Valley fever incidence by performing quantile regression on observed Valley fever incidence and mean annual temperature and precipitation (Figure 3.7). For our baseline period, our model predicts mean annual Valley fever incidence is likely to be greatest in the extreme southwestern U.S. and southwestern Texas (Figure 3.7). The model also predict high incidence in the Central Valley of California. For the baseline period, our model predicts up to 34,460 potential cases of Valley fever within Arizona, California, Nevada, New Mexico, and Utah, compared to approximately 9,500 observed cases per year (CDC, 2018a).

We then applied our quantile regression model to future climate projections for both RCP4.5 and RCP8.5. Our model predicts Valley fever potential incidence will increase over time throughout the extreme southwestern U.S., southern Great Plains, Central Valley of California, and the northwestern U.S. (Figure 3.7; Figure A.5). Using our baseline (invariant) human population estimates, we transformed incidence projections into the number of Valley fever cases (Figure 3.5e). The number of potential cases each year for RCP8.5 is projected to increase by 12% in the year 2035 and by 50% in the year 2095.

3.3.4 Compounding effects of climate change and human population projections on Valley fever

Increasing U.S. population will compound disease impacts caused by climate change. By 2095 for RCP8.5 assuming an invariant population, we estimate that the number of people living in the Valley fever endemic area will be 55.5 M (Table 3.1). When we account for both climate change and increasing population, this number increases by 32% (73.2 M) for the SSP2 population scenario and by 44% (80.1 M) for the SSP5 population scenario. In

Figure 3.7. We estimated an upper bound of future Valley fever incidence using a 90th percentile regression model for (a) our 2007 baseline period, (b) 2035, (c) 2065, and (d) 2095 for RCP8.5. Over time, our model predicts Valley fever incidence will increase throughout the extreme southwestern US and the southern Great Plains. Incidence will also increase throughout the Central Valley of California and in the northwestern US.

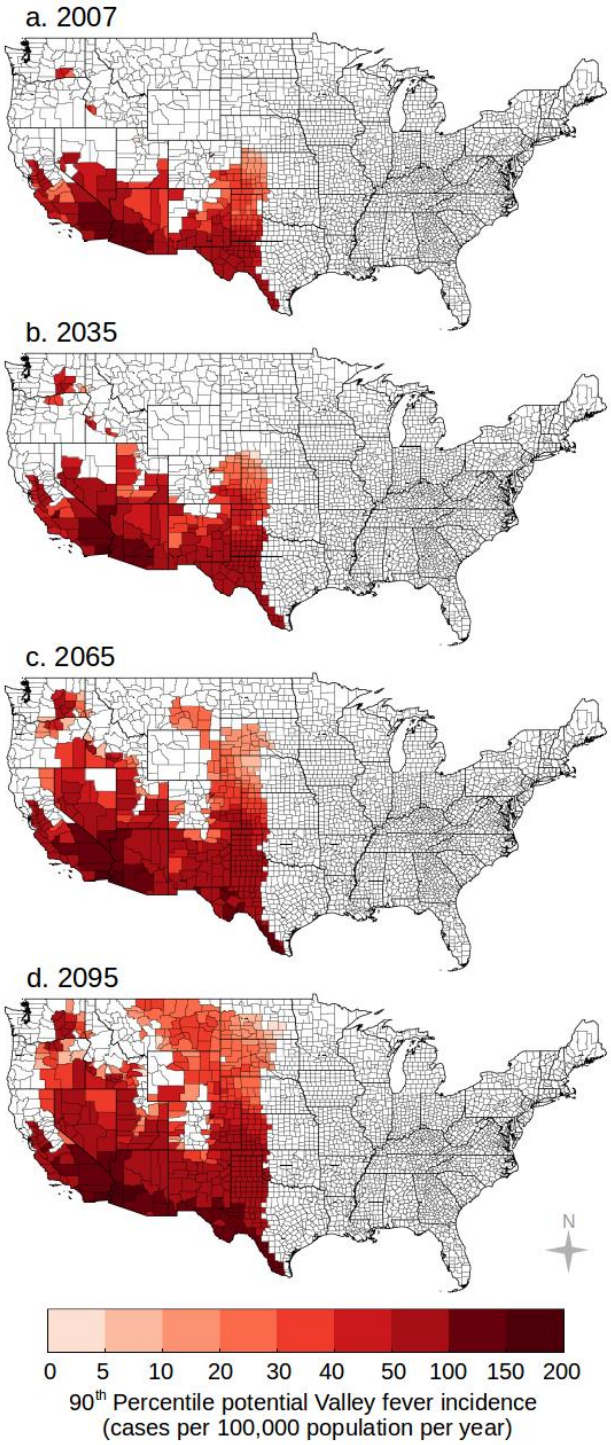

Table 3.1. Compounding effects of climate change and increasing human population on the number of people in millions living in the endemic region for Valley fever in the years 2035, 2065, and 2095, relative to our 2007 baseline population estimate of 47.5 M.

	RCP4.5 Climate			RCP8.5 Climate		
	2035	**2065**	**2095**	**2035**	**2065**	**2095**
No change in population (M)	49.9	52.1	52.7	50.1	55.0	55.5
SSP2 population scenario (M)	65.7	68.6	69.7	66.0	72.6	73.2
SSP5 population scenario (M)	71.9	75.0	76.2	72.2	79.4	80.1

concert, the number of potential Valley fever cases will increase by the same percent. The compounding effect between climate change and increasing population in the dry southwestern U.S. highlights the importance of developing more effective approaches for measuring and modeling geospatial patterns of *Coccidioides* spp. abundance and disease risk.

3.4 Discussion

3.4.1 Biogeography of Valley fever expansion

Our analysis identifies that a primary pathway for Valley fever expansion lies in the rain shadow of the Rocky Mountains. By the end of the 21st century, the climate-constrained area endemic to Valley fever will extend from the southern through the northern Great Plains. This is a predominant region for agriculture, which has a positive correlation with Valley fever incidence (Gorris et al., 2018). Further, climate projections indicate this region will experience an increased risk of drought (Cook et al., 2015). Together, intensifying drought and agriculture may increase the amount of dust loading

and thus human exposure to *Coccidioides* spp. It is notable in this context that the Valley fever expansion pathway predicted by our model is through areas affected by the 1930s Dust Bowl (Burnette & Stahle, 2013).

Not all states throughout the Great Plains are required to report Valley fever cases, which may limit our ability to monitor the potential spread of this disease. States in the Great Plains that do report have had minimal cases in recent years (CDC, 2019c). There is plausible evidence, however, that *Coccidioides* spp. inhabited this region before. Two buffalo that were radiocarbon dated to be 8500 years old, collected near Milburn, Custer County, Nebraska, showed signs of a fungal infection consistent with Valley fever; the buffalo may have migrated through endemic regions in the south before meeting their demise in Nebraska, or alternatively, the central Great Plains was an endemic region in the past (Morrow, 2006).

3.4.2 Increasing costs of Valley fever for human health

We expect the total number of Valley fever cases and subsequently total cost of disease will increase in concert with the expanding endemic area. Roughly 45% of people with Valley fever are hospitalized (Sondermeyer et al., 2013; Tsang et al., 2010). The estimated median total hospital charge per person in California from 2000–2011 was $55,000 (assuming 2011 USD; Sondermeyer et al., 2013). Based upon this hospitalization rate, the median total hospital charges (about $58,000 in 2015 USD), and the number of observed cases from 2000–2015 (149,286 cases), we estimate total hospitalization costs are abour $244 M per year (2015 USD) for our baseline period. Based on our predicted changes in the relative number of Valley fever cases (and assuming no change in human population) we estimate hospitalization costs due to climate change alone for the RCP8.5

scenario will rise to $274 M per year in 2035, $326 M per year in 2065, and $365 M per year in 2095 (2015 USD). These estimates do not include other costs associated with outpatient care and medications, missed days of work, or childcare (Colby & Ortman, 2014; Sondermeyer et al., 2013; Tsang et al., 2010), nor do they account for the compounding effects of future changes in U.S. population described above.

3.4.3 Improving future projections and sources of uncertainty

Our derived maps of Valley fever endemicity in 2035, 2065, and 2095 describe the disease range constrained solely by future climate. For these areas to become endemic, however, *Coccidioides* spp. needs to physically move into these new areas. This migration may be accomplished by the atmospheric transport of fungal spores in dust or by migration of infected animals, such as rodents (Taylor & Barker, 2019). To reduce uncertainties regarding rates of spread, more work is needed to systematically map the presence of *Coccidioides* spp. in both soils and atmospheric dust throughout the western U.S.

Our map of the area currently endemic to Valley fever may be helpful in the design of future sampling campaigns to gather occurrence data of *Coccidioides* spp. Once the presence of *Coccidioides* spp. in soils has been systematically mapped, we will be able to build a spatially explicit environmental niche model for *Coccidioides* ssp. directly from environmental surveillance data instead of epidemiological case reports (Miller, 2010; Peterson, 2006) and use this model to determine the response of the fungi to climate change (e.g., Escobar et al., 2016; Romero-Alvarez et al., 2017). As more positive occurrences of *Coccidioides* spp. in the soil are obtained, it will become increasingly critical to simultaneously measure soil properties such as alkalinity, pH, salinity, soil type, soil texture, along with the diversity and presence of other soil microbes to further refine the

environmental controls on fungal presence and abundance. High resolution occurrence maps could also help disentangle controls on disease incidence arising from different *Coccidioides* species (Baptista-Rosas et al., 2007; Colson et al., 2017; Lauer, 2017) as well as the impacts of heterogeneity in elevation and climate conditions within each county, especially for large counties throughout the western U.S. that span mountainous areas.

Concurrently, improved monitoring and reporting of Valley fever cases in states that currently have low or marginal disease incidence would allow for a more accurate delineation of contemporary climate controls. This is most critical for states where current climate conditions permit endemicity (Figure 3.3), yet the state is not currently reporting, including Colorado, Idaho, Kansas, Oklahoma, and Texas (CDC, 2018a). Proactive surveillance in states where climate does not currently permit endemicity but may in the future will help with monitoring disease spread.

Another factor that will likely modulate the number of Valley fever cases in the future is changes in the seasonal and interannual variability of precipitation. Precipitation in California is projected to shift to more intense periods of heavy and extreme rainfall, with moderate to small changes in the overall amount (Polade et al., 2017; Swain et al., 2018). These periods of greater moisture availability may increase fungal growth, while longer and more intense dry periods may enhance dust production and dispersal. In Arizona, summer rainfall brought by the North American monsoon is projected to weaken (Pascale et al., 2017), potentially leading to drier and dustier summers. It's also important to recognize that there is significant low frequency (decadal) internal variability in precipitation in the western U.S., driven for example by the Pacific Decadal Oscillation (PDO), that may seemingly dampen or amplify the effects of climate change (e.g., Lehner et

al., 2018). In our analysis, variability in precipitation causes some counties to switch back and forth over time in terms of their designation as endemic. For example, the estimated number of California counties endemic to Valley fever for RCP8.5 increases from 28 counties in 2035 to 31 counties in 2065, but then decreases to 30 counties in 2095 due to an increase in precipitation in San Francisco County, which was considered endemic in 2065. Evidence of precipitation variability can also be seen in the maps of precipitation change for RCP4.5 (Figure S2), where many areas that are drier in 2035 become wetter again in 2065, contrary to the stronger unidirectional pattern of change associated with anthropogenic forcing in RCP8.5.

We used a large set of CMIP5 model simulations to calculate the average projections of climate change for the U.S. Although some models perform better than others for the U.S. compared to historical observations, the multi-model mean tends to provide a reliable estimate of contemporary surface climate (Sheffield et al. 2013). With improved representation of ocean and atmospheric dynamics and higher spatial resolution, simulations contributed to the 6th Coupled Model Intercomparison Project (CMIP6; Eyring et al., 2016) will likely reduce uncertainties in future projections of temperature and precipitation for the U.S. (Stouffer et al., 2017). The higher quality climate information, along with improved downscaling techniques, will provide better boundary conditions for statistical and mechanistic models predicting changes in Valley fever endemic regions. However, uncertainty in climate projections is only one of the several different types of uncertainty limiting our ability to predict Valley fever endemicity.

Our model draws upon Valley fever incidence data, which implicitly links *Coccidioides* spp. presence with human cases of Valley fever. An important next step is the

development of a mechanistic model which separately simulates *Coccidioides* spp. abundance, transmission efficiency, and host heterogeneity as a function of different environmental and human demographic variables. As research on Valley fever and *Coccidioides* spp. continues, additional information such as the possible role of mammals in the fungal life cycle (Taylor & Barker, 2019; Barker, 2018), variations in ecological traits and ecosystems linked to different species of *Coccidioides* (Barker et al., 2012; Colson et al., 2017), and microbial competition (Lauer et al., 2019) will need further consideration for integration into both mechanistic and statistical models of disease incidence. This will be especially important if we learn different *Coccidioides* species have different virulence and tolerances for environmental controls, as this could affect the dispersal of disease and health impacts caused by climate change. As more occurrences of *Coccidioides* spp. in the soil are documented, adding any soil characteristics that limit the presence of the fungi into the model, such as alkalinity, salinity, soil type, and soil texture, may further refine the endemic area (Baptista-Rosas et al., 2007; Colson et al., 2017; Fisher et al., 2007; Maddy, 1957).

3.4.4 Coccidioidomycosis in a global context

Disease surveillance efforts throughout the U.S. and the comprehensive Valley fever case dataset provided the foundation for our study. However, Valley fever is not limited to the U.S. Our model, as well as the CDC endemicity model, depicts Valley fever endemicity spanning the U.S.-Mexico border. It is well known that *Coccidioides* spp. is present in Mexico; however, there has been minimal disease surveillance within the country (CDC, 2018b; Laniado-Laborin, 2007). Our future projections indicate the climate-constrained

endemic region may also extend north to the U.S.-Canada border by the end of the 21st century, potentially introducing *Coccidioides* spp. to a new country.

We found that the area endemic to Valley fever in the U.S., as well as the number of cases per year, will increase in response to climate change. Patterns of future change may be similar in other endemic areas within Central and South America. Apart from Mexico, countries that are likely endemic to Valley fever include Guatemala, Honduras, Argentina, Brazil, Paraguay, Bolivia, Venezuela, and Columbia (Colombo et al., 2011; Laniado-Laborin, 2007). International collaboration and Valley fever surveillance in these regions will help delineate the endemic boundaries, provide further information regarding the environmental factors structuring disease presence and incidence, and increase physician awareness (Cat et al., 2019).

3.4.5 Importance of integrating Valley fever into future climate change assessments

The U.S. Global Change Research Program recently suggested climate change may alter the spatial extent and number of Valley fever cases (Crimmins et al., 2016). Our study provides a first estimate to quantitatively describe this change. Furthermore, the Fourth National Climate Assessment report for the U.S. recognized the implications of drought on interannual variability of cases (Ebi et al., 2018). Although the area currently endemic to Valley fever is relatively smaller than other infectious diseases, like West Nile Virus (CDC, 2018c), we expect there may be similar or even larger negative health impacts from the exposure of new communities to Valley fever in response to climate change. In fact, recent mortality rates from Valley fever are similar, if not larger than those reported for West Nile virus. There are approximately 110 deaths per year from West Nile virus in the U.S. (mean 1999–2016; CDC, 2018c) compared to approximately 200 deaths per year from Valley

fever (mean 1990–2008; CDC, 2018a). Further, Valley fever cases have increased considerably since 2008, suggesting there may be additional negative impacts from this disease.

3.5 Conclusions

We combined a multi-state database of Valley fever incidence observations and climate projections to predict how climate change may influence the endemic area and number of Valley fever cases in the U.S. Using our climate-constrained niche model, we found the endemic area to Valley fever, as well as the number of cases per year, will increase in response to climate change. As temperatures increase and precipitation patterns change, most of the western U.S. will meet climate thresholds necessary for Valley fever endemicity. Through time, we found the endemic area will expand northward, most notably through the Great Plains. Expansion of the endemic area is suppressed farther east by regional increases in precipitation and the presence of moist air from the Gulf of Mexico. By 2095 for a high climate warming scenario (RCP8.5), our model predicts that 476 counties across 17 states may become endemic to Valley fever. This could result in up to 50% more annual Valley fever cases, before taking into account the compounding effect of future increases in human population. Estimating the regions that may become endemic to Valley fever can mitigate the health effects of this disease, as it will allow health care providers and citizens to prepare in advance. Our research is an example of the necessary bridge between climate science and human health as climate change reshapes areas endemic to infectious diseases.

Acknowledgements

M. E. Gorris is supported by a Department of Defense (DoD), National Defense Science & Engineering Graduate Fellowship (32 CFR 168a). K. K. Treseder acknowledges support from the U.S. NSF (EAR-1411942 and DEB-1457160) and the U.S. Department of Energy, Office of Science, Office of Biological and Environmental Research (BER), under Award Numbers DE-PS02-09ER09-25 and DE-SC001641. C. S. Zender gratefully acknowledges support from the Energy Exascale Earth System Model (E3SM) project, funded by the U.S. Department of Energy, Office of Science, Office of Biological and Environmental Research, from NASA's AIST, and from the Borrego Valley Endowment Fund. J. T. Randerson acknowledges support from the Gordon and Betty Moore Foundation (GBMF3269), NASA's SMAP, IDS, and CMS research programs, and the RUBISCO Scientific Focus Area that receives funding from the Regional and Global Modeling program within the Biological and Environmental Research division of DOE's Office of Science. We thank the Arizona Department of Health Services, the California Department of Public Health, the New Mexico Department of Health, the Nevada Department of Health and Human Services, and the Utah Department of Health for providing us with Valley fever case data from their respective state health agencies. Valley fever data may be obtained from the affiliated state health agencies. We acknowledge the World Climate Research Programme's Working Group on Coupled Modelling, which is responsible for CMIP, and we thank the climate modeling groups (listed in Table A.1. of this paper) for producing and making available their model output. For CMIP, the U.S. Department of Energy's Program for Climate Model Diagnosis and Intercomparison provides coordinating support and led development of software infrastructure in partnership with the Global Organization for Earth System Science Portals. The authors declare no competing financial interests.

Chapter 4

Climate controls on the spatial pattern of West Nile virus incidence in the United States

4.1 Introduction

West Nile virus (WNV; Flaviviridae: flavivirus) is the leading cause of mosquito-borne disease in humans in the United States (CDC, 2019b). West Nile virus is primarily transmitted between birds—the main viral host—and mosquitos—the viral vector. However, humans are accidental hosts that can contract WNV when bit by an infected mosquito. Approximately 20% of humans who are infected by WNV are symptomatic, with a small percent of cases developing into neuroinvasive disease (CDC, 2018d). West Nile virus was introduced to the U.S. in 1999 in New York (Kilpatrick, 2011). Each year after, WNV continued to spread further west until it was found throughout the conterminous U.S. in 2005. Although both the number of WNV cases and the spatial distribution of cases has varied considerably, over the past several years the total number of cases in the conterminous U.S. has stabilized at a level between 2,000 and 2,400 cases per year. Many of the cases occur in counties with large population centers in the U.S.; in contrast, WNV incidence has been particularly high in the northern Great Plains (Chuang & Wimberly, 2012; Peterson et al., 2013). Since each step of the WNV transmission cycle is sensitive to environmental conditions, climate may be structuring the spatial pattern of WNV incidence.

One important climate control on the WNV transmission cycle may be precipitation. Precipitation is an important control, regulating the distribution and permanence of landscape water bodies that bring mosquitos and birds into contact. The *Culex* genus of mosquitos, that frequently take blood meals from humans, is thought to be the most

important transmitter of WNV (Hamer et al., 2009; Kilpatrick et al., 2005; Turell et al., 2005). West Nile virus and *Culex* mosquitos are often found in temperate climate zones, while areas with higher moisture availability in maritime tropical climates favor more tropical mosquito species that are not as important for transmitting WNV (Ewing et al., 2016). Within the temperate climate zones, one species of mosquitoes that may be an exceptionally important transmitter of WNV is *Culex tarsalis* (Turell et al., 2005). *Cx. tarsalis* thrives in areas with irrigation (Lungstrom, 1954; Nielsen et al., 2008), which are prevalent in the agricultural regions throughout the Great Plains where levels of WNV incidence are relatively high. *Cx. tarsalis* is known to change its seasonal feeding preference between birds and other animals, including humans (Turnell et al., 2005). Therefore, this species could both amplify the presence of WNV in mosquitos by feeding on infected birds and be a primary transmitter of WNV to humans; this may be especially true if mosquitos, birds, and humans are all co-located around the limited water sources within irrigated rural areas.

In addition to precipitation, temperature may be another important climate control on the spatial structure of WNV incidence. Mosquitos have important physiological temperature limits that allow them to successfully overwinter and survive the summer heat (Rueda et al., 1990). Some of the temperature thresholds on *Culex* mosquitos have been well documented. *Cx. quinquefasciatus* generally lives in regions with summer temperatures between 24°C and 28°C and *Cx. pipiens* in regions with summer temperatures between 16°C and 24°C (Ciota et al., 2014; Dohm et al., 2002). *Cx. quinquefasciatus* survives well at temperatures around 20°C-30°C, but survival drops drastically below 15°C and above 34°C (Ciota et al., 2014). If temperatures become too warm, especially in the hot summer months, mosquito mortality may greatly increase (Ciota et al., 2014). Seasonal

temperatures also affect when birds migrate into a region, when they breed, and their habitat range (Dunn & Winkler, 1999; Marra et al., 2005). Specific bird species are thought to be important amplifiers of WNV transmission, especially the American robin (*Turdus migratorius*; hereafter "robins"; Hamer et al., 2009; Kilpatrick, 2011). The American crow (*Corvus brachyrhynchos*; hereafter "crows") may also play an important role in the WNV transmission cycle by supporting the overwintering of the virus as it is passed from crow to crow within overwintering roosts (Hinton et al., 2015; Montecino-Latorre et al., 2018). Hot weather during summer months, when mosquitos are generally more active, also may cause humans to limit the time they spend outdoors, thus limiting their exposure to mosquitos (Hedquist & Brazel, 2014).

Our goal was to explore what seasonal climate conditions constrain the spatial extent of WNV incidence across the U.S. Specifically, we aimed to answer: what climate conditions support the highest levels of WNV incidence? To do so, we compared two different methods for modeling present day mean annual WNV incidence: a machine learning algorithm and a Poisson regression model. We used county-level mean annual WNV incidence data to examine the statistical relationships between incidence and seasonal surface air temperature and seasonal precipitation. Then, we used seasonal climate variables as input for our two modeling approaches. The random forest model informed us where critical climate thresholds are for structuring the spatial pattern of West Nile virus incidence. We used important climate variables determined by our random forest model to develop a Poisson regression model to also describe the spatial pattern of WNV incidence. Both modeling approaches gave us an indication of the important climatic conditions that structure the spatial pattern of WNV incidence. In our discussion, we aimed

to answer: what biological mechanism related to the WNV transmission cycle do these important climate conditions likely describe? Our statistical models may provide a means to project changes in future WNV risk in response to climate change, since warming temperatures and changes in precipitation may shift the regions most affected by this disease.

4.2 Methods

4.2.1 West Nile virus data

We obtained human cases counts of WNV at the county-level by year for the conterminous U.S. from 1999-2017 from the U.S. Centers for Disease Control and Prevention (CDC). We converted case counts to WNV incidence (cases per 100,000 population) using annual county-level population estimates from the U.S. Census Bureau (U.S. Census Bureau, 2017; 2018). Since WNV was found throughout the conterminous U.S. in 2005, we limited our analyses of the contemporary spatial pattern of WNV cases and incidence to 2005-2017. In total, our WNV dataset included 31,465 disease cases, including both neuroinvasive and non-neuroinvasive cases. We performed our analysis at the county-level, which was the highest resolution available from the CDC for the de-identified, aggregated case data; the conterminous U.S. contains 3108 counties.

4.2.2 Climate data

We used monthly surface air temperature and precipitation from the Precipitation elevation Regressions on Independent Slopes Model, available as 4 km gridded products (Daly et al., 1994, 2008). To compare climate with our county-level WNV incidence data, we spatially averaged the native gridded climate data to the county-level using county shapefiles from the U.S. Census Bureau (https://www.census.gov/geo/maps-

data/data/tiger-line.html). We calculated three-month mean annual and mean seasonal climate variables from 2005-2017 for direct comparison to our WNV dataset (means of DJF, MAM, JJA, SON).

4.2.3 Random Forest model

We created a mean random forest model (R package "random forest") to explore which seasonal climate conditions are important in structuring the spatial pattern of WNV incidence in the U.S. We used mean seasonal temperature and precipitation as input to our model along with county-level mean annual WNV incidence observations. We created our mean random forest model by running 10 bootstrapped (with replacement) random forest models, each with 1,000 regression trees. We trained these random forest models using 70% of our county-level data (n=2175) and randomly selected 3 predictor variables as candidates at each split. To avoid overfitting, we used a node size of 4, so that each terminal node in our regression trees (i.e., leaves) described at least 4 counties. We averaged the county-level estimations of WNV incidence from the 10 bootstrapped random forest models to report our final estimation of county-level mean annual WNV incidence.

We tested the performance of each of the 10 bootstrapped random forest models by calculating the mean square error using 30% of our county-level data (n=933) as our testing dataset. The in-sample correlation coefficients for the 10 models range between 0.92 and 0.93, with an average of 0.93. The out of sample correlation coefficients for the 10 models range between 0.50 and 0.62, with an average of 0.58. The root mean square errors for the 10 random forest models range between 3.2 and 4.1 cases per 100,000 population per year, with an average of 3.7 cases per 100,000 population per year. The R^2 for our mean random forest model, calculated between the observed county-level mean annual

WNV incidence and our approximated mean annual WNV incidence was 0.86. We measured the importance of each climate variable in the model by calculating the decrease in modeled mean square error from randomly permuting each predictor variable.

To understand important splitting points for each of the seasonal climate predictors, we ran an additional regression tree using the predicted WNV incidence from our mean random forest model as our input training data (R package "rpart"). This created a summary tree similar in performance to the mean random forest model (RMSE = 2.1 cases per 100,000 population per year; $R^2 = 0.75$). This tree allowed us to explore the important climate thresholds that structured areas of higher and lower WNV incidence. This technique of creating a summary tree to look inside the "black box" of the random forest model was adopted from Faivre et al. 2016.

4.2.4 Poisson regression model

As an additional test of the importance of our explanatory climate variables, we used the top four important climate drivers from the random forest model to create a Poisson regression model of mean annual WNV. To directly compare the model coefficients across explanatory variables, we scaled each climate driver to fall within 0 and 1 using the minimum and maximum data values for each driver variable ($[x_i - x_{MIN}] / [x_{MAX} - x_{MIN}]$). Since we derived WNV incidence from count data, we assumed the WNV incidence data had a Poisson distribution and was over dispersed (mean = 2.2 cases per 100,000 population per year; variance = 32.5 cases per 100,000 population per year). To transform our non-integer incidence data into count-like data for input to our Poisson-distributed model, we multiplied our incidence data by 100 to convert it from cases per 100,000 population per year to cases per 10,000,000 population per year and rounded to the nearest integer (i.e.,

0.98 cases per 100,000 population per year became 98 cases per 10,000,000 population per year). We divided our model output by 100 to report our final model output of WNV incidence in cases per 100,000 population per year.

Informed by our mean random forest model, the input for our Poisson regression model included winter precipitation, winter temperature, and summer temperature. The psuedo-R^2 value for our model (calculated from residual and null deviance values) was 0.42. Adding the next important predictor to the model, SON precipitation, only raised the psuedo-R^2 value by 0.13 to 0.55.

4.3 Results

4.3.1 The mean spatial pattern and magnitude of West Nile virus in the U.S.

Despite interannual variability in the location and number of WNV cases (Figure 4.1a), the maps of mean annual WNV cases (Figure 4.1b) and mean annual WNV incidence (Figure 4.1c) show distinct spatial patterns. The highest number of mean annual WNV cases occur in counties with large cities. The 10 counties with the highest mean annual number of cases from 2005-2017 include Los Angeles (CA), Phoenix (AZ), Chicago (IL), Dallas (TX), Orange County, CA, Fort Worth (TX), Houston (TX), Riverside (CA), Bakersfield (CA), and Fort Collins (CO); together, this set accounts for 22% of the mean annual number of cases during this period. Apart from Chicago, IL and Detroit, MI, it is more challenging to identify large population centers by levels of WNV cases on the eastern half of the U.S.

Normalizing by population, the incidence map reveals a distinct v-shaped pattern of elevated WNV incidence throughout the Great Plains of the U.S. The high incidence region spans several northern states on the Canadian border (Montana, North Dakota, and

Figure 4.1. Total number of cases and mean spatial pattern of West Nile virus (WNV) in the US during 2005-2017, including (a) a time series of WNV cases for the conterminous US derived from data compiled by the CDC for the sum of neuroinvasive and non-neuroinvasive cases, (b) a county-level map of the number of mean annual WNV cases averaged from 2005-2017, and (c) a county-level map of mean annual incidence derived from the case data shown in panel (b) and annual, county-level US Census population estimates.

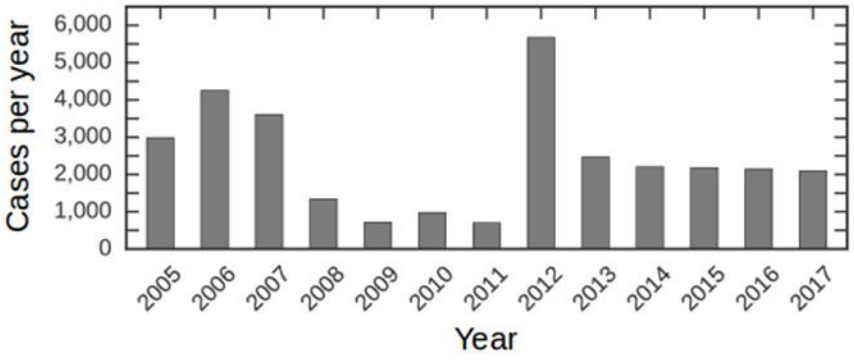

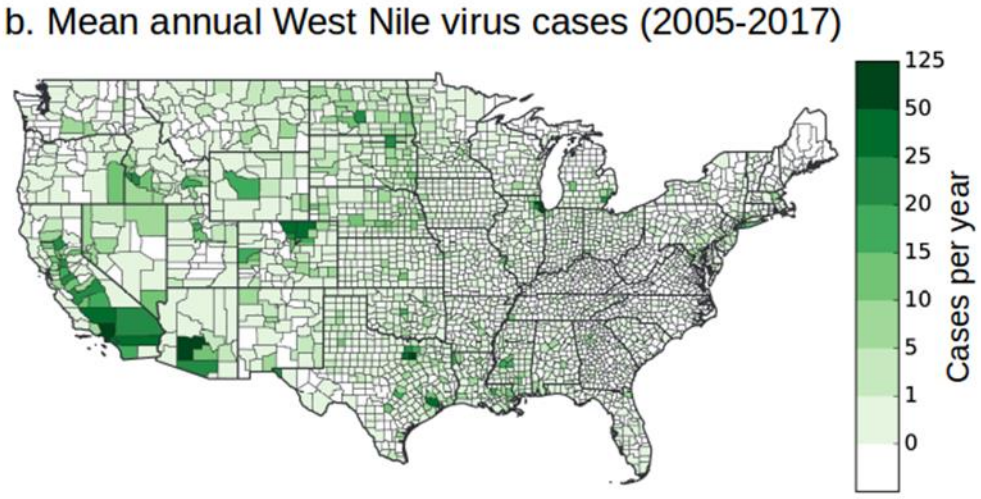

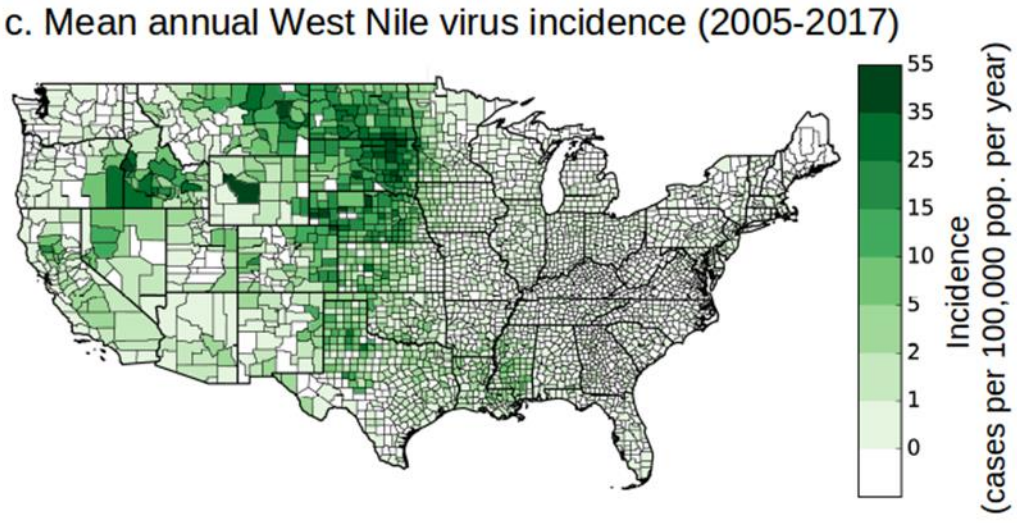

western Minnesota) and narrows to the south through Wyoming, South Dakota, Nebraska, Colorado, western Kansas, western Oklahoma, northeastern New Mexico, and northwestern Texas. There is also a hotspot of elevated WNV incidence in southern Idaho and along the Oregon-Idaho border on the southern Columbia Plateau. WNV incidence is low in the eastern U.S., except for a pocket of moderate incidence throughout Louisiana, southeastern Arkansas, and Mississippi in the southern Mississippi River Valley. In subsequent analysis, our goal is to identify the climate drivers that help explain the v-shaped zone of elevated incidence, and more generally, the full spatial pattern of incidence shown in Figure 4.1.

4.3.2 Statistical relationships between seasonal climate and levels of West Nile virus incidence

By comparing county-level mean annual WNV incidence with seasonal precipitation and temperature variables, we found that areas with dry and cold winters support higher levels of incidence (Figures 4.2 and 4.3). From visual inspection, an important threshold occurs for winter (DJF) precipitation at a level of about 30 mm/month (Figure 4.2a). 675 counties have a precipitation level below this threshold, yet this set of counties has a mean annual incidence of 7.9 ± 9.6 cases per 100,000 population per year. In contrast, the 2,433 counties above this threshold have a mean annual incidence of 0.7 ± 2.2 cases per 100,000 population per year. This factor of 11 difference in incidence for these two sets is highly significant when evaluated using a student's T test. Low precipitation during other seasonal periods is also associated with higher incidence, but with less well-defined breakpoints.

Similarly, counties that have winter temperatures below 0°C have higher levels of WNV incidence, approximately 4.0 ± 8.0 cases per 100,000 population per year (Figure

Figure 4.2. Incidence and histograms of the county number as a function of precipitation. Four seasonal intervals are shown: a) winter (DJF), (b) spring (MAM), (c) summer (JJA), and (d) fall (SON). In each histogram, the number of counties was aggregated in 10 mm/month precipitation bins. Mean annual incidence and mean monthly precipitation variables during 2005-2017 were used to create the plots.

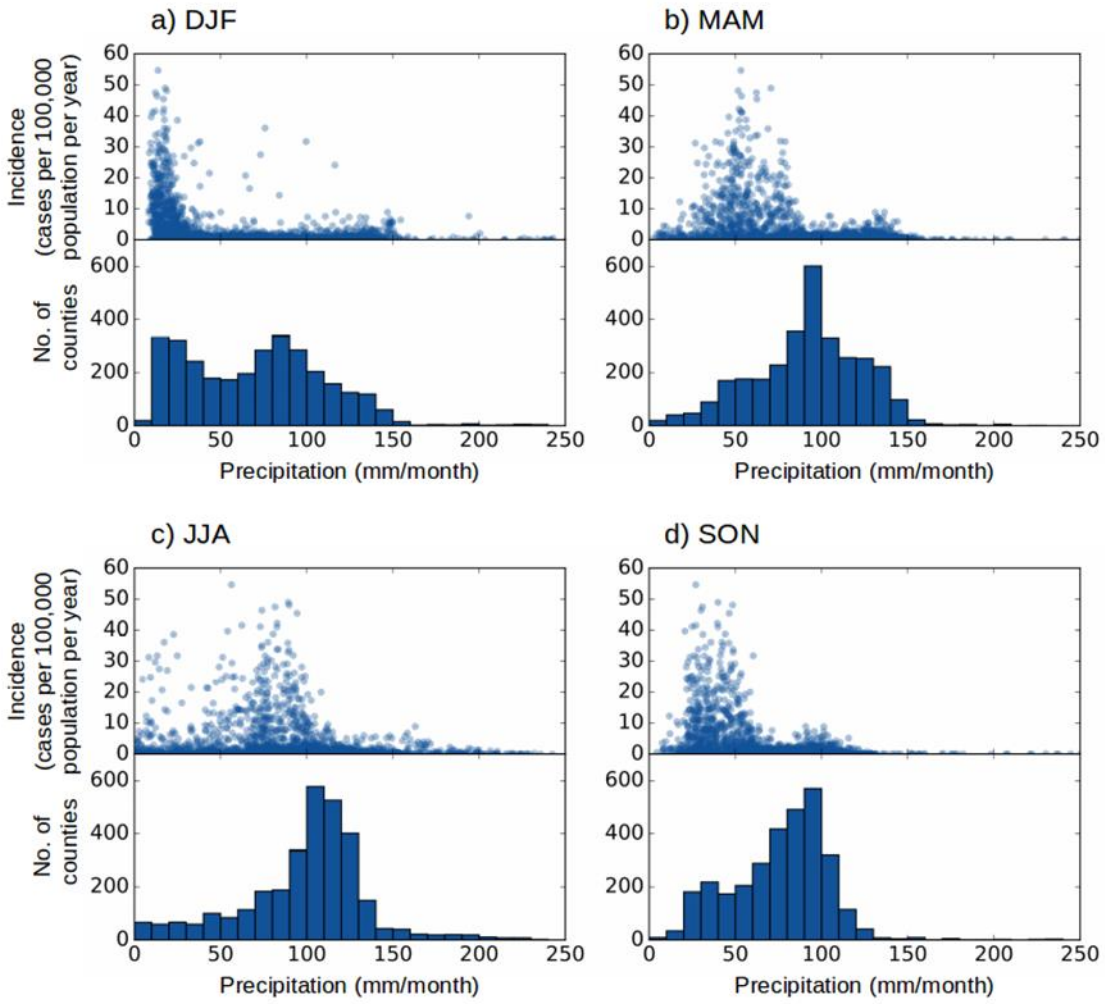

Figure 4.3. Incidence and histograms of county number as a function of air temperature. Four seasonal intervals are shown: a) winter (DJF), (b) spring (MAM), (c) summer (JJA), and (d) fall (SON). In each histogram, the number of counties was aggregated in 2°C temperature bins. Mean annual incidence and mean surface air temperature during 2005-2017 were used to create these plots.

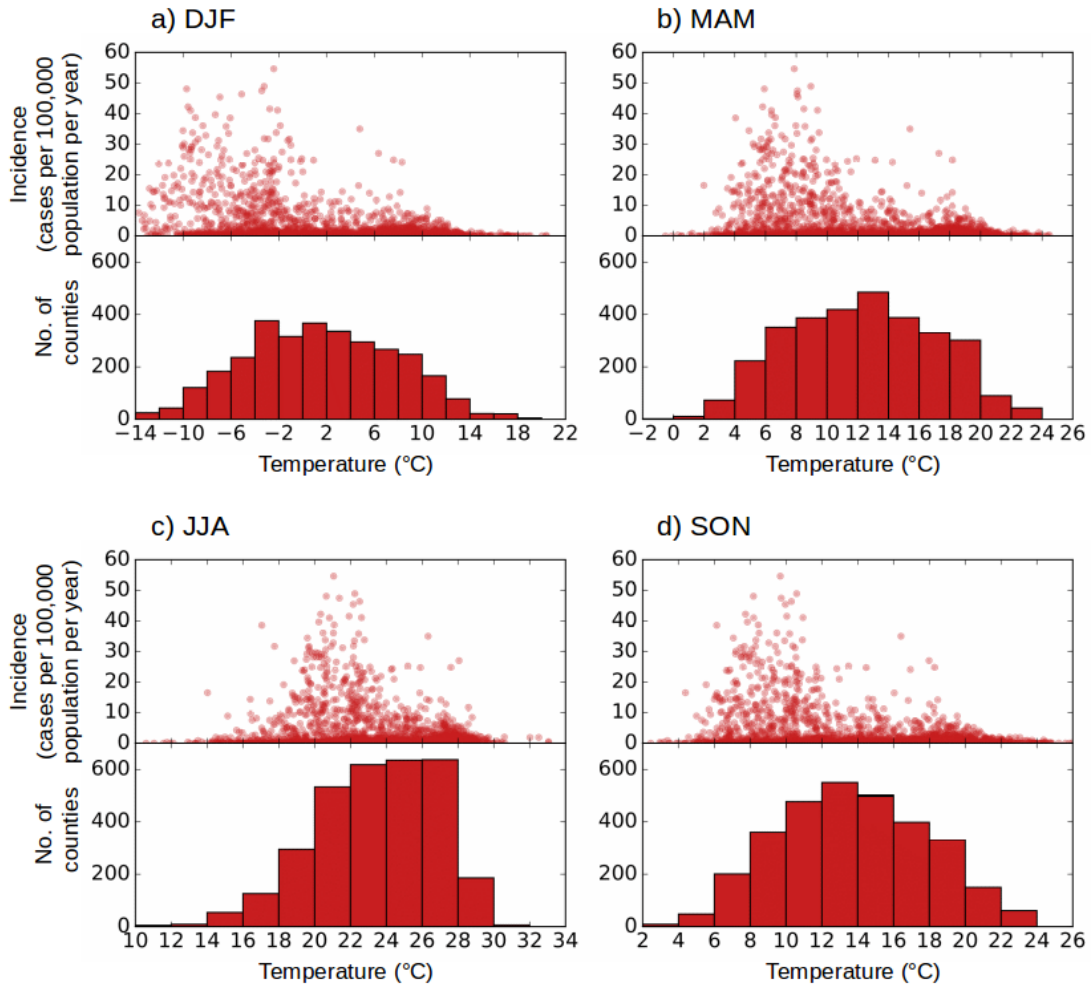

4.3a). In contrast, counties with winter temperature above 0°C have lower incidence (0.9 ± 2.3 cases per 100,000 population per year). Cooler temperatures during other seasonal intervals also favor higher levels of WNV incidence (Figure 4.3b,d). West Nile virus incidence was relatively low in counties that have summer temperatures above 24°C (Figure 4.3c), which may reflect the physiological temperature limits on the WNV transmission cycle.

To further explore the relationship between seasonal climate drivers and mean annual WNV incidence, we calculated the county-level univariate linear correlation between each seasonal climate driver and mean annual WNV incidence (Table 4.1). Among all seasonal climate drivers, fall precipitation has the strongest negative correlation with WNV incidence. Counties with lower fall precipitation have higher WNV incidence. Moderately strong negative relationship between precipitation and WNV incidence also occur during winter and spring. Among the seasonal temperature variables, winter temperature has the strongest negative relationship with WNV incidence, but with a magnitude much lower than the fall, winter, and spring precipitation variables. The fractions of variance explained by these single variables provide a baseline for evaluating the success of more complex models described below.

When building and interpreting our models of WNV incidence, it is also important to consider the collinearity among the different climate drivers. The spatial structure of temperature is correlated highly among all the different seasons (Figure 4.4; 0.80-0.99), whereas seasonal precipitation exhibits relatively higher levels of correlation among fall, winter, and spring seasons (0.75-0.82) but not between summer and other seasons (0.23-0.51). Across temperature and precipitation variables, correlations were considerably

Table 4.1. The county-level univariate correlation coefficient of each seasonal climate variable on the spatial pattern of West Nile virus in the U.S. using linear regression. All values are significant at $p < 0.000$.

	Explanatory variables			
	Precipitation		**Temperature**	
Season	Pearson r	R^2	Pearson r	R^2
DJF	-0.36	0.13	-0.28	0.08
MAM	-0.35	0.12	-0.23	0.05
JJA	-0.24	0.06	-0.13	0.02
SON	-0.42	0.17	-0.25	0.06

Figure 4.4. A spatial correlation matrix between the 8 seasonal climate variables across all counties in the conterminous U.S. The matrix displays the Pearson correlation coefficient between each pair of predictor variables. Each predictor variable consisted of a vector with 3108 elements, with each element representing the mean of climate for a single county.

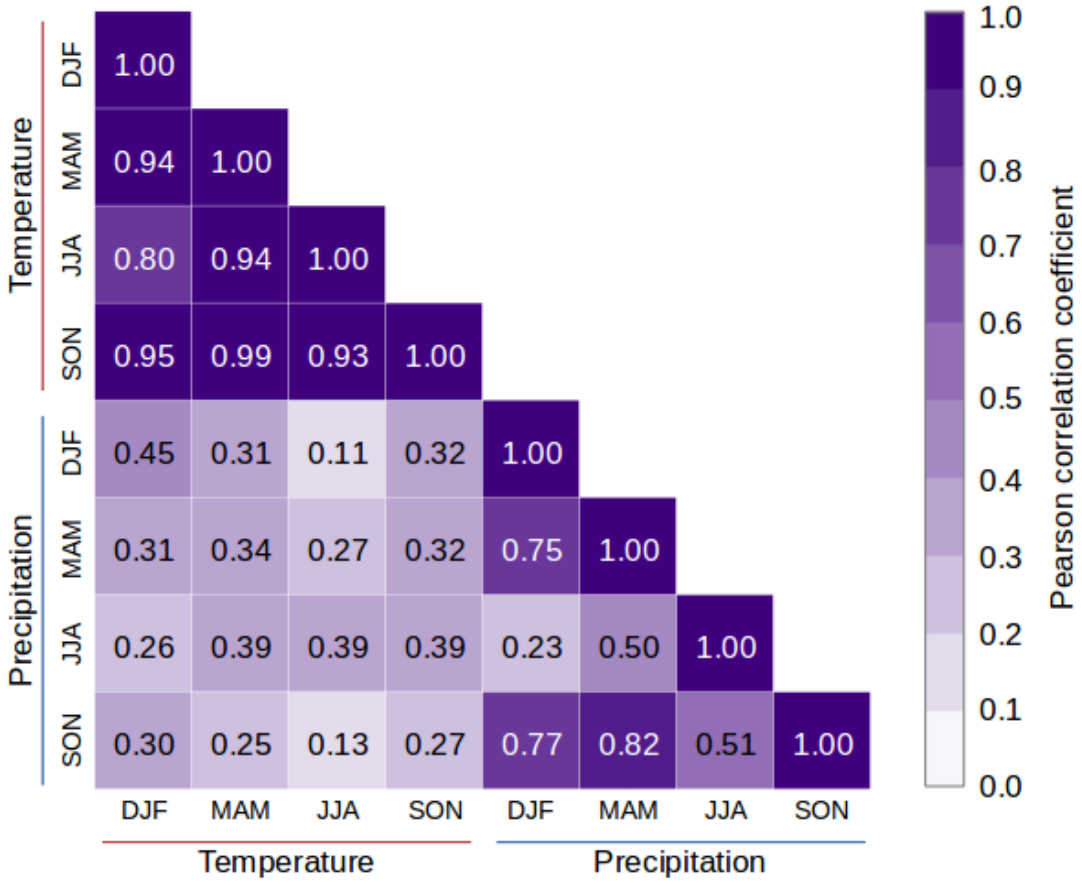

lower (0.11-0.45) with the largest positive correlation occurring between precipitation and temperature during winter.

4.3.3 A random forest model of the mean spatial structure of West Nile virus incidence

We created a mean random forest model to predict the spatial structure of WNV incidence and explore relationships between the seasonal climate drivers and WNV incidence. Our summary regression tree indicates winter precipitation, fall precipitation, winter temperature, and summer temperature were the four most important conditional splits to determine the county-level WNV incidence (Table 4.2). Counties that have dry and cold winters, mild summer temperatures, and dry falls are assigned the highest level of WNV incidence. Counties with lower levels of WNV incidence had wetter winter and fall seasons.

Our mean random forest model successfully captures the v-shaped area of increased WNV incidence throughout the Great Plains (Figure 4.5). The model also produces a smooth pattern of WNV incidence between counties, even though there is county-level heterogeneity in the observed mean annual incidence data (Figure 4.1c). This smoothed map may be a better estimate of WNV risk, since the county-level heterogeneity is likely driven by factors not related to climate, such as the availability of county-level healthcare services and variability in the accuracy of reporting. Our mean random forest model also captures the hotspot of WNV incidence along the Idaho-Oregon border on the southern Columbia Plateau, but underestimates the levels of WNV incidence there compared to observations (Figure 4.5b). Overall, our model had a slight high incidence bias throughout

Table 4.2. The county-level conditional climate splits identified by the summary regression tree created from the mean random forest predictions. Precipitation has units of mm/month and air temperature has units of °C.

Split 1	Split 2	Split 3	Split 4	Split 5	WNV Incidence	# of Counties
DJF P ≥ 21.9					0.95	2691
	SON P ≥ 60.4				0.47 *	2280
	SON P < 60.4				3.61 *	411
DJF P < 21.9					10.71	417
	DJF T ≥ -1.9				4.69 *	157
	DJF T < -1.9				14.34	260
		JJA T < 19.6			7.44 *	66
		JJA T ≥ 19.6			16.69	194
			DJF T ≥ -6.0		14.46 *	110
			DJF T < -6.0		19.60	84
				SON P ≥ 52.3	10.31 *	13
				SON P < 52.3	21.30 *	71

** indicates the split was a final node (i.e., leaf)*

Figure 4.5. A map of mean annual WNV incidence (cases per 100,000 population per year) predicted by the mean random forest model, where each county is the average of output across the 10 random forest models (a) and the county-level model bias compared with CDC observations (b).

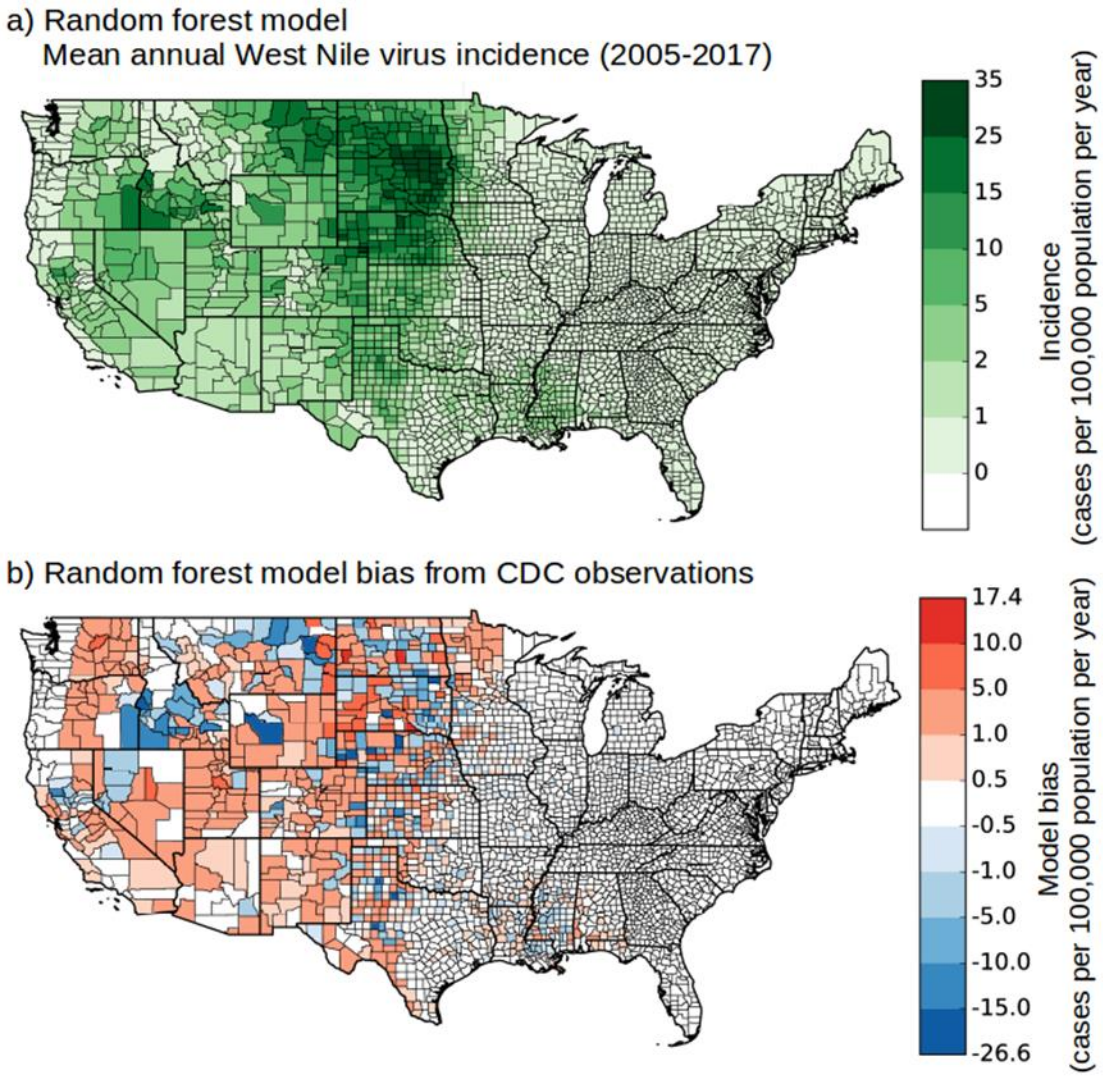

the western U.S., but underestimates the incidence in the highest incidence counties, including those in the central Great Plains.

We mapped the conditional breaks for each of the four important seasonal climate predictors to compare the spatial structure of the conditional breaks in the mean random forest model to mean annual WNV incidence (Figure 4.6). The conditional split for winter precipitation produces a similar v-shaped area throughout the Great Plains as mean annual WNV incidence (Figure 4.6a). The conditional pattern of fall precipitation is an important factor for limiting WNV incidence levels in the eastern U.S. The winter and summer temperature conditional breaks are staggered latitudinally compared to the precipitation breaks, which may suggest that temperatures constrain the latitudinal differences in WNV magnitude. For example, the highest levels of WNV incidence are in the northern Great Plains, which have relatively cooler winter and summer temperatures.

We calculated the importance measure of each seasonal climate predictor across the 10 bootstrapped random forest models by measuring the percent increase in mean square error that resulted from randomly permuting each variable (Table 4.3). Identical to our summary tree output, winter temperature, summer temperature, winter precipitation, and fall precipitation were the most important variables for structuring the spatial pattern of WNV incidence.

4.3.4 A Poisson regression model of the mean spatial structure of West Nile virus incidence

We used the important seasonal climate predictors identified by our random forest model to create a Poisson regression model of the spatial structure of mean annual WNV

Figure 4.6. The conditional breaks in the summary regression tree for the four most important predictor variables: (a) winter (DJF) precipitation, (b) winter (DJF) temperature, (c) fall (SON) precipitation, and (d) summer (JJA) temperature. The left side of the colorbar indicates the seasonal climate conditional break, while the right side of the colorbar indicates the average county-level WNV incidence value for each split, identified by the summary regression tree created from the mean random forest predictions.

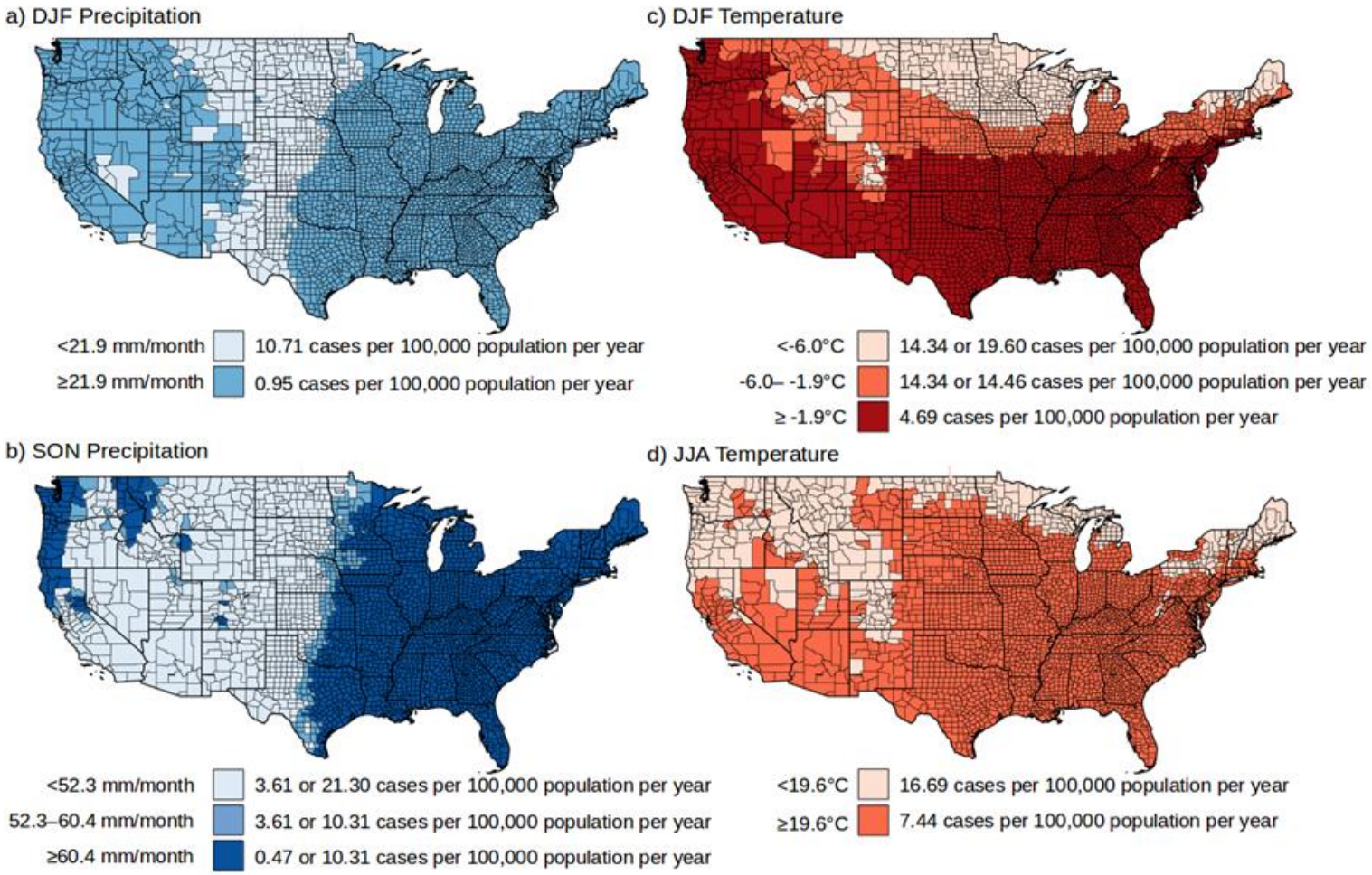

Table 4.3. The importance measure of each seasonal climate variable averaged across the 10 bootstrapped random forest models reported as the decrease in MSE, as well as the standard deviation and range of the decrease in MSE across the 10 models, and the Poisson regression model coefficient for three of the most important predictor variables.

Explanatory variable		Decrease in MSE	Standard Deviation	Range	Poisson regression coefficient
DJF	Precipitation	20.3 *	1.9	17.5–23.0	-13.1
MAM	Precipitation	7.8	1.1	6.0–9.5	
JJA	Precipitation	8.3	1.5	6.0–11.4	
SON	Precipitation	15.5	1.7	12.9–17.9	
DJF	Temperature	11.7 *	0.6	11.1–12.9	-2.3
MAM	Temperature	6.2	0.8	5.2–8.0	
JJA	Temperature	9.8 *	0.6	8.9–10.5	1.3
SON	Temperature	7.3	0.6	6.3–8.2	

*Note: * indicates the variable was included in the Poisson regression model.*

incidence. This model will allow us to understand how each seasonal climate variable affects WNV incidence when taken together.

We incorporated three of the top predictor variables from the random forest model as input to our Poisson model, including winter temperature, summer temperature, and winter precipitation. Our Poisson model suggests counties with dry and cold winters and warmer summers have the highest levels of WNV incidence (Table 4.3). The largest model coefficient is applied to winter precipitation, followed by winter temperature.

Our Poisson model broadly captures the v-shaped area of higher WNV incidence throughout the Great Plains (Figure 4.7a). It successfully predicts low levels of incidence along the northwest Pacific coast and eastern U.S. However, this model with fewer degrees of freedom compared to the random forest model, overestimates levels of WNV incidence throughout much of the western U.S. and Midwest and underestimates the areas of

Figure 4.7. A map of the annual WNV incidence (cases per 100,000 population per year) predicted from our Poisson regression model (a) and the county-level model bias compared to CDC observations (b).

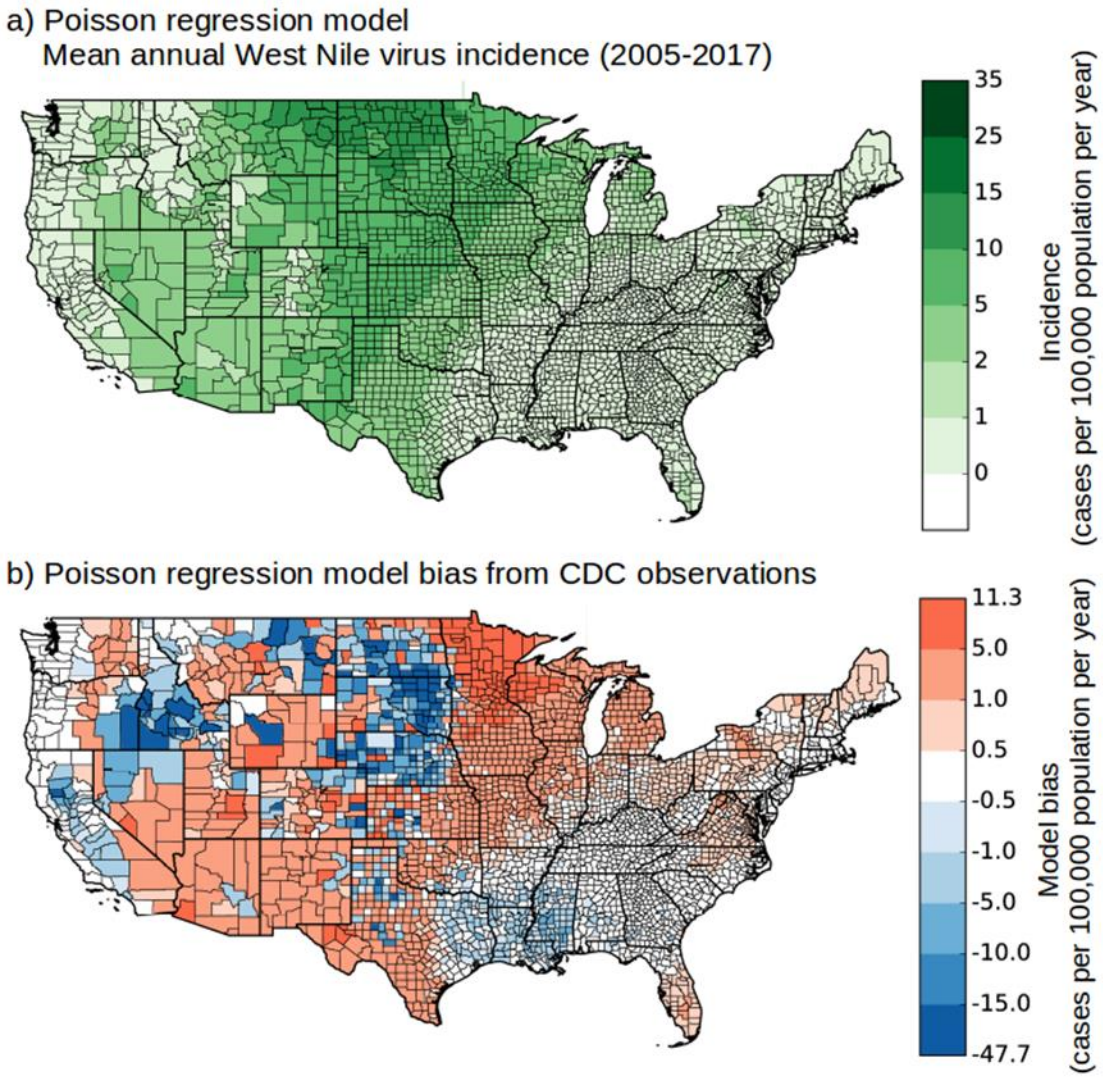

increased WNV incidence, including in the northern Great Plains (Figure 4.7b). The model considerably overpredicts WNV incidence throughout the southwestern U.S. and does not capture the pockets of increased incidence in the southern Columbia Plateau and southern Mississippi River Valley.

4.4 Discussion

4.4.1 The influence of climate on the spatial pattern of West Nile virus incidence

Climate conditions are likely structuring both the mean spatial extent of WNV incidence and the interannual variability in the number and location of disease cases across the conterminous U.S. Our study is the first to use climate conditions to constrain the mean spatial extent and level of WNV incidence, in comparison to previous studies that have mainly focused on the interannual relationships between climate and WNV at county or regional levels. Our models suggest winter precipitation, winter temperature, and summer temperature are the most important seasonal climate predictors of the spatial pattern of county-level mean annual WNV incidence. A threshold in winter precipitation was critical for shaping the v-shaped structure of higher WNV incidence. Counties that had winter precipitation below 21.9 mm/month fell within this v-shape and on average had incidence levels over 11 times higher than counties that were wetter. Cold winter temperatures were important for constraining the areas containing the highest incidence levels. Among the counties that had dry winters below 21.9 mm/month, counties that had winter temperatures below -1.9°C on average had incidence levels of 14.3 cases per 100,000 population per year compared to counties with warmer winters with average incidence levels 3 times lower (4.7 cases per 100,000 population per year). Collectively, these variables constrain the v-shaped pattern of higher WNV incidence throughout the Great

Plains, in both the random forest model and Poisson model. Using these three seasonal climate conditions together may provide a means to predict the future spatial extent of WNV risk in response to climate change. However, sub-regional patterns of WNV incidence are likely structured by a series of environmental variables, including vegetation type (Brownstein et al., 2002; Ezenwa et al., 2007; Gibbs et al., 2006; Ruiz et al., 2004), land use (Bowden et al., 2011), and hydrology (Shaman et al., 2010).

4.4.2 Spatial controls on West Nile virus incidence compared to interannual controls

Previous work examining the interannual variability in WNV cases also found temperature and precipitation to be important drivers of WNV cases. However, the relationships between these variables and WNV incidence was fundamentally different. From year to year, warmer winters and springs led to an increase in WNV cases throughout the U.S. (Hahn et al., 2015; Manore et al., 2014; Wimberly et al., 2014). This may allow more mosquitos to overwinter and begin an earlier breeding season in spring. The large number of U.S. West Nile virus cases in 2012 in the southern Great Plains followed an anomalously warm spring and moderate summer, possibly allowing an earlier breeding season but not reaching the mosquitos physiological temperature limits in summer (Hahn et al., 2015). Although our models suggest that regions with colder winter temperatures support higher mean levels of WNV incidence, areas that have anomalously warmer winters may lead to above average levels of WNV cases.

The role of precipitation on interannual WNV levels varies spatially (DeGroote et al., 2008; Landesman et al., 2007; Shaman et al., 2010; Wang et al., 2010; Wimberly et al. 2014). Generally, lower levels of precipitation cause places that are already dry (e.g., western U.S.) to have lower levels of WNV incidence, and places that are typically wet (e.g.,

eastern U.S.) to have higher WNV incidence (Hahn et al., 2015; Landesman et al., 2007). Our spatial model found that areas with dry and cold winters and mild summers supported higher levels of WNV incidence, however interannual climate variability is likely to modulate this pattern through a different set of biological mechanisms.

We used climate conditions to model the spatial extent of WNV, which allowed us to broadly estimate fine-scale processes that influence the structure of WNV incidence. We explored what aspect of the WNV transmission cycle may support higher WNV incidence levels under dry and cold winters, examining the role of birds, humans, and mosquitos.

4.4.3 The spatial pattern of West Nile virus incidence in relation to birds

Birds play an important role in the transmission of WNV by acting as viral reservoir host. For this reason, the presence of birds is known to module the rate of WNV transmission (Bergsman et al., 2016; Ezenwa et al., 2005; Kilpatrick et al., 2006). One of the most important bird species to the spread of WNV, considered the key reservoir host, is robins (Kilpatrick et al., 2006). Even in ecosystems where robins aren't abundant, they can account for most mosquito feedings (Kilpatrick et al., 2006). Unlike other species, robin population levels aren't affected by WNV (George et al., 2015), but removing robins from a community does decrease WNV transmission (Kilpatrick et al., 2006). Robins are ubiquitously present throughout the conterminous U.S. and are present year-round in the Great Plains (Fink et al., 2018). There is a relatively high abundance of robins in the Great Plains compared to other parts of the U.S. during the non-breeding season (DJF), pre-breeding migration (FMAM), and post-breeding migration (SOND; Fink et al., 2018). The large quantity of robins that migrate through this area may play a role in WNV transmission cycle, since there are more potential viral hosts. However, robins don't seem

to be the key determinant of the spatial pattern of increased WNV incidence, since they are also present outside of the areas of highest WNV incidence.

Another important bird species for WNV transmission is the crow. Although crow population levels have suffered from WNV (LaDeau et al., 2011; Yaremych et al., 2004), crows may be relatively unimportant for the amplification of WNV (Kilpatrick et al., 2006) since they make up a very small percent of mosquito feedings (Molaei et al., 2006). However, crows are still a highly competent host for WNV (McLean et al., 2001) and new findings suggest they may play an important role in overwintering the virus (Montecino-Latorre et al., 2018). Crows live in large winter roosts and may allow WNV to persist throughout winter by continually spreading the disease from bird to bird (Hinton et al., 2015; Montecino-Latorre et al., 2018). Crows are also present year-round in the Great Plains (Fink et al. 2018), so the presence of WNV in the crow populations may accelerate bird to mosquito transmission in spring when mosquitos emerge (Montecino-Latorre et al., 2018). However, crows are also found throughout much of the eastern U.S., where there are lower levels of WNV incidence.

4.4.4 The spatial pattern of West Nile virus incidence in relation to humans

To study the relative levels of WNV in the U.S., we chose to create our model based on disease incidence rather than case counts. Because the highest levels of WNV incidence occur in generally lower populated areas, especially throughout the northern Great Plains, the abundance of humans does not appear to be a controlling or limiting factor of the spatial extent of WNV.

Because the ratio of mosquitos to humans may be important for WNV transmission, previous studies have incorporated population density as a predictor of WNV incidence.

However, these studies found mixed results where suburbs and rural areas were associated with both higher and lower levels of incidence (Gibbs et al., 2006; Ruiz et al., 2004, 2007; Schweitzer et al., 2006). Higher levels of human immunity in a population can reduce the number of WNV cases (Paull et al., 2017). This may be an important factor when predicting the interannual levels of WNV cases, but human immunity likely doesn't structure the spatial extent of the disease. Estimates of population seroprevalence in the U.S. is low (less than 14%), so most of the population is still susceptible to WNV (Murphy et al., 2005; Paull et al., 2017; Peterson et al., 2013). Socioeconomic status and population demographics may also influence the structure of WNV incidence (Brownstein et al., 2002; Harrigan et al., 2010; Hayes et al., 2005; Liu et al., 2009). At the county-level, differences in healthcare may cause some of the heterogeneity in case counts, especially if people need to travel to population centers to seek medical services.

Humans behavior and the amount of time spent outdoors is also affected by the weather and climate (Chen & Ng, 2012). People may choose to remain indoors during the hot and humid summer months, causing less human exposure to infected mosquitos (Hedquist & Brazel, 2014). The northern Great Plains is an area that has a lot of agriculture (U.S. Department of Agriculture, 2019), so people probably spend more time outdoors in this region. Agriculture and irrigated croplands may also provide additional water resources necessary for the mosquito-breeding lifecycle; one study found that county-level WNV incidence in the northern Great Plains increased with the amount of irrigated cropland (Wimberly et al., 2008). Although humans may not be the main component structuring the area of increased WNV incidence, they could inadvertently be supporting it.

4.4.5 The spatial pattern of West Nile virus incidence in relation to mosquitos

Mosquitos may be the main driver of the spatial extent of WNV. Although many species can carry WNV, some species are more easily infected, better at amplifying the virus, and more successful at transmitting the disease to a host than others (Goddard et al., 2002; Sardelis et al., 2001; Turell et al. 2000, 2001, 2003). WNV has been found throughout North America in 59 different mosquito species (Godsey et al., 2001; Hayes et al., 2005; Komar et al., 2003; Turell et al., 2005). *Cx. tarsalis* is likely the most important mosquito vector for WNV within the northern Great Plains since it's an effective vector and primarily breeds in rural habitats (Chuang et al., 2011; Turell et al., 2005; Wimberly et al., 2008). It is possible for this species to acquire WNV through vertical transmission and carry the virus through diapause into the following year (Nelms et al., 2013).

A spatial analysis of the 2003 WNV levels in the northern Great Plains found climatically-averaged temperature and precipitation best described the spatial pattern of disease (Wimberly et al., 2008). This study by Wimberly et al. (2008) hypothesized these climate conditions may be capturing the geographical extent of *Cx. tarsalis*. Wimberly et al. (2008) found average monthly precipitation between May and July at approximately 67 mm/month was optimal for WNV amplification and transmission in the northern Great Plains, when analyzing a region across North Dakota, South Dakota, Nebraska, eastern Montana, and Wyoming. Counties with higher or lower levels of precipitation were predicted to have lower levels of incidence. Our study across the conterminous U.S. broadly supports the idea of a precipitation optimum during spring and early summer. As shown in Figure 4.2b, there is a broad optimum of incidence between 40 and 100 mm/month of precipitation during spring. Although there were over 1,215 counties (~40% of all

counties) above 100 mm/month, incidence never exceeded 10 cases per 100,000 population per year.

East of the northern Great Plains, precipitation increases and *Aedes vexans* and *Culex pipiens* may assume the role of most important vector (DeGroot et al., 2008; Wimberly et al., 2008). This supports the success of *Cx. tarsalis* as a vector for WNV under drier conditions. This positive relationship may describe the effects of temperature on the amplification of mosquitos as WNV vectors, potentially by influencing the mosquito incubation rate (Reisen et al., 2006).

The important seasonal climate drivers of the spatial structure of WNV incidence is likely describing the ecological niche of key mosquito species driving the transmission of WNV. The absence of these key mosquito species in other regions of the U.S. may explain the lower levels of WNV incidence, especially in the eastern U.S. where there is greater human populations and the presence of important bird species. Understanding that the presence of mosquitos is likely driving most of the spatial structure in disease incidence will be important for future predictive models of WNV in response to climate change.

4.4.6 The potential effects of climate change on West Nile virus incidence

Climate change may shift the spatial extent and magnitude of WNV incidence in the U.S. if warming temperatures and changes in precipitation change the environmental range of birds and mosquitos. Annual average air temperatures in the U.S. are projected to increase from 1.6°C-6.6°C by the end of the 21st century (Hayhoe et al., 2018). Warming temperatures may cause the mosquitos to inhabit locations farther north, especially if warmer winters ease the challenge for mosquitos to successfully overwinter. At the same time, warming in the south may cause temperatures to become too warm for the habitat of

key WNV mosquito species. Warming may also cause tropical mosquito species to migrate further north and compete with temperate mosquito species.

The temperature controls on mosquito habitats may cause the highest risk of WNV to travel northward from the U.S. into Canada. Enhanced surveillance of WNV risk along the U.S.-Canada border and collaboration between U.S. and Canadian health agencies may benefit risk analysis of WNV in this region. The Canadian Prairie Provinces (Manitoba, Saskatchewan, and Alberta) north of the northern Great Plains already report the highest levels of WNV incidence in Canada (Chen et al., 2013). One of the first projections of WNV risk in North America—mainly based upon temperatures in the warmest month, seasonal precipitation, and annual precipitation—found an increased risk of WNV in Canada throughout the 21st century (Harrigan et al., 2014). This is consistent with projections that the geographical range of *Culex* mosquitos in Canada will expand further north (Chen et al., 2013; Hangoh et al., 2012). However, little to no change in precipitation throughout the Great Plains coupled with warming temperatures (Hayhoe et al., 2018), especially in winter, may cause temperate mosquito populations such as *Cx. tarsalis* to migrate further north, thus reducing the total health burden from WNV across the U.S. Systematically mapping the presence of mosquitos species and their abundance in the U.S. and Canada is necessary for a better understanding of the important mosquito species for the transmission of WNV, their relation to the environment, and projections of disease spread.

4.5 Conclusions

We used both a random forest model and a statistical model to explore how seasonal temperatures and precipitation structure the spatial pattern of WNV incidence in the U.S. Our mean random forest model indicated regions in the U.S. with cold and dry

winters, mild summers, and dry falls support the highest levels of WNV incidence. Specifically, areas with winter precipitation below 21.9 mm/month and winter temperatures below -1.9°C had the highest levels of WNV incidence. Driven by winter temperature, summer temperatures, winter precipitation, and fall precipitation, both our random forest model and statistical model captured the v-shaped spatial structure of observed mean annual WNV incidence in the U.S., with the highest levels of WNV incidence in the northern Great Plains. Our spatial predictive model is most likely describing the ecological niche of important mosquito species for the transmission of WNV. Our models may be used to predict the response of WNV incidence to climate change, since shifts in precipitation and increasing temperatures may cause mosquitos to change their environmental range.

Acknowledgements

We thank Jennifer Lehman and the Arboviral Diseases Branch team at the National Center of Emerging Zoonotic Infectious Diseases of the U.S. Centers for Disease Control and Prevention for providing us with WNV case data. ME Gorris received support from a Department of Defense (DoD) National Defense Science and Engineering Graduate Fellowship (32 CFR 168a). JT Randerson is supported by the U.S. Department of Energy Office of Science Division Biological and Environmental Research through the RUBISCO project and by the Gordon and Betty Moore Foundation (GBMF3269).

Chapter 5

Conclusions

5.1 Summary of Results

The goal of my dissertation was to create frameworks for analyzing how climate change may affect the spatial distribution of two important environmental infectious diseases in the U.S. In order to estimate future projections of each disease, I first studied the relationships between each infectious disease and the environment. Then, I created models to describe the current geographical extent of each disease.

In Chapter 2, I examined the climate and environmental conditions that structure Valley fever disease dynamics across the southwestern U.S. To do so, I compiled the first multi-state dataset of Valley fever cases. The mean annual cycle of incidence varied throughout the southwestern U.S. and peaked following periods of low precipitation and soil moisture. From year-to-year, however, autumn incidence was higher following cooler, wetter, and productive springs in the San Joaquin Valley of California. In south-central Arizona, incidence increased significantly through time. By 2015, incidence in this region was more than double the rate in the San Joaquin Valley. I found that Valley fever incidence was greatest in areas that were concurrently hot and dry. These endemic areas could potentially be defined by climate thresholds.

In Chapter 3, I used these climate thresholds to estimate the area endemic to Valley fever using a climate niche model derived from the contemporary climate and disease incidence data. I created a climate-constrained niche model by defining counties as endemic if they have mean annual temperatures above 10.7°C and mean annual precipitation below 600 mm/year. I then used this model with projections of climate from

Earth system models to assess how endemic areas will change during the 21st century. By 2100 in a high warming scenario, our model predicts the area of climate-limited endemicity will more than double, the number of affected states will increase from 12 to 17, and the number of Valley fever cases will increase by 50%. The Valley fever endemic region will expand north into dry western states, including Idaho, Wyoming, Montana, Nebraska, South Dakota, and North Dakota. Precipitation will limit the disease from spreading into states farther east and along the central and northern Pacific coast. This was the first quantitative estimate of how climate change may influence Valley fever in the U.S.

In Chapter 4, I identified the seasonal climate variables that structure the spatial extent of West Nile virus incidence in humans across the conterminous U.S. I used present day mean annual West Nile virus incidence using county-level CDC case reports from 2005-2017, monthly-mean climate variables from PRISM, and random forest and multiple linear regression algorithms to create predictive models of West Nile virus incidence for the U.S. I found that dry winters coupled with cold winters led to the highest levels of West Nile virus incidence: counties with winter precipitation levels less than 22.5 mm/month and winter temperatures less than 1.9°C had incidence 13 times greater than counties that were wetter and warmer. I argue these cold and dry conditions are optimal for mosquitos to act as West Nile virus transmission vectors. The statistical models I created may be used to project changes in West Nile virus incidence in response to climate change.

My dissertation research provides the foundation for assessing how Valley fever and West Nile virus may be affected by climate change. Although it is debated whether or not climate change will cause a net increase in the overall burden of infectious disease, I found evidence that the health burden from Valley fever is likely to increase in response to

climate change. The basis of the disease prediction frameworks I developed could also be applied to other environmental infectious diseases in the U.S., like tick-borne diseases (e.g., Lyme Disease), or diseases endemic to other regions in the world, like dengue virus. Continued research modeling the future burden of environmental infectious diseases in the U.S. is critical for implementing effective disease surveillance and mitigation programs. These projections may ultimately alleviate the future burden of environmental infectious diseases caused by climate change.

5.2 Future research

5.2.1 Projections of West Nile virus incidence in response to climate change

The predictive models of West Nile virus incidence I developed in Chapter 4 provide a means for estimating future projections of West Nile virus in response to climate change. As a preliminary analysis, I used my random forest model and climate projections from 30 downscaled CMIP5 Earth system models (BCSD data) to estimate how the spatial structure of West Nile virus incidence will respond to climate change throughout the 21st century for RCP8.5, a high greenhouse gas emissions scenario. I found that as temperatures warm, especially in the winter months, the region of highest West Nile virus incidence will shift northwards into Canada (Figure 5.1). However, areas conducive to moderate levels of West Nile virus incidence will shift into regions with greater human populations, which may increase the overall number of disease cases by 60% by year 2100 for the RCP8.5 climate change scenario (assuming invariant population).

Figure 5.1. I used a random forest model to estimate how the spatial structure of WNV incidence will respond to climate change from our (a) 2011 baseline period for the years (b) 2035, (c) 2065, and (d) 2095 for the RCP8.5 scenario. Over time, our model predicts the areas with the highest WNV incidence will shift northward, presumably into Canada.

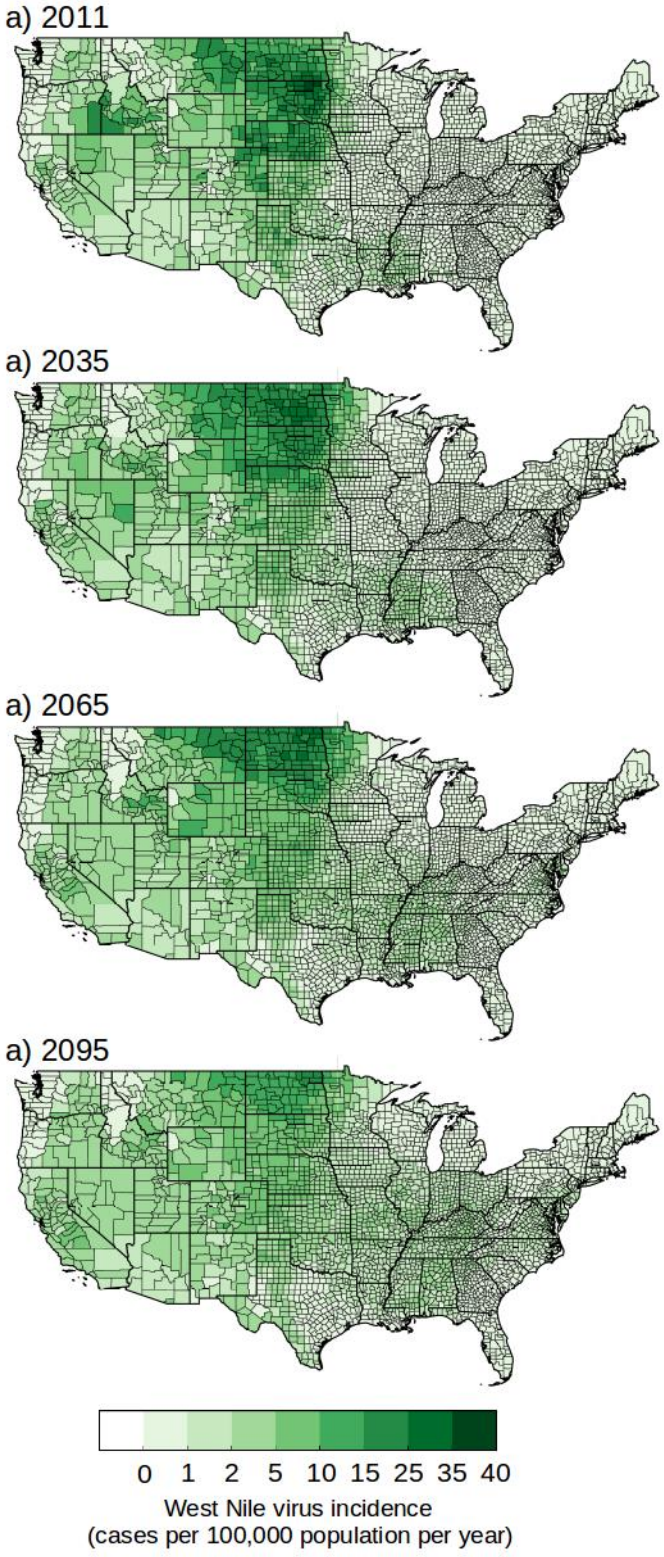

The ability of our model to assess changes in future West Nile virus risk in response to climate change may be useful for disease surveillance and mitigation. I will continue to optimize the predictive model of West Nile virus incidence to test the robustness of this response. I will also consider a moderate greenhouse gas emissions scenario, RCP4.5, as well as future projections of human population.

5.2.2 Applying our Valley fever niche model to the western hemisphere

Valley fever is not limited to the U.S. Soil samples positive for *Coccidioides* ssp. and Valley fever cases have been identified in a number of countries throughout North, Central, and South America (Colombo et al., 2011; Laniado-Laborin, 2007). However, there is limited knowledge on where the endemic regions are throughout the western hemisphere. It is well known that *Coccidioides* spp. is present in Mexico; however, there has been minimal disease surveillance within the country (CDC, 2018b; Laniado-Laborin, 2007). Apart from Mexico, countries that are likely endemic to Valley fever include Guatemala, Honduras, Argentina, Brazil, Paraguay, Bolivia, Venezuela, and Columbia (Colombo et al., 2011; Laniado-Laborin, 2007). In the U.S., I found that the area endemic to Valley fever, as well as the number of cases per year, may increase in response to climate change. These patterns of future change may be similar in other endemic areas. An important next step in my research on Valley fever is to apply my climate-constrained niche model to the western hemisphere to predict the areas currently endemic to Valley fever.

I created a preliminary map of the areas endemic to Valley fever throughout the western hemisphere using my climate-constrained niche model (Figure 5.2). I followed the methods in Chapter 3 and used 4 km^2 gridded mean annual temperature and mean annual

Figure 5.2. Regions of the western hemisphere identified as endemic by our climate-constrained niche model. Areas with a mean annual temperature greater than or equal to 10.7°C and a mean annual precipitation level less than or equal to 600 mm/yr are colored in magenta.

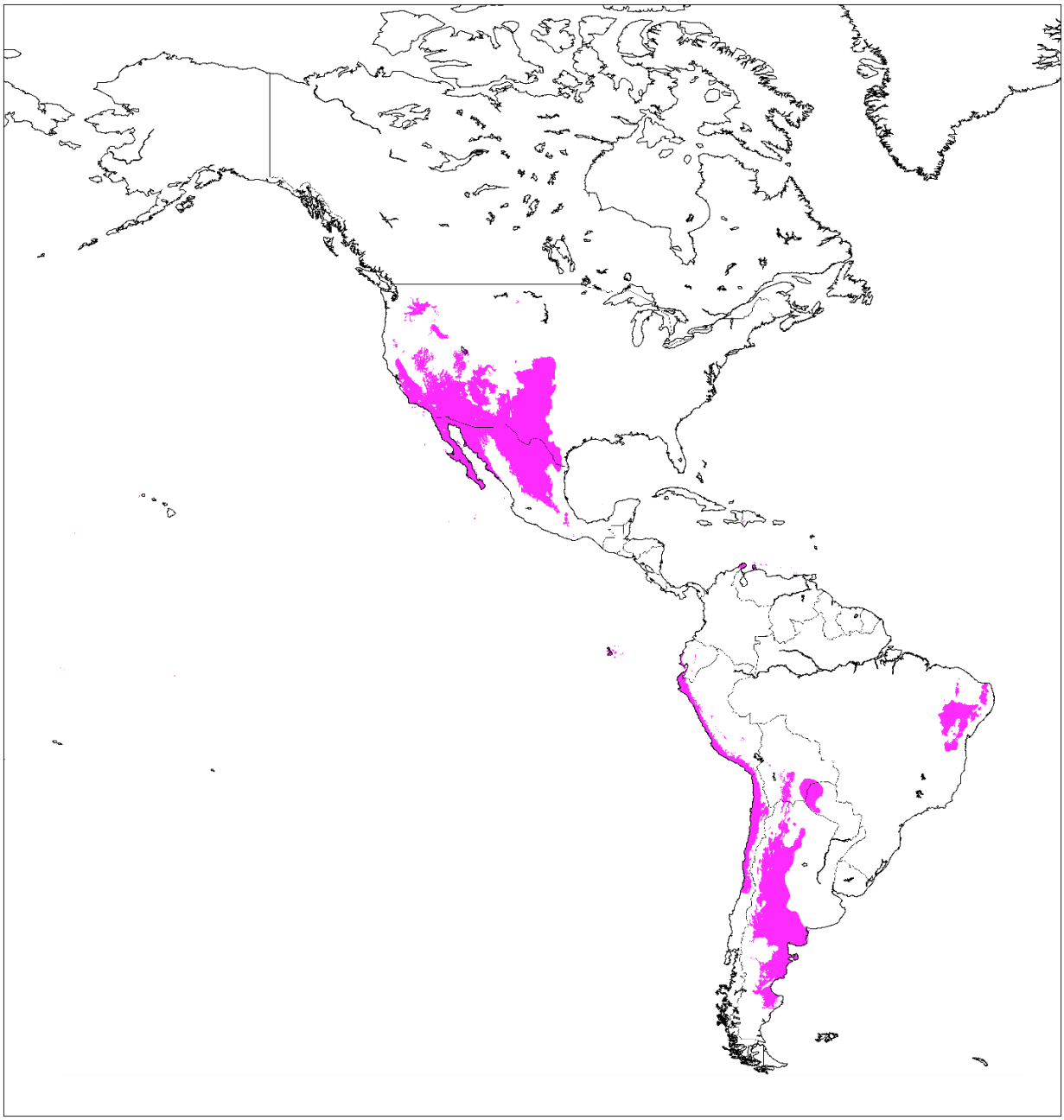

precipitation data from TerraClimate (averaged from 2000-2015; Abatzoglou et al., 2018). The areas that meet our climate thresholds are plotted in magenta: that is, areas that have mean annual temperatures greater than or equal to 10.7°C and mean annual precipitation less than or equal to 600 mm/year. Many of the countries that have reported Valley fever cases outside the U.S. are highlighted in the map, including Mexico, Venezuela, Brazil, Argentina, Paraguay, and Bolivia. It is important to recognize that I trained our initial climate-constrained niche model for the U.S., which may not be sufficient for a model of endemicity that spans the western hemisphere. In future work, I plan to use additional reference points to help refine the temperature and precipitation thresholds to define endemic areas, especially as the Valley fever community continues to learn more about disease incidence outside of the U.S. or other species of *Coccidioides*.

5.2.3 Creating a *Coccidioides* ssp. soil sampling database

To continue learning about the lifecycle of *Coccidioides* ssp., how the fungi respond to the environment, its relationships among microbial communities, and where the fungi are present, researchers should continue environmental surveillance. Creating a systematic soil extraction and DNA sequencing protocol would help standardize surveillance studies. Analyzing the fungal DNA with high-throughput sequencing (e.g., Illumina) would allow a variety of research questions to be studied, including comparing isolates among soil samples and human patients. Our climate-constrained niche model may provide guidance to scientists wishing to isolate *Coccidioides* ssp. from the environment, especially by identifying geographical locations where *Coccidioides* ssp. have not previously been found. In turn, additional occurrence data points of *Coccidioides* ssp. in the environment, as well as

the associated soil properties where it was found, would allow me to validate my model and add additional important environmental parameters as they are discovered.

5.2.4 Interannual variability of Valley fever cases

I used mean annual incidence data to estimate the area endemic to Valley fever. However, the number of disease cases will likely vary from year to year across the endemic region. The number of disease cases may be controlled by a variety of environmental and non-environmental factors, including climate conditions, human activity, changes in disease reporting practices, and changes in healthcare practices. Interannual variations in the amount and timing of precipitation likely influence both the abundance of *Coccidioides* ssp. in the environment and the dispersion of spores (Park et al., 2005; Gorris et al., 2018). An important area for future research is creating short-term predictive models of the number of Valley fever cases, on the time scale of months to years. Understanding how climate affects both the interannual variability of Valley fever cases as well as the area endemic to Valley fever will help attribute future changes in case counts to climatic controls versus other non-climatic factors.

A challenge to analyzing the interannual variability of Valley fever cases is obtaining the appropriate Valley fever case data. In order to protect patient identities, case data is often released only for large counties or regions with higher enough population, aggregated to the month or annual time scale, and distributed with no identifiable demographic information. This limits the research questions one could explore. A stronger collaboration between the CDC, state health agencies, and research organizations may help alleviate some of this challenge. In order to explore how climatic and non-climatic factors influence the number of Valley fever cases, case count data should be available at the finest

spatial scale (at least county-level), at the monthly time scale, and paired with important patient demographic information including the age, race, and gender. Incorporating these additional data parameters into both interannual models and spatial models of incidence may refine our current and future projections of Valley fever.

REFERENCES

Abatzoglou, J. T., Dobrowski, S. Z., Parks, S. A., Hegewisch, K. C. (2018). Terraclimate, a high-resolution global dataset of monthly climate and climatic water balance from 1958-2015, *Scientific Data*, 5, 170191. https://doi.org/10.1038/sdata.2017.191

Ampel, N. M. (2010). What's behind the increasing rates of coccidioidomycosis in Arizona and California?. *Current Infectious Disease Reports*, 12(3), 211–216. https://doi.org/10.1007/s11908-010-0094-3

Arizona Department of Health Services (2012). Arizona—valley fever report, 2007–2011. Arizona Department of Health Services. Phoenix, AZ. Retrieved from http://vfce.arizona.edu/sites/vfce/files/5-year-review-07-11.pdf

Arizona Department of Health Services (2013). Valley fever 2012 annual report. Arizona Department of Health Services. Phoenix, AZ. Retrieved from http://www.azdhs.gov/documents/preparedness/epidemiology-disease-control/valley-fever/reports/valley-fever-2012.pdf

Balbus, J., Crimmins, A., Gamble, J. L., Easterling, D. R., Kunkel, K. E., Saha, S., & Sarofim, M. C. (2016). Ch. 1: Introduction: Climate Change and Human Health. In The Impacts of Climate Change on Human Health in the United States: A Scientific Assessment. (pp. 25–42). Washington, DC: U.S. Global Change Research Program. http://dx.doi.org/10.7930/J0VX0DFW

Baptista-Rosas, R. C., Catalán-Dibene, J., Romero-Olivares, A. L., Hinojosa, A., Cavazos T., & Riquelme, M. (2012). Molecular detection of *Coccidioides* spp. from environmental samples in Baja California: linking valley fever to soil and climate conditions. *Fungal Ecology*, 5(2), 177–190. https://doi.org/10.1016/j.funeco.2011.08.004

Baptista-Rosas, R. C., Hinojosa, A., & Riquelme, M. (2007). Ecological niche modeling of *Coccidioides* spp. in western North American deserts. *Annals of the New York Academy of Sciences*, 1111(1), 35–46. https://doi.org/10.1196/annals.1406.003

Barker, B. M. (2018). Coccidioidomycosis in animals. In S. Seyedmousavi, G. de Hoog, J. Guillot, and P. Verweij (Eds.), Emerging and Epizootic Fungal Infections in Animals (pp. 81–114). Springer, Cham. https://doi.org/10.1007/978-3-319-72093-7_4

Barker, B. M., Litvintseva, A. P., Riquelme, M., & Vargas-Gastélum, L. (2019). *Coccidioides* ecology and genomics. *Medical Mycology*, 57(Supplement_1), S21–S29. https://doi.org/10.1093/mmy/myy051

Barker, B. M., Tabor, J. A., Shubitz, L. F., Perrill, R., & Orbach, M. J. (2012). Detection and phylogenetic analysis of *Coccidioides posadasii* in Arizona soil samples. *Fungal Ecology*, 5(2), 163–176. https://doi.org/10.1016/j.funeco.2011.07.010

Beard, C. B., Eisen, R. J., Barker, C. M., Garofalo, J. F., Hahn, M., Hayden, … & Schramm, P. J. (2016). Ch. 5: Vector-borne diseases. In The Impacts of Climate Change on Human Health in the United States: A Scientific Assessment (129–156). Washington, DC: U.S. Global Change Research Program. http://dx.doi.org/10.7930/J0765C7V

Bercovitch, R. S., Catanzaro, A., Schwartz, B. S., Pappagianis, D., Watts, D. H., & Ampel, N. M. (2011). Coccidioidomycosis during pregnancy: a review and recommendations for management. *Clinical Infectious Diseases*, 53(4), 363–368. https://doi.org/10.1093/cid/cir410

Bergsman, L. D., Hyman, J. M., & Manore, C. A. (2016). A mathematical model for the spread of West Nile virus in migratory and resident birds. *Mathematical Biosciences & Engineering*, 13(2), 401–424. https://doi.org/10.3934/mbe.2015009

Benedict, K., & Park, B. J. (2014). Invasive fungal infections after natural disasters. *Emerging Infectious Diseases*, 20(3), 349–355. https://doi.org/10.3201/eid2003.131230

Blair, J. E., & Logan, J. L. (2001). Coccidioidomycosis in solid organ transplantation. *Clinical Infectious Diseases*, 33(9), 1536–1544. https://doi.org/10.1086/323463

Boryan, C., Yang, Z., Mueller, R., & Craig, M. (2011). Monitoring U.S. agriculture: the U.S. Department of Agriculture, National Agricultural Statistics Service cropland data layer Program. *Geocarto International*, 26(5), 341–358. https://doi.org/10.1016/j.atmosenv.2015.11.004

Boryan, C., Yang, Z., & Di, L. (2012). Deriving 2011 cultivated land cover data sets using USDA National Agricultural Statistics Service historic cropland data layers. In Proceedings of Geoscience and Remote Sensing Symposium, 6297–6300. Munich, Germany: 2012 IEEE International. https://doi.org/10.1109/IGARSS.2012.6352699

Bosilovich, M. G., Akella, S., Coy, L., Cullather, R., Draper, C., Gelaro, R., ... & Wargan, K. (2015). MERRA-2: Initial evaluation of the climate (Tech. Rep. NASA/TM-2015-10, 43). Greenbelt, MD: NASA Goddard Space Flight Center. Retrieved from https://gs6101-gmao.gsfc.nasa.gov/pubs/docs/Bosilovich803.pdf

Bowden, S. E., Magori, K., & Drake, J. M. (2011). Regional differences in the association between land cover and West Nile virus disease incidence in humans in the United States. *The American Journal of Tropical Medicine and Hygiene*, 84(2), 234–238. https://doi.org/10.4269/ajtmh.2011.10-0134

Brownstein, J. S., Rosen, H., Purdy, D., Miller, J. R., Merlino, M., Mostashari, F., & Fish, D. (2002). Spatial analysis of West Nile virus: rapid risk assessment of an introduced vector-borne zoonosis. *Vector Borne and Zoonotic Diseases*, 2(3), 157–164. https://doi.org/10.1089/15303660260613729

Bureau of Transportation Statistics (2016). Passenger travel facts and figures 2016. Washington, D. C.: U.S. Department of Transportation. Retrieved from http://www.rita.dot.gov/bts/sites/rita.dot.gov.bts/files/PTFF%202016_full.pdf

Burnette, D. J., & Stahle, D. W. (2013). Historical perspective on the dust bowl drought in the central United States. *Climatic Change*, 116(3-4), 479–494. https://doi.org/10.1007/s10584-012-0525-2

Cat, L. A., Gorris, M. E., Randerson, J. T., Riquelme, M., & Treseder, K. K. (2019). Crossing the Line: Human Disease and Climate Change Across Borders. *Journal of Environmental Health*, 81(8), 14–22. https://neha.org/node/60622

Caldwell, C. T. (1932). Coccidioidal granuloma: a report of three cases recognized in Texas. *Texas State Journal of Medicine*, 28, 327–333.

California Department of Public Health (2013). Hazard Evaluation System and Information Service, Preventing work-related coccidioidomycosis (valley fever). Sacramento, CA: California Department of Public Health,. Retrieved from http://www.elcosh.org/record/document/3684/d001224.pdf

Campins, H. (1961). Coccidioidomycosis. Comments on the case histories in Venezuela. *Mycopathologia*, 15, 306–316. https://doi.org/10.1007/BF02136335

Catalán-Dibene, J., Johnson, S. M., Eaton, R., Romero-Olivares, A. L., Baptista-Rosas, R. C., Pappagianis, D., & Riquelme, M. (2014). Detection of coccidioidal antibodies in serum of a small rodent community in Baja California, Mexico. *Fungal Biology*, 118(3), 330–339. https://doi.org/10.1016/j.funbio.2014.01.006

Cayan, D., Tyree, M., Kunkel, K. E., Castro, C., Gershunov, A., Barsugli, J., … Duffy, P. (2013). Ch. 6: Future climate: projected average. In G. Garfin, A. Jardine, R. Merideth, M. Black, and S. LeRoy (Eds.), Assessment of Climate Change in the Southwest United States: A Report Prepared for the National Climate Assessment (pp. 153–196). Washington, D. C.: Island Press.

Centers for Disease Control and Prevention (2012). Telebriefing on West Nile virus update. http://www.cdc.gov/media/releases/2012/t0822_west_nile_update.html

Centers for Disease Control and Prevention (2015). National Notifiable Diseases Surveillance System, Data Collection and Reporting. Atlanta, GA: CDC. Retrieved from https://wwwn.cdc.gov/nndss/data-collection.html

Centers for Disease Control and Prevention (2017a). Sources of valley fever (coccidioidomycosis). Atlanta, GA: CDC. Retrieved from https://www.cdc.gov/fungal/diseases/coccidioidomycosis/causes.html

Centers for Disease Control and Prevention (2018a). Valley Fever (Coccidioidomycosis) Statistics. Retrieved from https://www.cdc.gov/fungal/diseases/coccidioidomycosis/statistics.html

Centers for Disease Control and Prevention (2018b). Valley Fever Awareness. Retrieved from https://www.cdc.gov/features/valleyfever/index.html

Centers for Disease Control and Prevention (2018c). West Nile virus Final Cumulative Maps & Data for 1999–2017. Retrieved from https://www.cdc.gov/westnile/statsmaps/cumMapsData.html

Centers for Disease Control and Prevention (2018d). West Nile virus, Symptoms, Diagnosis, & Treatment. Retrieved from https://www.cdc.gov/westnile/symptoms/index.html

Centers for Disease Control and Prevention (2019a). Chikungunya virus in the United States. Retrieved from https://www.cdc.gov/chikungunya/geo/united-states.html

Centers for Disease Control and Prevention (2019b). West Nile virus. Retrieved from https://www.cdc.gov/westnile/index.html

Centers for Disease Control and Prevention (2019c). West Nile virus, Cumulative Maps and Data. Retrieved from https://www.cdc.gov/westnile/statsmaps/cumMapsData.html

Chang, D. C., Anderson, S., Wannemuehler, K., Engelthaler, D. M., Erhart, L., Sunenshine, R. H., et al. (2008). Testing for coccidioidomycosis among patients with community-acquired pneumonia. *Emerging Infectious Diseases*, 14(7), 1053–1059. https://doi.org/10.3201/eid1407.070832

Chen, C., Jenkins, E., Epp, T., Waldner, C., Curry, P., & Soos, C. (2013). Climate change and West Nile virus in a highly endemic region of North America. *International Journal of Environmental Research and Public Health*, 10(7), 3052–3071. https://doi.org/10.3390/ijerph10073052

Chen, L. & Ng, E. (2012). Outdoor thermal comfort and outdoor activities: a review of research in the past decade. *Cities*, 29(2), 118-125. https://doi.org/10.1016/j.cities.2011.08.006

Chretien, J. P., Anyamba, A., Small, J., Britch, S., Sanchez, J. L., Halbach, A. C., ... & Linthicum, K. J. (2015). Global climate anomalies and potential infectious disease risks: 2014-2015. *PLoS Currents*, 7. https://doi.org:10.1371/currents.outbreaks.95fbc4a8fb4695e049baabfc2fc8289f

Chuang, T.W. & Wimberly, M.C. (2012). Remote sensing of climatic anomalies and West Nile virus incidence in the northern Great Plains of the United States. *PLoS One*, 7(10), p.e46882. https://doi.org/10.1371/journal.pone.0046882

Chuang, T. W., Hildreth, M. B., Vanroekel, D. L., & Wimberly, M. C. (2011). Weather and land cover influences on mosquito populations in Sioux Falls, South Dakota. *Journal of Medical Entomology*, 48(3), 669–679. https://doi.org/10.1603/me10246

Ciota, A. T., Matacchiero, A. C., Kilpatrick, A. M., & Kramer, L. D. (2014). The effect of temperature on life history traits of Culex mosquitoes. *Journal of Medical Entomology*, 51(1), 55–62. https://doi.org/10.1603/ME13003

City of El Paso Department of Public Health (2015). Notifiable conditions report. El Paso, TX: City of El Paso Department of Public Health. Retrieved from https://www.elpasotexas.gov/~/media/files/coep/public%20health/epidemiology/2015%20epidemiology%20reports/notifiable%20conditions%20report%20_dec15_ir_ver2.ashx

Colby, S. L., & Ortman, J. M. (2014). Projections of the Size and Composition of the U.S. Population: 2014 to 2060, Current Population Reports (Report No.: P25-1143) Washington, DC: US Census Bureau.

Colombo, A. L., Tobón, A., Restrepo, A., Queiroz-Telles, F., & Nucci, M. (2011). Epidemiology of endemic systemic fungal infections in Latin America. *Medical Mycology*, 49(8), 785–798. https://doi.org/10.3109/13693786.2011.577821

Colson, A. J., Vredenburgh, L., Guevara, R. E., Rangel, N. P., Kloock, C. T., & Lauer, A. (2017). Large-scale land development, fugitive dust, and increased coccidioidomycosis incidence in the Antelope Valley of California, 1999–2014. *Mycopathologia*, 182(5-6), 439–458. https://doi.org/10.1007/s11046-016-0105-5

Comrie, A. C. (2005). Climate factors influencing coccidioidomycosis seasonality and outbreaks. *Environmental Health Perspectives*, 13(6), 688–692. https://doi.org/10.1289/ehp.7786

Cook, B. I., Ault, T. R., & Smerdon, J. E. (2015). Unprecedented 21st century drought risk in the American Southwest and Central Plains. *Science Advances*, 1(1), e1400082. https://doi.org/10.1126/sciadv.1400082

Coopersmith, E. J., Bell, J. E., Benedict, K., Shriber, J., McCotter, O., & Cosh, M. H. (2017). Relating coccidioidomycosis (valley fever) incidence to soil moisture conditions. *GeoHealth*, 1(1), 51–63. https://doi.org/10.1002/2016GH000033

The Cornell Lab of Ornithology (2019). American robin (turdus migratorious) Distribution, Migration, and Habitat. Retrieved from https://birdsna.org/Species-Account/bna/species/amerob/distribution

Crimmins, A., Balbus, J., Gamble, J. L., Beard, C. B., Bell, J. E., Dodgen, D., et al. (Eds.). (2016). The Impacts of Climate Change on Human Health in the United States: A Scientific Assessment. Washington, DC: US Global Change Research Program. http://dx.doi.org/10.7930/J0R49NQX

Crum, N. F., Lederman, E. R., Stafford, C. M., Parrish, J. S., & Wallace, M. R. (2004). Coccidioidomycosis: a descriptive survey of a reemerging disease, Clinical characteristics and current controversies. *Medicine*, 83(3), 149–175. https://doi.org/10.1097/01.md.0000126762.91040.fd

Daly, C., Halbleib, M., Smith, J. I., Gibson, W. P., Doggett, M. K., Taylor, G. H., Curtis, J., & Pasteris, P. P. (2008). Physiographically sensitive mapping of climatological temperature and precipitation across the conterminous United States. *International Journal of Climatology*, 28(15), 2031–2064. https://doi.org/10.1002/joc.1688

Daly, C., Neilson, R. P., & Phillips, D. L. (1994). A statistical-topographic model for mapping climatological precipitation over mountainous terrain. *Journal of Applied Meteorology*, 33(2), 140–158. https://doi.org/10.1175/1520-0450(1994)033<0140:ASTMFM>2.0.CO;2

Darsie Jr., R. F., & Ward, R. A. (1981). Identification and geographical distribution of the mosquitos of North America, north of Mexico (pp. 234-274). Fresno, CA: American Mosquito Control Association.

Davies, B. W., Smith, J. M., Hink, E. M., & Durairaj, V. D. (2017). Increased incidence of rhino-orbital-cerebral mucormycosis after Colorado flooding. *Ophthalmic Plastic & Reconstructive Surgery*, 33(3S), S148–S151. https://doi.org/10.1097/IOP.0000000000000448

de Macêdo, R. C., Rosado, A. S., da Mota, F. F., Cavalcante, M. A., Eulálio, K. D., Filho, A. D., … Wanke, B. (2011). Molecular identification of *Coccidioides* spp. in soil samples from Brazil. *BMC Microbiology*, 11(1). 108. https://doi.org/10.1186/1471-2180-11-108

DeGroote, J. P., Sugumaran, R., Brend, S. M., Tucker, B. J., & Bartholomay, L. C. (2008). Landscape, demographic, entomological, and climatic associations with human disease incidence of West Nile virus in the state of Iowa, USA. *International Journal of Health Geographics*, 7(1), 19. https://doi.org/10.1186/1476-072X-7-19

Deser, C., Phillips, A., Bourdette, V., & Teng, H. (2012). Uncertainty in climate change projections: the role of internal variability. *Climate Dynamics*, 38(3-4), 527–546. https://doi.org/10.1007/s00382-010-0977-x

Didan, K. (2015). MOD13C2 MODIS/Terra Vegetation Indices Monthly L3 Global 0.05Deg CMG V006, NASA EOSDIS Land Processes CAAD. Sioux Falls, SD: USGS Earth Resources Observation and Science (EROS) Center. https://doi.org/10.5067/MODIS/MOD13C2.006

Dohm, D. J., O'Guinn, M. L., & Turell, M. J. (2002). Effect of environmental temperature on the ability of *Culex pipiens* (Diptera: Culicidae) to transmit West Nile virus. *Journal of Medical Entomology*, 39(1), 221–225. https://doi.org/10.1603/0022-2585-39.1.221

Durry, E., Pappagianis, D., Werner, S. B, Hutwagner, L., Sun, R. K., Maurer, M., McNeil, M. M., & Pinner, R. W. (1997). Coccidioidomycosis in Tulare County, California, 1991: reemergence of an endemic disease. *Journal of Medical and Veterinary Mycology*, 35(5), 321–326. https://doi.org/10.1080/02681219780001361

Easterling, D. R., Arnold, J. R., Knutson, T., Kunkel, K. E., LeGrande, A. N., Leung, L. R., et al. (2017). Precipitation Change in the United States. In D. J. Wuebbles, D. W. Fahey, K. A. Hibbard, D. J. Dokken, B. C. Stewart, & T. K. Maycock (Eds.), Climate Science Special Report: Fourth National Climate Assessment, Volume I. Washington, DC: US Global Change Research Program, 207–230. https://doi:10.7930/J0H993CC

Ebi, K. L., Balbus, J. M., Luber, G., Bole, A., Crimmins, A., Glass, G., et al. (2018). Human Health. In D. R. Reidmiller, D. R., Avery, C. W., Easterling, D. R., Kunkel, K. E., Lewis, K. L. M., Maycock, T. K., & Stewart, B. C. (Eds.), Impacts, Risks, and Adaptation in the United States: Fourth National Climate Assessment, Volume II (pp. 539–571). Washington, DC: U.S. Global Change Research Program. https://doi.org/10.7930/NCA4.2018.CH14

Edwards, P. Q., & Palmer, C. E. (1957). Prevalence of sensitivity to coccidioidin, with special reference to specific and nonspecific reactions to coccidioidin and to histoplasmin. *CHEST Journal*, 31(1), 35–60. https://doi.org/10.1378/chest.31.1.35

Elconin, A. F., Egeberg, R. O., & Lubarsky, R. (1957). Growth pattern of *Coccidioides immitis* in the soil of an endemic area, In Proceedings of the Symposium on Coccidioidomycosis (pp. 168–170).

Epstein, P. R. (2001). Climate change and emerging infectious diseases. *Microbes and Infection*, 3(9), 747–754. https://doi.org/10.1016/S1286-4579(01)01429-0

Epstein, P. (2010). The ecology of climate change and infectious diseases: comment. *Ecology*, 91(3), 925–928. http://www.jstor.org/stable/25661125

Escobar, L. E., Romero-Alvarez, D., Leon, R., Lepe-Lopez, M. A., Craft, M. E., Borbor-Cordova, M. J., & Svenning, J. C. (2016). Declining prevalence of disease vectors under climate change. *Scientific Reports*, 6. https://doi.org/10.1038/srep39150

Eulálio, K. D., de Macêdo, R. C., Cavalcanti, M. A., Martins, L. M., Lazéra, M. S., & Wanke, B. (2001). *Coccidioides immitis* isolated from armadillos (*Dasypus novemcinctus*) in the state of Piauí, northeast Brazil. *Mycopathologia*, 149(2), 57–61. https://doi.org/10.1023/A:1007273019647

Ewing, D. A., Cobbold, C. A., Purse, B. V., Nunn, M. A., & White, S. M. (2016). Modelling the effect of temperature on the seasonal population dynamics of temperate mosquitoes. *Journal of Theoretical Biology*, 400, 65–79. https://doi.org/10.1016/j.jtbi.2016.04.008

Eyring, V., Bony, S., Meehl, G. A., Senior, C. A., Stevens, B., Stouffer, R. J., & Taylor, K. E. (2016). Overview of the Coupled Model Intercomparison Project Phase 6 (CMIP6)

experimental design and organization. *Geoscientific Model Development*, 9(5), 1937–1958. https://doi.org/10.5194/gmd-9-1937-2016

Ezenwa, V. O., Godsey, M. S., King, R. J., & Guptill, S. C. (2005). Avian diversity and West Nile virus: testing associations between biodiversity and infectious disease risk. *Proceedings of the Royal Society B: Biological Sciences*, 273(1582), 109–117. https://doi.org/10.1098/rspb.2005.3284

Ezenwa, V. O., Milheim, L. E., Coffey, M. F., Godsey, M. S., King, R. J., & Guptill, S. C. (2007). Land cover variation and West Nile virus prevalence: patterns, processes, and implications for disease control. *Vector-Borne and Zoonotic Diseases*, 7(2), 173–180. https://doi.org/10.1089/vbz.2006.0584

Faivre, N. R., Jin, Y., Goulden, M. L., & Randerson, J. T. (2016). Spatial patterns and controls on burned area for two contrasting fire regimes in Southern California. *Ecosphere*, 7(5), e01210. https://doi.org/10.1002/ecs2.1210

Fink, D., Auer, T., Johnston, A., Strimas-Mackey, M., Iliff, M., & Kelling, S. (2018). eBird Status and Trends. Version: November 2018. Ithaca, New York: Cornell Lab of Ornithology. Retrieved from https://ebird.org/science/status-and-trends

Fisher, F. S., Bultman, M. W., Johnson, S. M., Pappagianis, D., & Zaborsky, E. (2007). *Coccidioides* niches and habitat parameters in the southwestern United States: a matter of scale. *Annals of the New York Academy of Sciences*, 1111(1), 47–72. https://doi.org/10.1196/annals.1406.031

Friedman, L., Smith, C. E., Pappagianis, D., & Berman, R. J. (1956). Survival of *Coccidioides immitis* under controlled conditions of temperature and humidity. *American Journal of Public Health and the Nations Health*, 46(10), 1317–1324. https://doi.org/10.2105/AJPH.46.10.1317

Gage, K. L., Burkot, T. R., Eisen, R. J. and Hayes, E. B. (2008). Climate and vectorborne diseases. *American Journal of Preventive Medicine*, 35(5), 436–450. https://doi.org/10.1016/j.amepre.2008.08.030

Garfin, G., Franco, G., Blanco, H., Comrie, A., Gonzalez, P., Piechota, T., Smyth, R., & Waskom, R. (2014). Ch. 20: Southwest, In J. M. Melillo, T. C. Richmond, G. W. Yohe (Eds.), Climate change impacts in the United States: the third national climate assessment (pp. J462–486). Washington D. C.: U.S. Global Change Research Program. https://doi.org/10.7930/J08G8HMN

George, T. L., Harrigan, R. J., LaManna, J. A., DeSante, D. F., Saracco, J. F., & Smith, T. B. (2015). Persistent impacts of West Nile virus on North American bird populations. *Proceedings of the National Academy of Sciences*, 112(46), 14290–14294. https://doi.org/10.1073/pnas.1507747112

Gibbs, S. E., Wimberly, M. C., Madden, M., Masour, J., Yabsley, M. J., & Stallknecht, D. E. (2006). Factors affecting the geographic distribution of West Nile virus in Georgia, USA: 2002–2004. *Vector-Borne & Zoonotic Diseases*, 6(1), 73–82. https://doi.org/10.1089/vbz.2006.6.73

Godsey Jr, M. S., Blackmore, M. S., Panella, N. A., Burkhalter, K., Gottfried, K., Halsey, L. A., ... & Lambert, A. (2005). West Nile virus epizootiology in the southeastern United States, 2001. *Vector-Borne & Zoonotic Diseases*, 5(1), 82–89. https://doi.org/10.1089/vbz.2005.5.82

Gorris, M. E., Cat, L. A., Zender, C. S., Treseder, K. K., & Randerson, J. T. (2018). Coccidioidomycosis dynamics in relation to climate in the southwestern United States. *GeoHealth*, 2(1), 6–24. https://doi.org/10.1002/2017GH000095

Greene, D. R., Koenig, G., Fisher, M. C., & Taylor, J. W. (2000). Soil isolation and molecular identification of *Coccidioides immitis*. *Mycologia*, 92(3), 406–410, https://doi.org/10.2307/3761498

Griffin, D. W. (2007). Atmospheric movement of microorganisms in clouds of desert dust and implications for human health. *Clinical Microbiology Reviews*, 20(3), 459–477. https://doi.org/10.1128/CMR.00039-06

Gubler, D. J., Reiter, P., Ebi, K. L., Yap, W., Nasci, R., & Patz, J. A. (2001). Climate variability and change in the United States: potential impacts on vector-and rodent-borne diseases. *Environmental Health Perspectives*, 109(suppl 2), 223–233. https://doi.org/10.1289/ehp.109-1240669

Hahn, M. B., Monaghan, A. J., Hayden, M. H., Eisen, R. J., Delorey, M. J., Lindsey, N. P., ... & Fischer, M. (2015). Meteorological conditions associated with increased incidence of West Nile virus disease in the United States, 2004–2012. *The American Journal of Tropical Medicine and Hygiene*, 92(5), 1013–1022. https://doi.org/10.4269/ajtmh.14-0737

Hamer, G. L., Kitron, U. D., Goldberg, T. L., Brawn, J. D., Loss, S. R., Ruiz, M. O., ... & Walker, E. D. (2009). Host selection by *Culex pipiens* mosquitoes and West Nile virus amplification. *The American Journal of Tropical Medicine and Hygiene*, 80(2), 268–278. https://doi.org/10.4269/ajtmh.2009.80.268

Harp, E. L., & Jibson, R. W. (1996). Landslides triggered by the 1994 Northridge, California, earthquake. *Bulletin of the Seismological Society of America*, 86(1B), S319–S332.

Harrigan, R. J., Thomassen, H. A., Buermann, W., Cummings, R. F., Kahn, M. E., & Smith, T. B. (2010). Economic conditions predict prevalence of West Nile virus. *PLoS One*, 5(11), e15437. https://doi.org/10.1371/journal.pone.0015437

Harrigan, R. J., Thomassen, H. A., Buermann, W., & Smith, T. B. (2014). A continental risk assessment of West Nile virus under climate change. *Global Change Biology*, 20(8), 2417–2425. https://doi.org/10.1111/gcb.12534

Hauer, M. E. (2019). Population projections for US counties by age, sex, and race controlled to shared socioeconomic pathway. *Scientific Data*, 6, 190005. https://doi.org/10.1038/sdata.2019.5

Hayes, E. B., Komar, N., Nasci, R. S., Montgomery, S. P., O'Leary, D. R., & Campbell, G. L. (2005). Epidemiology and transmission dynamics of West Nile virus disease. *Emerging Infectious Diseases*, 11(8), 1167–1173. https://doi.org/10.3201/eid1108.050289a

Hayhoe, K., Wuebbles, D. J., Easterling, D. R., Fahey, D. W., Doherty, S., Kossin, J., et al. (2018) Our Changing Climate. In D. R. Reidmiller, C. W. Avery, D. R. Easterling, K. E. Kunkel, K. L. M. Lewis, T. K. Maycock, & B. C. Stewart (Eds.), Impacts, Risks, and Adaptation in the United States: Fourth National Climate Assessment, Volume II (pp. 72–144). Washington, DC: U.S. Global Change Research Program. https://doi:10.7930/NCA4.2018.CH2

Hector, R. F., Rutherford, G. W., Tsang, C. A., Erhart, L. M., McCotter, O., Anderson, S. M., … Galgiani, J. N. (2011). The public health impact of coccidioidomycosis in Arizona and California. *International Journal of Environmental Research and Public Health*, 8(4), 1150–1173. https://doi.org/10.3390/ijerph8041150

Hirschmann, J. V. (2007). The early history of coccidioidomycosis: 1892–1945. *Clinical Infectious Diseases*, 44(9), 1202–1207. https://doi.org/10.1086/513202

Hinton, M. G., Reisen, W. K., Wheeler, S. S., & Townsend, A. K. (2015). West Nile virus activity in a winter roost of American crows (Corvus brachyrhynchos): is bird-to-bird transmission important in persistence and amplification? *Journal of Medical Entomology*, 52(4), 683–692. https://doi.org/10.1093/jme/tjv040

Hongoh, V., Berrang-Ford, L., Scott, M. E., & Lindsay, L. R. (2012). Expanding geographical distribution of the mosquito, Culex pipiens, in Canada under climate change. *Applied Geography*, 33, 53–62. https://doi.org/10.1016/j.apgeog.2011.05.015

Huete, A., Didan, K., Miura, T., Rodriguez, E. P., Gao, X., & Ferreira, L. G. (2002). Overview of the radiometric and biophysical performance of the MODIS vegetation indices. *Remote Sensing of Environment*, 83(1), 195–213. https://doi.org/10.1016/S0034-4257(02)00096-2

Huete, A., Didan, K., van Leeuwen, W., Miura, T., & Glenn, E. (2010). MODIS vegetation indices, In B. Ramachandran, C. Justice, M. Abrams (Eds.), Land remote sensing and global environmental change (pp. 579–602). New York, NY: Springer. https://doi.org/10.1007/978-1-4419-6749-7_26

Hugenholtz, P. (1957). Climate and coccidioidomycosis, In Proceedings of the symposium on Coccidioidomycosis (575, pp. 136–143). Washington D.C.: U.S. Public Health Services.

Huppert, M., Levine, H. B., Sun, S. H., & Peterson, E. T. (1967). Resistance of vaccinated mice to typical and atypical strains of *Coccidioides immitis*. *Journal of Bacteriology*, 94(4), 924–927.

Jones, J. M., Koski, L., Khan, M., Brady, S., Sunenshine, R., & Komatsu, K.K. (2017). Coccidioidomycosis: An underreported cause of death—Arizona, 2008–2013. *Medical Mycology*, 56(2), 172–179. https://doi.org/10.1093/mmy/myx041

Kerrick, S. S., Lundergan, L. L., & Galgiani, J. N. (1985). Coccidioidomycosis at a university health service. *American Review of Respiratory Disease*, 131(1), 100–102. https://doi.org/10.1164/arrd.1985.131.1.100

Kilpatrick, A. M. (2011). Globalization, land use, and the invasion of West Nile virus. *Science*, 334(6054), 323–327. https://doi.org/10.1126/science.1201010

Kilpatrick, A. M., Daszak, P., Jones, M. J., Marra, P. P., & Kramer, L. D. (2006). Host heterogeneity dominates West Nile virus transmission. *Proceedings of the Royal Society B: Biological Sciences*, 273(1599), 2327–2333. https://doi.org/10.1098/rspb.2006.3575

Kilpatrick, A. M., Kramer, L. D., Campbell, S. R., Alleyne, E. O., Dobson, A. P., & Daszak, P. (2005). West Nile virus risk assessment and the bridge vector paradigm. *Emerging Infectious Diseases*, 11(3), 425–429. https://doi.org/10.3201/eid1103.040364

Kilpatrick, A. M., Meola, M. A., Moudy, R. M. & Kramer, L. D. (2008). Temperature, viral genetics, and the transmission of West Nile virus by *Culex pipiens* mosquitoes. *PLoS Pathogens*. 4, e1000092. https://doi.org/10.1371/journal.ppat.1000092

Kolivras, K. N., & Comrie, A. C. (2003). Modeling valley fever (coccidioidomycosis) incidence on the basis of climate conditions. *International Journal of Biometeorology*, 47(2), 87–101. https://doi.org/10.1007/s00484-002-0155-x

Komar, N. (2003). West Nile virus: epidemiology and ecology in North America. *Advances in Virus Research*, 61, 185–234. https://doi.org/10.1016/S0065-3527(03)61005-5

Komatsu, K., Vaz, V., McRill, C., Colman, T., Comrie, A., Sigel, K., … Park, B. (2003). Increase in Coccidioidomycosis—Arizona, 1998–2001. *MMWR Morbidity and Mortality Weekly Report*, 52(6), 109–112. https://doi.org/10.1001/jama.289.12.1500

Koski, L., Sylvester, T., Narang, J., & Sunenshine, R. (2016). Estimating trends of coccidioidomycosis in an endemic area after laboratory reporting changes: Maricopa County, 2006–2014. *Proceedings of the 60th annual Coccidioidomycosis Study Group meeting*, 60, 59.

Kunkel, K. E., Stevens, L. E., Stevens, S. E., Sun, L., Janssen, E., Wuebbles, D., Redmond, K. T., & Dobson, J. G. (2013). Regional Climate Trends and Scenarios for the U.S. National

Climate Assessment: Part 5. In Climate of the Southwest U.S. (Tech. rep. NESDIS 142–5, 51–70). Washington, D. C.: National Oceanic and Atmospheric Administration.

Lacy, G. H., & Swatek, F. E. (1974). Soil ecology of *Coccidioides immitis* at Amerindian middens in California. *Applied Microbiology*, 27(2), 379–388.

LaDeau, S. L., Calder, C. A., Doran, P. J., & Marra, P. P. (2011). West Nile virus impacts in American crow populations are associated with human land use and climate. *Ecological Research*, 26(5), 909–916. https://doi.org/10.1007/s11284-010-0725-z

Lafferty, K. D. (2009). The ecology of climate change and infectious diseases. *Ecology*, 90(4), 888–900. https://doi.org/10.1890/08-0079.1

Lafferty, K. D. (2010). The ecology of climate change and infectious diseases: reply. *Ecology*, 91(3), 928–929. https://doi.org/10.1890/09-1656.1

Lafferty, K. D. and Mordecai, E. A. (2016). The rise and fall of infectious disease in a warmer world. *F1000Research*, 5. https://doi.org/10.12688/f1000research.8766.1

Landesman, W. J., Allan, B. F., Langerhans, R. B., Knight, T. M., & Chase, J. M. (2007). Inter-annual associations between precipitation and human incidence of West Nile virus in the United States. *Vector-Borne and Zoonotic Diseases*, 7(3), 337–343. https://doi.org/10.1089/vbz.2006.0590

Laniado-Laborin, R. A. (2007). Expanding understanding of epidemiology of coccidioidomycosis in the Western hemisphere. *Annals of the New York Academy of Sciences*, 1111(1), 19–34. https://doi.org/10.1196/annals.1406.004

Lauer, A. (2017). Coccidioidomycosis: increasing incidence of an “orphan” disease in response to environmental changes. In C. Hurst (Ed.), Modeling the Transmission and Prevention of Infectious Disease (Vol. 4, pp. 151–185). Springer, Cham. https://doi.org/10.1007/978-3-319-60616-3_6

Lauer, A., Baal, J. D., Baal, J. C., Verma, M., & Chen, J. M. (2012). Detection of *Coccidioides immitis* in Kern County, California, by multiplex PCR. *Mycologia*, 104(1), 62–69. https://doi.org/10.3852/11-127

Lauer, A., Baal, J. D., Mendes, S. D., Casimiro, K. N., Passaglia, A. K., Valenzuela, A. H., & Guibert, G. (2019). Valley fever on the rise—searching for microbial antagonists to the fungal pathogen *Coccidioides immitis*. *Microorganisms*, 7(2), 31–47. https://doi.org/10.3390/microorganisms7020031

Lauer, A., Talamantes, J., Olivares, L. R. C., Medina, L. J., Baal, J. D. H., Casimiro, K., et al. (2014). Combining forces-the use of landsat TM satellite imagery, soil parameter information, and multiplex PCR to detect *Coccidioides immitis* growth sites in Kern County, California. *PloS One*, 9(11), e111921:1–14. https://doi.org/10.1371/journal.pone.0111921

Lehner, F., Deser, C., Simpson, I. R., & Terray, L. (2018). Attributing the U.S. Southwest's recent shift into drier conditions. *Geophysical Research Letters*, 45, 6251–6261. https://doi.org/10.1029/2018GL078312

Lin, Y. 2007. Mesoscale dynamics (pp. 413–420). Cambridge University Press. https://doi.org/10.1017/CBO9780511619649

Litvintseva, A.P., Marsden-Huag, N., Hurst, S., Hill, H., Gade, L., Driebe, E. M., … Chiller, T. (2014). Valley fever: finding new places for an old disease: *Coccidioides immitis* found in Washington State soil associated with recent human infection. *Clinical Infectious Diseases*, 60(1), e1–3. https://doi.org/10.1093/cid/ciu681

Liu, A., Lee, V., Galusha, D., Slade, M. D., Diuk-Wasser, M., Andreadis, T., ... & Rabinowitz, P. M. (2009). Risk factors for human infection with West Nile Virus in Connecticut: a multi-year analysis. *International Journal of Health Geographics*, 8(1), 67. https://doi.org/10.1186/1476-072X-8-67

Liu, L.-Y., Li, X.-Y., Shi, P.-J., Gao, S.-Y., Wang, J.-H., Ta, W.-Q., … Xiao, B.-L. (2007). Wind erodibility of major soils in the farming–pastoral ecotone of China. *Journal of Arid Environments*, 68(4), 611–623. https://doi.org/10.1016/j.jaridenv.2006.08.011

Louie, L., Ng, S., Hajjeh, R., Johnson, R., Vugia, D., Werner, S. B., Talbot, R., & Klitz, W. (1999). Influence of host genetics on the severity of coccidioidomycosis. *Emerging Infectious Diseases*, 5(5), 672–680. https://doi.org/10.3201/eid0505.990508

Lungstrom, L. (1954). Biological studies on Culex tarsalis (Diptera Culicidae) in Kansas. *Transactions of the Kansas Academy of Science*, 57(1), 86–96. https://doi.org/10.2307/3625649

Maddy, K. T. (1957). Ecological factors of the geographic distribution of *Coccidioides immitis*. *Journal of the American Veterinary Medical Association*, 130(11), 475–476.

Maddy, K. T. (1958). The geographic distribution of *Coccidioides immitis* and possible ecological implications. *Arizona Medicine*, 15(3), 178–188.

Maddy, K. T. (1965). Observations on *Coccidioides immitis* found growing naturally in soil. *Arizona Medicine*, 22(4), 281–288.

Manore, C. A., Davis, J. K., Christofferson, R. C., Wesson, D. M., Hyman, J. M., & Mores, C. N. (2014). Towards an early warning system for forecasting human West Nile virus incidence. *PLoS Currents*, 6. https://doi.org/10.1371.currents.outbreaks.ed6f0f8a61d20ae5f32aaa5c2b8d3c23

Marsden-Haug, N., Goldoft, M., Ralston, C., Limaye, A. P., Chua, J., Hill, H., … Chiller, T. (2012). Coccidioidomycosis Acquired in Washington State. *Clinical Infectious Diseases*, 56(6), 847–850. https://doi.org/10.1093/cid/cis1028

Maurer, E. P., Brekke, L., Pruitt, T., & Duffy, P. B. (2007). Fine-resolution climate projections enhance regional climate change impact studies. *Eos, Transactions American Geophysical Union*, 88(47), 504–504. https://doi.org/10.1029/2007EO470006

McConnell, J. R., Aristarain, A. J., Banta, J. R., Edwards, P. R., & Simoes, J. C. (2007). 20th-Century doubling in dust archived in an Antarctic Peninsula ice core parallels climate change and desertifications in South America. *Proceedings of the National Academy of Sciences*, 104(14), 5743–5748. https://doi.org/10.1073/pnas.0607657104

McLean, R.G., Ubico, S. R., Docherty, D. E., Hansen, W. R., Sileo, L., & McNamara, T. S. (2001). West Nile virus transmission and ecology in birds. *Annals of the New York Academy of Sciences*, 951(1), 54–57. https://doi.org/10.1111/j.1749-6632.2001.tb02684.x

Miller, J. (2010). Species distribution modeling. *Geography Compass*, 4(6), 490–509. https://doi.org/10.1111/j.1749-8198.2010.00351.x

Molaei, G., Andreadis, T. G., Armstrong, P. M., Anderson, J. F., & Vossbrinck, C. R. (2006). Host feeding patterns of Culex mosquitoes and West Nile virus transmission, northeastern United States. *Emerging Infectious Diseases*, 12(3), 468–474. https://doi.org/10.3201/eid1203.051004

Molod, A., Takacs, L., Suarez, M., & Bacmeister, J. (2015). Development of the GEOS-5 atmospheric general circulation model: evolution from MERRA to MERRA2. *Geoscientific Model Development*, 8(5), 1339–1356.

Montecino-Latorre, D., & Barker, C. M. (2018). Overwintering of West Nile virus in a bird community with a communal crow roost. *Scientific Reports*, 8(1), 6088. https://doi.org/10.1038/s41598-018-24133-4

Morrow, W. (2006). Holocene coccidioidomycosis: Valley Fever in early Holocene bison (Bison antiquus). *Mycologia*, 98(5), 669–677.

Moss, R. H., Edmonds, J. A., Hibbard, K. A., Manning, M. R., Rose, S. K., Van Vuuren, D. P., et al. (2010). The next generation of scenarios for climate change research and assessment. *Nature*, 463, 747–756. https://doi.org/10.1038/nature08823

Murphy, T. D., Grandpre, J., Novick, S. L., Seys, S. A., Harris, R. W., & Musgrave, K. (2005). West Nile virus infection among health-fair participants, Wyoming 2003: assessment of symptoms and risk factors. *Vector-Borne & Zoonotic Diseases*, 5(3), 246–251. https://doi.org/10.1089/vbz.2005.5.246

Neblett Fanfair, R., Benedict, K., Bos, J., Bennett, S. D., Lo, Y. C., Adebanjo, T., ... & Drew, C. (2012). Necrotizing cutaneous mucormycosis after a tornado in Joplin, Missouri, in 2011. *New England Journal of Medicine*, 367(23), 2214–2225. https://doi.org/10.1056/NEJMoa1204781

Needham, G. R., & Teel, P. D. (1991). Off-host physiological ecology of ixodid ticks. *Annual Review of Entomology*, 36(1), 659–681. https://doi.org/10.1146/annurev.en.36.010191.003303

Neff, J. C., Ballantyne, A. P., Farmer, G. L., Mahowald, N. M., Conroy, J. L., Landry, C. C., … Reynolds, R. L. (2008). Increasing eolian dust deposition in the western United States linked to human activity. *Nature Geoscience*, 1(3), 189–195. https://doi.org/10.1038/ngeo133

Nelms, B. M., Fechter-Leggett, E., Carroll, B. D., Macedo, P., Kluh, S., & Reisen, W. K. (2013). Experimental and natural vertical transmission of West Nile virus by California Culex (Diptera: Culicidae) mosquitoes. *Journal of Medical Entomology*, 50(2), 371–378. https://doi.org/10.1603/ME12264

Nguyen, C., Barker, B. M., Hoover, S., Nix, D. E., Ampel, N. M., Frelinger, J. A., Orbach, M. J., & Galgiani, J. N. (2013). Recent advances in our understanding of the environmental, epidemiological, immunological, and clinical dimensions of coccidioidomycosis. *Clinical Microbiology Reviews*, 26(3), 505–525. https://doi.org/10.1128/CMR.00005-13

Nielsen, C. F., Armijos, M. V., Wheeler, S., Carpenter, T. E., Boyce, W. M., Kelley, K., ... & Reisen, W. K. (2008). Risk factors associated with human infection during the 2006 West Nile virus outbreak in Davis, a residential community in northern California. *The American Journal of Tropical Medicine and Hygiene*, 78(1), 53–62. https://doi.org/10.4269/ajtmh.2008.78.53

Odio, C. D., Marciano, B. E., Galgiani, J. N., & Holland, S. M. (2017). Risk factors for disseminated coccidioidomycosis, United States. *Emerging Infectious Diseases*, 23(2), 308–311. https://doi.org/10.3201/eid2302.160505

O'Neill, B. C., Kriegler, E., Riahi, K., Ebi, K. L., Hallegatte, S., Carter, T. R., et al. (2014). A new scenario framework for climate change research: the concept of shared socioeconomic pathways. *Climatic Change*, 122(3), 387–400. https://doi.org/10.1007/s10584-013-0905-2

Pappagianis, D. (1994). Marked increase in cases of coccidioidomycosis in California: 1991, 1992, and 1993. *Clinical Infectious Diseases*, 19(Suppl 1), S14–S18.

Park, B. J., Sigel, K., Vaz, V., Komatsu, K., McRill, C., Phelan, M., … Hajjeh, R. A. (2005). An epidemic of coccidioidomycosis in Arizona associated with climatic changes, 1998–2001. *Journal of Infectious Diseases*, 191(11), 1981–1987. https://doi.org/10.1086/430092

Pascale, S., Boos, W. R., Bordoni, S., Delworth, T. L., Kapnick, S. B., Murakami, H., et al. (2017). Weakening of the North American monsoon with global warming. *Nature Climate Change*, 7(11), 806–813. https://doi.org/10.1038/NCLIMATE3412

Paull, S. H., Horton, D. E., Ashfaq, M., Rastogi, D., Kramer, L. D., Diffenbaugh, N. S., & Kilpatrick, A. M. (2017). Drought and immunity determine the intensity of West Nile virus

epidemics and climate change impacts. *Proceedings of the Royal Society B: Biological Sciences*, 284(1848). https://doi.org/10.1098/rspb.2016.2078

Perera, P., Stone, S., Talan, D. A., Moran, G. J., & Pinner, R. (2002). Coccidioidomycosis in workers at an archeologic site–Dinosaur National Monument, Utah, June–July 2001. *Annals of Emergency Medicine*, 39(5), 566–567. https://doi.org/10.1067/mem.2002.123550

Peterson, A. T. (2006). Ecologic niche modeling and spatial patterns of disease transmission. *Emerging Infectious Diseases*, 12(12), 1822–1826. https://doi.org/10.3201/eid1212.060373

Petersen, L. R., Carson, P. J., Biggerstaff, B. J., Custer, B., Borchardt, S. M., & Busch, M. P. (2013). Estimated cumulative incidence of West Nile virus infection in US adults, 1999–2010. *Epidemiology & Infection*, 141(3), 591–595. https://doi.org/10.1017/S0950268812001070

Petersen, L. R., Marshall, S. L., Barton-Dickson, C., Hajjeh, R. A., Lindsley, M. D., Warnock, D. W., … Morgan, J. (2004). Coccidioidomycosis among workers at an archeological site, northeastern Utah. *Emerging Infectious Diseases*, 10(4), 637–42. https://doi.org/10.3201/eid1004.030446

Phillips, S. J., Anderson, R. P., & Schapire, R. E. (2006). Maximum entropy modeling of species geographic distributions. *Ecological Modelling*, 190(3–4), 231–259. https://doi.org/10.1016/j.ecolmodel.2005.03.026

Polade, S. D., Gershunov, A., Cayan, D. R., Dettinger, M. D., & Pierce, D. W. (2017). Precipitation in a warming world: Assessing projected hydro-climate changes in California and other Mediterranean climate regions. *Scientific Reports*, 7(1), 10783. https://doi.org/10.1038/s41598-017-11285-y

Reclamation, 2013. Downscaled CMIP3 and CMIP5 Climate and Hydrology Projections: Release of Downscaled CMIP5 Climate Projections, Comparison with preceding Information, and Summary of User Needs, prepared by the U.S. Department of the Interior, Bureau of Reclamation, Technical Services Center, Denver, Colorado. 47 pp. https://gdo-dcp.ucllnl.org/downscaled_cmip_projections/techmemo/downscaled_climate.pdf

Reisen, W. K., Fang, Y., & Martinez, V. M. (2014). Effects of temperature on the transmission of West Nile virus by Culex tarsalis (Diptera: Culicidae). *Journal of Medical Entomology*, 43(2), 309–317. https://doi.org/10.1093/jmedent/43.2.309

Rienecker, M. M., Suarez, M. J., Gelaro, R., Todling, R., Bacmeister, J., Liu, E., … Woollen, J. (2011). MERRA: NASA's modern-era retrospective analysis for research and applications. *Journal of Climate*, 24(14), 3624–3648. https://doi.org/10.1175/JCLI-D-11-00015.1

Rodell, M., & Beaudoing, H. K. (2007). GLDAS Noah Land Surface Model L4 Monthly 0.25 x 0.25 degree V2.1. Greenbelt, MD: Goddard Earth Sciences Data and Information Services Center (GES DISC). https://doi.org/10.5067/7NP2052IA62C

Rodell, M., Houser, P. R., Jambor, U. E. A., Gottschalck, J., Mitchell, K., Meng, C. J., … Entin, J. K. (2004). The global land data assimilation system. *Bulletin of the American Meteorological Society*, 85(3), 381–394. https://doi.org/10.1175/BAMS-85-3-381

Romero-Alvarez, D., Escobar, L. E., Varela, S., Larkin, D. J., & Phelps, N. B. (2017). Forecasting distributions of an aquatic invasive species (*Nitellopsis obtusa*) under future climate scenarios. *PloS One*, 12(7), e0180930:1–24. https://doi.org/10.1371/journal.pone.0180930

Rosenstein, N. E., Emery, K. W., Werner, S. B., Kao, A., Johnson, R., Rogers, D., … Perkins, B. A. (2001). Risk factors for severe pulmonary and disseminated coccidioidomycosis: Kern County, California, 1995–1996. *Clinical Infectious Diseases*, 32(5), 708–715. https://doi.org/10.1580/10806032(2001)012[0216:AOCL]2.0.CO;2

Ruiz, M. O., Chaves, L. F., Hamer, G. L., Sun, T., Brown, W. M., Walker, E. D., ... & Kitron, U. D. (2010). Local impact of temperature and precipitation on West Nile virus infection in Culex species mosquitoes in northeast Illinois, USA. *Parasites & Vectors*, 3(1), 19. https://doi.org/10.1186/1756-3305-3-19

Ruiz, M. O., Tedesco, C., McTighe, T. J., Austin, C., & Kitron, U. (2004). Environmental and social determinants of human risk during a West Nile virus outbreak in the greater Chicago area, 2002. *International Journal of Health Geographics*, 3(1), 8. https://doi.org/10.1186/1476-072X-3-8

Ruiz, M. O., Walker, E. D., Foster, E. S., Haramis, L. D., & Kitron, U. D. (2007). Association of West Nile virus illness and urban landscapes in Chicago and Detroit. *International Journal of Health Geographics*, 6(1), 10. https://doi.org/10.1186/1476-072X-6-10

Sardelis, M. R., Turell, M. J., Dohm, D. J., & O'Guinn, M. L. (2001). Vector competence of selected North American *Culex* and *Coquillettidia* mosquitoes for West Nile virus. *Emerging Infectious Diseases*, 7(6), 1018–1022. https://doi.org/10.3201/eid0706.010617

Schweitzer, B. K., Kramer, W. L., Sambol, A. R., Meza, J. L., Hinrichs, S. H., & Iwen, P. C. (2006). Geographic factors contributing to a high seroprevalence of West Nile virus-specific antibodies in humans following an epidemic. *Clinical and Vaccine Immunology*, 13(3), 314–318. https://doi.org/10.1128/CVI.13.3.314-318.2006

Shaman, J., & Day, J. F. (2007). Reproductive phase locking of mosquito populations in response to rainfall frequency. *PLoS One*, 2(3), e331. https://doi.org/10.1371/journal.pone.0000331

Shaman, J., Day, J. F., & Komar, N. (2010). Hydrologic conditions describe West Nile virus risk in Colorado. *International Journal of Environmental Research and Public Health*, 7(2), 494–508. https://doi.org/10.3390/ijerph7020494

Sheffield, J., Barrett, A. P., Colle, B., Nelun Fernando, D., Fu, R., Geil, K. L., et al. (2013). North American climate in CMIP5 experiments. Part I: Evaluation of historical simulations of continental and regional climatology. *Journal of Climate*, 26(23), 9209–9245. https://doi.org/10.1175/JCLI-D-12-00592.1

Shriber, J., Conlon, K. C., Benedict, K., McCotter, O., & Bell, J. E. (2017). Assessment of Vulnerability to Coccidioidomycosis in Arizona and California*. International Journal of Environmental Research and Public Health*, 14(7), 680. https://doi.org/10.3390/ijerph14070680

Smith, C. E., Beard, R. R., Rosenberger, H. G., & Whiting, E. G. (1946b). Effect of season and dust control on coccidioidomycosis. *Journal of the American Medical Association*, 132(14), 833–838. https://doi.org/10.1001/jama.1946.02870490011003

Smith, C. E., Beard, R. R., Whiting, E. G., & Rosenberger, H. G. (1946a). Varieties of coccidioidal infection in relation to the epidemiology and control of the diseases. *American Journal of Public Health and the Nations Health*, 36(12), 1394–402. https://doi.org/10.2105/AJPH.36.12.1394

Smith, K. R., Woodward, A., Campbell-Lendrum, D., Chadee, D. D., Honda, Y., Liu, Q., … & Sauerborn, R. (2014) Human health: impacts, adaptation, and co-benefits. In C. B. Field, V. R. Barros, D. J. Dokken, K. J. Mach, M. D. Mastrandrea, T.E. Bilir, M. Chatterjee, K. L. Ebi, Y. O. Estrada, R. C. Genova, B. Girma, E. S. Kissel, A. N. Levy, S. MacCracken, P. R. Mastrandrea, and L. L.White (Eds.), Climate Change 2014: Impacts, Adaptation, and Vulnerability. Part A: Global and Sectoral Aspects. Contribution of Working Group II to the Fifth Assessment Report of the Intergovernmental Panel on Climate Change (pp. 709–754). Cambridge, United Kingdom and New York, NY, USA: Cambridge University Press. https://www.ipcc.ch/site/assets/uploads/2018/02/WGIIAR5-Chap11_FINAL.pdf

Sondermeyer, G., Lee, L., Gilliss, D., Tabnak, F., & Vugia, D. (2013). Coccidioidomycosis-associated hospitalizations, California, USA, 2000–2011. *Emerging Infectious Diseases*, 19(10), 1590–1598. https://doi.org/10.3201/eid1910.130427

Sotomayor, C., Madrid, G. S., & Torres, E. A. (1960). Aislamiento de *Coccidioides immitis* del suelo de Hermosillo, Sonora México. *Revista Latinoamericana de Microbiologia*, 3(4), 237–238.

Stacy, P. K. R., Comrie, A. C., & Yool, S. R. (2012). Modeling valley fever incidence in Arizona using a satellite-derived soil moisture proxy. *GIScience and Remote Sensing*, 49(2), 299–316. https://doi.org/10.2747/1548-1603.49.2.299

Stewart, R.A., & Meyer, K.F. (1932). Isolation of *Coccidioides immitis* (Stiles) from the soil. *Proceedings of the Society for Experimental Biology and Medicine*, 29(8), 937–938. https://doi.org/10.3181/00379727-29-6159

Stocker, T. F., Qin, D., Plattner, G. K., Tignor, M., Allen, S. K., Boschung, J., et al. (Eds.). (2013). Intergovernmental Panel on Climate Change. Climate Change 2013: The Physical Science Basis. Contribution of Working Group I to the Fifth Assessment Report of the Intergovernmental Panel on Climate Change. Cambridge and New York: Cambridge University Press. http://www.ipcc.ch/report/ar5/wg1/

Stouffer, R. J., Eyring, V., Meehl, G. A., Bony, S., Senior, C., Stevens, B., & Taylor, K. E. (2017). CMIP5 scientific gaps and recommendations for CMIP6. *Bulletin of the American Meteorological Society*, 98(1), 95–105. https://doi.org/10.1175/BAMS-D-15-00013.1

Swain, D. L., Langenbrunner, B., Neelin, J. D., & Hall, A. (2018). Increasing precipitation volatility in twenty-first-century California. *Nature Climate Change*, 8(5), 427–437. https://doi.org/10.1038/s41558-018-0140-y

Swatek, F. E. (1975). The epidemiology of coccidioidomycosis, In Y. Al-Doory, The Epidemiology of Human Mycotic Diseases (pp. 75–102). Springfield, IL: Charles C. Thomas.

Swatek, F. E., & Omieczynski, D. T. (1970), Isolation and identification of *Coccidioides immitis* from natural sources. *Mycopathologia*, 41(1), 155–166. https://doi.org/10.1007/BF02051491

Swatek, F. E., Omieczynski, D. T., & Plunkett, O. A. (1967). *Coccidioides immitis* in California, In Proceedings of the 2nd Coccidioidomycosis Symposium (pp. 255–264). Tucson, AZ: University of Arizona Press.

Talamantes, J., Behseta, S., & Zender, C. S. (2007). Fluctuations in climate and incidence of coccidioidomycosis in Kern County, California: A review. *Annals of the New York Academy of Sciences*, 1111(1), 73–82. https://doi.org/10.1196/annals.1406.028

Tamerius, J. D., & Comrie, A. C. (2011). Coccidioidomycosis incidence in Arizona predicted by seasonal precipitation. *PLoS One*, 6(6), e21009. https://doi.org/10.1371/journal.pone.0021009

Taylor, J. W., & Barker, B. M. (2019). The endozoan, small-mammal reservoir hypothesis and the life cycle of *Coccidioides* species. *Medical Mycology*, 57(Supplement_1), S16–S20. https://doi.org/10.1093/mmy/myy039

Taylor, K. E., Stouffer, R. J., & Meehl, G. A. (2012). An overview of CMIP5 and the experiment design. *Bulletin of the American Meteorological Society*, 93(4), 485–498. https://doi.org/10.1175/BAMS-D-11-00094.1

Thompson, G. R. (2011). Pulmonary coccidioidomycosis. *Seminars in Respiratory and Critical Care Medicine*, 32(6), 754–763. https://doi.org/10.1055/s-0031-1295723

Tong, D. Q., Wang, J. X. L., Gill, T. E., Lei, H., & Wang, B. (2017). Intensified dust storm activity and Valley fever infection in the southwestern United States. *Geophysical Research Letters*, 44(9), 4304–4312. https://doi.org/10.1002/2017GL073524

Tsang, C. A., Anderson, S. M., Imholte, S. B., Erhart, L. M., Chen, S., Park, B. J., … Sunenshine, R.H. (2010). Enhanced surveillance of coccidioidomycosis, Arizona, USA, 2007–2008. *Emerging Infectious Diseases*, 16(11), 1738–1744. https://doi.org/10.3201/eid1611.100475

Turabelidze, G., Aggu-Sher, R. K., Jahanpour, E., & Hinkle, C. J. (2015). Coccidioidomycosis in a state where it is not known to be endemic – Missouri, 2004–2013. *MMWR Morbidity and Mortality Weekly Report*, 64, 636–639. Retrieved from https://www.cdc.gov/mmwr/preview/mmwrhtml/mm6423a3.htm.

Turell, M. J., O'Guinn, M., & Oliver, J. (2000). Potential for New York mosquitoes to transmit West Nile virus. *The American Journal of Tropical Medicine and Hygiene*, 62(3), 413-414. https://doi.org/10.4269/ajtmh.2000.62.413

Turell, M. J., O'Guinn, M. L., Dohm, D. J., & Jones, J. W. (2001). Vector competence of North American mosquitoes (Diptera: Culicidae) for West Nile virus. *Journal of Medical Entomology*, 38(2), 130–134. https://doi.org/10.1603/0022-2585-38.2.130

Turell, M. J., Bunning, M., Ludwig, G. V., Ortman, B., Chang, J., Speaker, T., ... & McNamara, T. (2003). DNA vaccine for West Nile virus infection in fish crows (*Corvus ossifragus*). *Emerging Infectious Diseases*, 9(9), 1077–1081. https://doi.org/ 10.3201/eid0909.030025

Turell, M. J., Dohm, D. J., Sardelis, M. R., O'guinn, M. L., Andreadis, T. G., & Blow, J. A. (2005). An update on the potential of North American mosquitoes (Diptera: Culicidae) to transmit West Nile virus. *Journal of Medical Entomology*, 42(1), 57–62. https://doi.org/10.1093/jmedent/42.1.57

U.S. Census Bureau (2011a). Intercensal estimates of the resident population for counties: April 1, 2000 to July 1, 2010. Suitland, MD: U.S. Census Bureau. Retrieved from http://www.census.gov/data/tables/time-series/demo/popest/intercensal-2000-2010-counties.html

U.S. Census Bureau (2011b). Population Distribution and Change: 2000 to 2010. Suitland, MD: U.S. Census Bureau. Retrieved from https://www.census.gov/prod/cen2010/briefs/c2010br-01.pdf

U.S. Census Bureau (2015). Counties population totals tables: 2010–2015. Suitland, MD: U.S. Census Bureau,. Retrieved from http://www.census.gov/data/tables/2015/demo/popest/counties-total.html

U.S. Census Bureau (2016). Annual estimates of the resident population: April 1, 2010 to July 1, 2016. Retrieved from

https://factfinder.census.gov/faces/tableservices/jsf/pages/productview.xhtml?pid=PEP_2016_PEPANNRES&prodType=table

U.S. Census Bureau (2017). Intercensal estimates of the resident population for counties: April 1, 2000 to July 1, 2010. Suitland, MD: US Census Bureau. Retrieved from http://www.census.gov/data/tables/time-series/demo/popest/intercensal-2000-2010-counties.html

U.S. Census Bureau (2018). Annual Estimates of the Resident Population: April 1, 2010 to July 1, 2017. Suitland, MD: US Census Bureau, American FactFinder. Retrieved from https://factfinder.census.gov/faces/tableservices/jsf/pages/productview.xhtml?src=bkmk

U.S. Department of Agriculture (2019). CropScape Cropland Data Layers. National Agricultural Statistics Service. Retrieved from https://nassgeodata.gmu.edu/CropScape/

U.S. Geological Survey (2017). California Water Science Center: California's Central Valley. Reston, VA: U.S. Geological Survey. Retrieved from https://ca.water.usgs.gov/projects/central-valley/about-central-valley.html

Vargas-Gastélum, L., Romero-Olivares, A. L., Escalante, A. E., Rocha-Olivares, A., Brizuela, C., & Riquelme, M. (2015). Impact of seasonal changes on fungal diversity of a semi-arid ecosystem revealed by 454 pyrosequencing. *Federation of European Microbiological Societies Microbiology Ecology*, 91(5), fiv044:1–13. https://doi.org/10.1093/femsec/fiv044

Wang, G., Minnis, R. B., Belant, J. L., & Wax, C. L. (2010). Dry weather induces outbreaks of human West Nile virus infections. *BMC Infectious Diseases*, 10(1), 38. https://doi.org/10.1186/1471-2334-10-38

Werner, S. B., & Pappagianis, D. (1973). Coccidioidomycosis in northern California, An outbreak among archeology students near Red Bluff. *California Medicine*, 119(3), 16–20.

Werner, S. B., Pappagianis, D., Heindl, I., & Mickel, A. (1972). An epidemic of coccidioidomycosis among archeology students in northern California. *New England Journal of Medicine*, 286(10), 507–512. https://doi.org/10.1056/NEJM197203092861003

Wilken, J. A., Marquez, P., Terashita, D., NcNary, J., Windham, G., & Materna, B. (2014). Coccidioidomycosis among cast and crew members at an outdoor television filming event—California, 2012. *MMWR Morbidity and Mortality Weekly Report*, 63(15), 331–324. Retrieved from https://www.cdc.gov/mmwr/pdf/wk/mm6315.pdf

Wilken, J. A., Sondermeyer, G., Shusterman, D., McNary, J., Vugia, D. J., McDowell, A., … Gold, D. (2015). Coccidioidomycosis among workers constructing solar power farms, California, USA, 2011–2014. *Emerging Infectious Diseases*, 21(11), 1997–2005. https://doi.org/10.3201/eid2111.150129

Williams, P. L., Sable, D. L., Mendez, P., & Smyth, L. T. (1979). Symptomatic coccidioidomycosis following a severe natural dust storm, An outbreak at the Naval Air Station, Lemoore. *California Chest*, 76(5), 566–570. https://doi.org/10.1378/chest.76.5.566

Wimberly, M. C., Hildreth, M. B., Boyte, S. P., Lindquist, E., & Kightlinger, L. (2008). Ecological niche of the 2003 West Nile virus epidemic in the northern Great Plains of the United States. *PLoS One*, 3(12), e3744. https://doi.org/10.1371/journal.pone.0003744

Wimberly, M. C., Lamsal, A., Giacomo, P., & Chuang, T. W. (2014). Regional variation of climatic influences on West Nile virus outbreaks in the United States. *The American Journal of Tropical Medicine and Hygiene*, 91(4), 677–684. https://doi.org/10.4269/ajtmh.14-0239

Woods, C. W., McRill, C., Plikaytis, B. D., Rosenstein, N. E., Mosley, D., Boyd, D., … Hajjeh R. A. (2000). Coccidioidomycosis in human immunodeficiency virus-infected persons in Arizona, 1994–1997: incidence, risk factors, and prevention. *The Journal of Infectious Diseases*, 181(4), 1428–1434. https://doi.org/10.1086/315401

Yaremych, S. A., Warner, R. E., Mankin, P. C., Brawn, J. D., Raim, A., & Novak, R. (2004). West Nile virus and high death rate in American crows. *Emerging Infectious Diseases*, 10(4), 709–711. https://doi.org/10.3201/eid1004.030499

Zender, C. S., & Talamantes, J. (2006). Climate controls on valley fever incidence in Kern County, California. *International Journal of Biometeorology*, 50(3), 174–182. https://doi.org/10.1007/s00484-005-0007-6

Appendix A

Supporting Information for Ch. 3: Expansion of coccidioidomycosis endemic regions in the United States in response to climate change

Table A.1. BCSD models used for climate projections, averaged to the county-level from 0.125° × 0.125° resolution.

Modeling Center	Institute ID	Model Name	Num. endemic counties 2095 RCP4.5	Num. endemic counties 2095 RCP8.5	Citation
Commonwealth Scientific and Industrial Research Organization (CSIRO) and Bureau of Meteorology (BOM), Australia	CSIRO-BOM	ACCESS1.0	376	537	Collier, M., and Uhe, P. (2012). CMIP5 datasets from the ACCESS1.0 and ACCESS1.3 coupled climate models. Centre for Australian weather and Climate Research.
Beijing Climate Center, China Meteorological Administration	BCC	BCC-CSM1.1 BCC-CSM1.1(m)	300 431	466 456	Gao F., Xin X., and Wu T. (2012). Study on the prediction of regional and global temperature in decadal time scale with BCC_CSM1.1 (in Chinese). *Chinese Journal of Atmospheric Sciences*.
Canadian Centre for Climate Modelling and Analysis	CCCMA	CanESM2	315	343	Arora, V. K., Boer, G. J., Christian, J. R., Curry, C. L., Denman, K. L., Zahariev, K., et al. (2009). The effect of terrestrial photosynthesis down regulation on the twentieth-century carbon budget simulated with the CCCma Earth System Model. *Journal of Climate*, 22(22), 6066-6088.
National Center for Atmospheric Research	NCAR	CCSM4	293	427	Meehl, G. A., Washington, W .M., Arblaster, J. M., Hu, A., Teng, H., Tebaldi, C., et al. (2012). Climate system response to external forcings and climate change

					projections in CCSM4. *Journal of Climate*, 25(11), 3661-3683.
Community Earth System Model Contributors	NSF-DOE-NCAR	CESM1(BGC) CESM1(CAM5)	309 337	493 506	Long, M. C., Lindsay, K., Peacock, S., Moore, J. K., and Doney, S. C. (2013). Twentieth-century oceanic carbon uptake and storage in CESM1 (BGC). *Journal of Climate*, 26(18), 6775-6800. Meehl, G. A., Washington, W. M., Arblaster, J. M., Hu, A., Teng, H., Kay, J. E., et al. (2013). Climate change projections in CESM1 (CAM5) compared to CCSM4. *Journal of Climate*, 26(17), 6287-6308.
Centro Euro-Mediterraneo per I Cambiamenti Climatici	CMCC	CMCC-CM	398	495	Fogli, P. G. , Manzini, E., Vichi, M., Alessandri, A., Patara, L., Gualdi, S., et al. (2009). INGV-CMCC Carbon (ICC): A Carbon Cycle Earth System Model. *CMCC Research Papers*, RP0061, 31. Vichi, M. Manzini, E., Fogli, P., Alessandri, A., Patara, L., Scoccimarro, E., et al. (2011). Global and regional ocean carbon uptake and climate change: sensitivity to a substantial mitigation scenario. *Climate Dynamics*, issn 0930-7575, 1-19
Centre National de Recherches Météorologiques / Centre Européen de Recherche et Formation Avancée en Calcul Scientifique	CNRM-CERFACS	CNRM-CM5	295	435	Voldoire, A., Sanchez-Gomez, E., Mélia, D. S., Decharme, B., Cassou, C., Sénési, S., et al. (2013). The CNRM-CM5. 1 global climate model: description and basic evaluation. *Climate*

					Dynamics, 40(9-10), 2091-2121.
Commonwealth Scientific and Industrial Research Organization in collaboration with Queensland Climate Change Centre of Excellence	CSIRO-QCCCE	CSIRO-Mk3.6.0	323	462	Collier, M. A., Jeffrey, S. J., Rotstayn, L. D., Wong, K. K., Dravitzki, S. M., Moseneder, C., et al. (2011). The CSIRO-Mk3. 6.0 Atmosphere-Ocean GCM: participation in CMIP5 and data publication. In International Congress on Modelling and Simulation–MODSIM.
LASG, Institute of Atmospheric Physics, Chinese Academy of Sciences and CESS,Tsinghua University	LASG-CESS	FGOALS-g2	348	521	Li, L., Lin, P., Yu, Y., Wang, B., Zhou, T., Liu, L., et al. (2013). The flexible global ocean-atmosphere-land system model, Grid-point Version 2: FGOALS-g2. Advances in Atmospheric Sciences, 30(3), 543-560.
The First Institute of Oceanography, SOA, China	FIO	FIO-ESM	254	351	Qiao, F., Song, Z., Bao, Y., Song, Y., Shu, Q., Huang, C., and Zhao, W. (2013). Development and evaluation of an Earth System Model with surface gravity waves. *Journal of Geophysical Research: Oceans*, 118(9), 4514-4524.
NOAA Geophysical Fluid Dynamics Laboratory	NOAA GFDL	GFDL-CM3 GFDL-ESM2G GFDL-ESM2M	314 282 295	408 408 438	Griffies, S. M., Winton, M., Donner, L. J., Horowitz, L. W., Downes, S. M., Farneti, R., et al. (2011). The GFDL CM3 coupled climate model: characteristics of the ocean and sea ice simulations. *Journal of Climate*, 24(13), 3520-3544. Dunne, J. P., John, J. G., Adcroft, A. J., Griffies, S. M., Hallberg, R. W., Shevliakova, E., et al. (2012). GFDL's ESM2

					global coupled climate–carbon earth system models. Part I: Physical formulation and baseline simulation characteristics. *Journal of Climate*, 25(19), 6646-6665. Dunne, J. P., John, J. G., Shevliakova, E., Stouffer, R. J., Krasting, J. P., Malyshev, S. L., et al. (2013). GFDL's ESM2 global coupled climate–carbon earth system models. Part II: carbon system formulation and baseline simulation characteristics. *Journal of Climate*, 26(7), 2247-2267.
NASA Goddard Institute for Space Studies	NASA GISS	GISS-E2-R	223	399	Schmidt, G. A., Kelley, M., Nazarenko, L., Ruedy, R., Russell, G. L., Aleinov, I., et al. (2014). Configuration and assessment of the GISS ModelE2 contributions to the CMIP5 archive. *Journal of Advances in Modeling Earth Systems*, 6(1), 141-184.
National Institute of Meteorological Research/Korea Meteorological Administration	NIMR/KMA	HadGEM2-AO	450	552	Baek, H. J., Lee, J., Lee, H. S., Hyun, Y. K., Cho, C., Kwon, W. T., et al. (2013). Climate change in the 21st century simulated by HadGEM2-AO under representative concentration pathways. Asia-Pacific *Journal of Atmospheric Sciences*, 49(5), 603-618. Collins, W. J., Bellouin, N., Doutriaux-Boucher, M., Gedney, N., Hinton, T., Jones, C. D., et al. (2008).

					Evaluation of the HadGEM2 model. Hadley Cent. Tech. Note, 74.
Met Office Hadley Centre (additional HadGEM2-ES realizations contributed by Instituto Nacional de Pesquisas Espaciais)	MOHC (additional realizations by INPE)	HadGEM2-CC HadGEM2-ES	430 415	505 464	Bellouin, N., Collins, W. J., Culverwell, I. D., Halloran, P. R., Hardiman, S. C., Hinton, T. J., et al. (2011). The HadGEM2 family of met office unified model climate configurations. *Geoscientific Model Development*, 4(3), 723-757. Collins, W. J., Bellouin, N., Doutriaux-Boucher, M., Gedney, N., Hinton, T., Jones, C. D., et al. (2008). Evaluation of the HadGEM2 model. Hadley Cent. Tech. Note, 74.
Institute for Numerical Mathematics	INM	INM-CM4	260	424	Volodin, E. M., Dianskii, N. A., and Gusev, A. V. (2010). Simulating present-day climate with the INMCM4. 0 coupled model of the atmospheric and oceanic general circulations. Izvestiya, *Atmospheric and Oceanic Physics*, 46(4), 414-431.
Institut Pierre-Simon Laplace	IPSL	IPSL-CM5A-LR IPSL-CM5A-MR IPSL-CM5B-LR	378 372 290	528 660 372	Dufresne, J. L., Foujols, M. A., Denvil, S., Caubel, A., Marti, O., Aumont, O., et al. (2013). Climate change projections using the IPSL-CM5 Earth System Model: from CMIP3 to CMIP5. *Climate Dynamics*, 40(9-10), 2123-2165.
Atmosphere and Ocean Research Institute (The University of Tokyo), National Institute for	MIROC	MIROC5	382	568	Watanabe, M., Suzuki, T., O'ishi, R., Komuro, Y., Watanabe, S., Emori, S., et al. (2010). Improved climate simulation by

Environmental Studies, and Japan Agency for Marine-Earth Science and Technology					MIROC5: Mean states, variability, and climate sensitivity. *Journal of Climate*, 23(23), 6312-6335.
Japan Agency for Marine-Earth Science and Technology, Atmosphere and Ocean Research Institute (The University of Tokyo), and National Institute for Environmental Studies	MIROC	MIROC-ESM MIROC-ESM-CHEM	332 414	464 512	Watanabe, S., Hajima, T., Sudo, K., Nagashima, T., Takemura, T., Okajima, H., et al. (2011). MIROC-ESM 2010: Model description and basic results of CMIP5-20c3m experiments. *Geoscientific Model Development*, 4(4), 845.
Max-Planck-Institut für Meteorologie (Max Planck Institute for Meteorology)	MPI-M	MPI-ESM-LR MPI-ESM-MR	299 372	403 445	Giorgetta, M. A., Jungclaus, J., Reick, C. H., Legutke, S., Bader, J., Böttinger, M., et al. (2013). Climate and carbon cycle changes from 1850 to 2100 in MPI-ESM simulations for the Coupled Model Intercomparison Project phase 5. *Journal of Advances in Modeling Earth Systems*, 5(3), 572-597.
Meteorological Research Institute	MRI	MRI-CGCM3	221	370	Yukimoto, S., Adachi, Y., Hosaka, M., Sakami, T., Yoshimura, H., Hirabara, M., et al. (2012). A new global climate model of the Meteorological Research Institute: MRI-CGCM3—model description and basic performance. *Journal of the Meteorological Society of Japan*. Ser. II, 90, 23-64.
Norwegian Climate Centre	NCC	NorESM1-M	416	505	Bentsen, M., Bethke, I., Debernard, J.B., Iversen, T., Kirkevåg, A., Seland, Ø., et al. (2013). The Norwegian earth system model, NorESM1-M—Part 1: Description and basic evaluation of the

					physical climate. *Geoscientific Model Development*, 6(3), 687-720.
Multi-model mean ± standard deviation			**330 ± 62**	**476 ± 69**	

Table A.2. Model performance metrics relative to the CDC endemicity map and projections of Valley fever metrics for year 2095 for RCP8.5 climate change scenario, for both the climate-constrained niche model and the two Maxent models used in the sensitivity analysis. In the final column, a state is reported as endemic if one or more counties within the state has a climate that permits endemicity.

Model	Accuracy	Recall	Percent change in population living in endemic region relative to 2007	Number of endemic states in 2095	States endemic in 2095
Climate-constrained niche model	94.6%	64.7%	17%	17	AZ, CA, CO, ID, KS, MT, ND, NE, NV, NM, OK, OR, SD, TX, UT, WA, WY
Two-variable Maxent: annual temperature and annual precipitation	96.3%	37.6%	18%	15	AZ, CA, CO, ID, KS, MT, NE, NV, NM, OK, OR, TX, UT, WA, WY
Three-variable Maxent: January temperature, July temperature, and annual precipitation	96.8%	53.5%	16%	14	AZ, CA, CO, ID, KS, NE, NV, NM, OK, OR, TX, UT, WA, WY

Table A.3. The number of counties within each state considered endemic for each time period by the climate-constrained niche model for the RCP8.5 climate change scenario. The number of endemic counties for the RCP4.5 climate change scenario is listed second in parenthesis. The total number of counties within the state is listed in the first column.

State	2007	2035		2065		2095	
Arizona	15	15	(15)	15	(15)	15	(15)
California	29	28	(28)	31	(28)	30	(28)
Colorado	11	22	(21)	32	(27)	38	(30)
Idaho	2	7	(4)	19	(10)	23	(13)
Kansas	31	32	(32)	30	(30)	32	(32)
Montana	0	0	(0)	8	(0)	34	(0)
Nebraska	3	12	(10)	26	(22)	27	(26)
Nevada	6	9	(9)	16	(14)	17	(14)
New Mexico	23	29	(29)	32	(31)	33	(31)
North Dakota	0	0	(0)	0	(0)	25	(0)
Oklahoma	5	6	(6)	6	(5)	9	(6)
Oregon	0	3	(2)	9	(6)	14	(8)
South Dakota	0	0	(0)	22	(9)	30	(12)
Texas	84	92	(91)	94	(87)	99	(88)
Utah	5	14	(10)	17	(14)	21	(14)
Washington	3	7	(6)	12	(10)	12	(11)
Wyoming	0	0	(0)	6	(0)	17	(2)

Figure A.1. Mean annual temperature anomalies calculated from the mean of the 30 CMIP5 models under both RCP4.5 (a-c) and RCP8.5 climate scenarios (d-f) in years (a,d) 2035, (b,e) 2065, and (c,f) 2095. Future warming throughout the contiguous U.S. is highest in the northern states and warming is most pronounced for the RCP8.5 climate scenario. These anomalies were estimated relative to a 2000–2015 baseline period (mean of 2007) described in the main text.

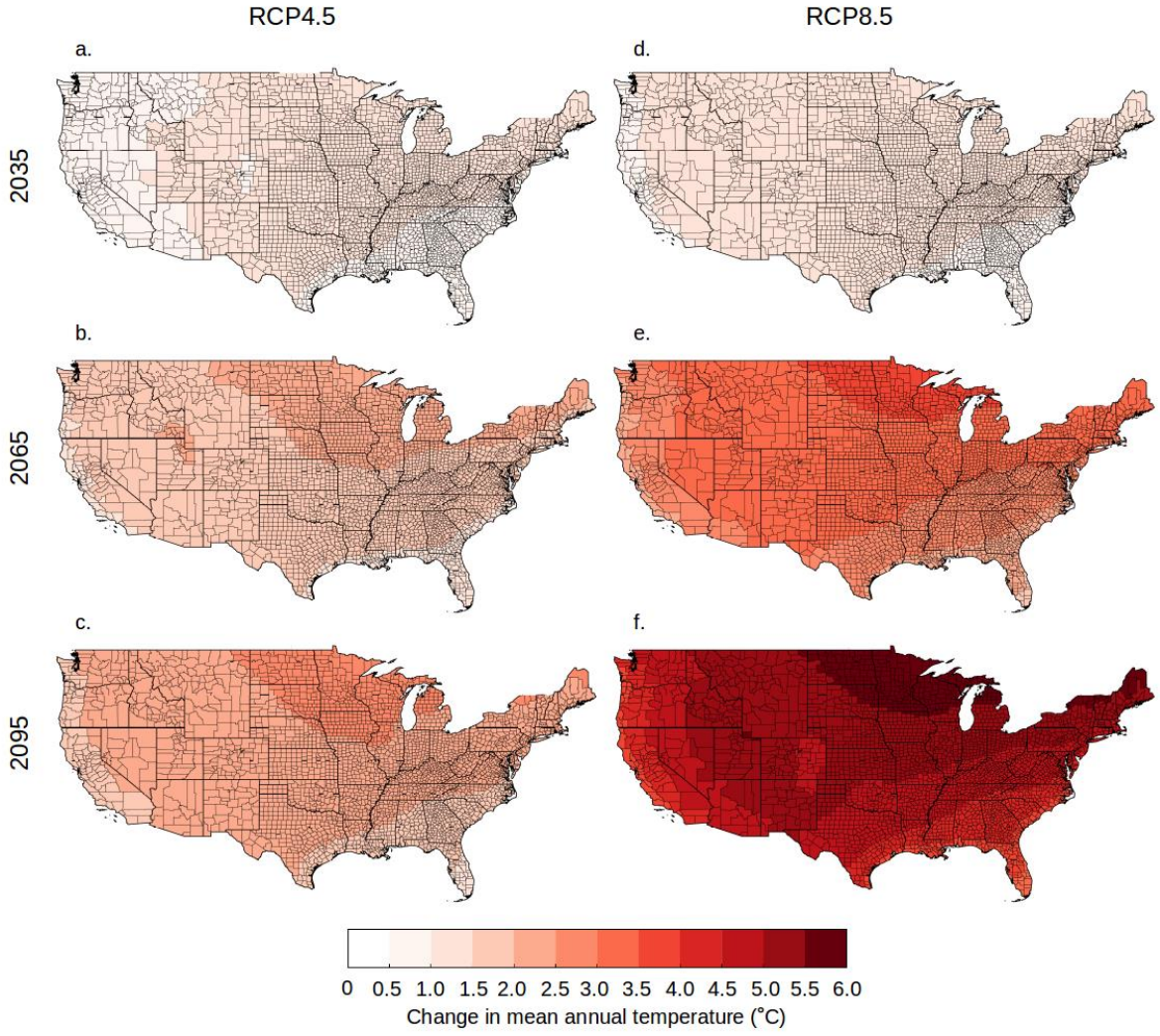

Figure A.2. Mean annual precipitation anomalies calculated from the mean of the 30 CMIP5 Earth system models for both RCP4.5 (a-c) and RCP8.5 climate scenarios (d-f) in years (a,d) 2035, (b,e) 2065, and (c,f) 2095. The south-central Great Plains and southwestern U.S. become drier while the Pacific Northwest and eastern U.S. become wetter. These changes are more pronounced for RCP8.5 climate. These anomalies were estimated relative to a 2000–2015 baseline period (mean of 2007) described in the main text.

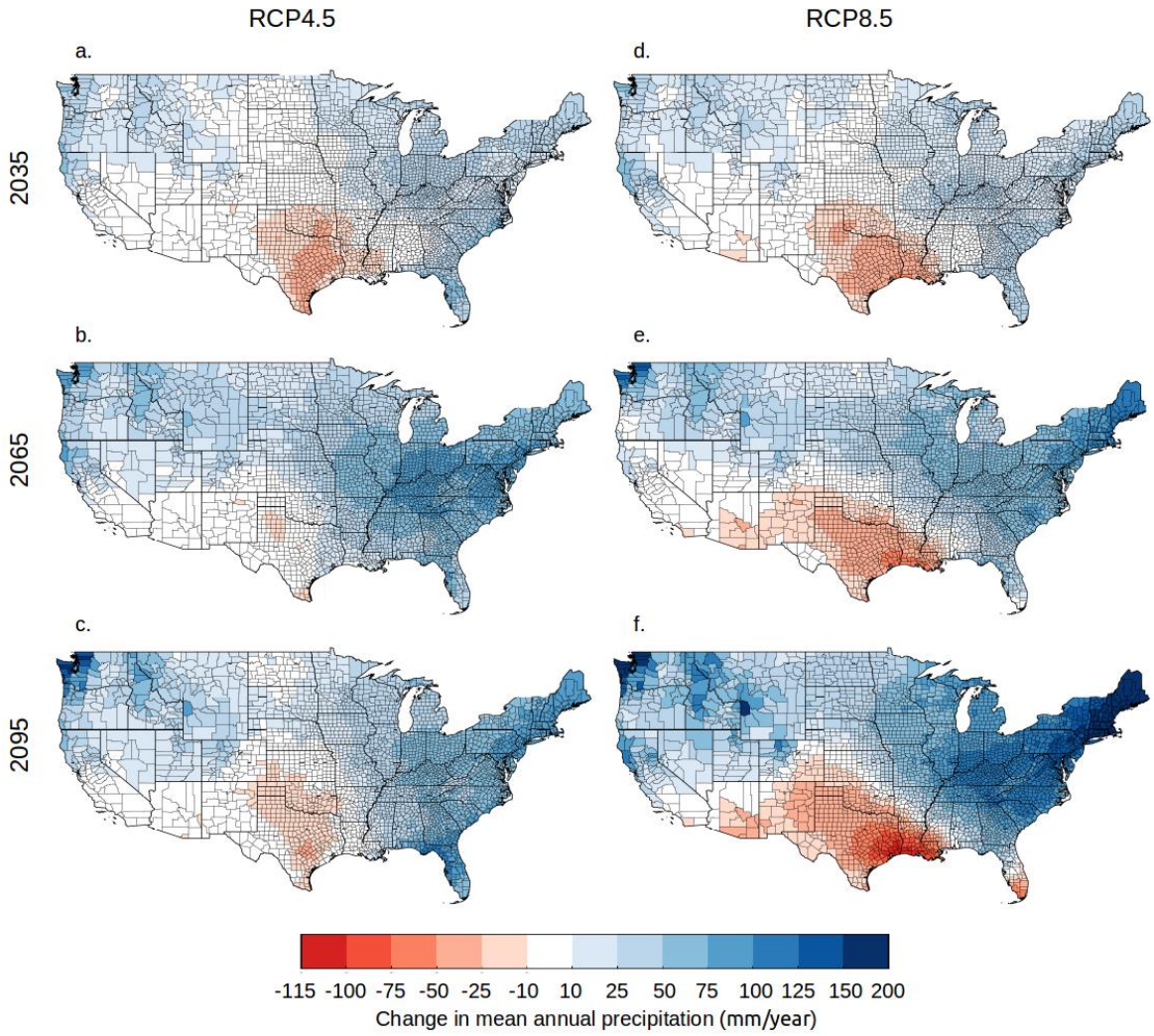

Figure A.3. For the RCP4.5 climate change scenario, areas where climate permits Valley fever endemicity are shown for years (a) 2035, (b) 2065, and (c) 2095. Areas where mean annual temperature permits endemicity are shown in red, areas where mean annual precipitation permits endemicity are shown in blue, and areas where both temperature and precipitation permit endemicity are shown in magenta, following the color scheme used in Figure 3 in the main text. The area endemic to Valley fever will extend farther north in future decades for the RCP4.5 climate scenario, especially in the rain shadows of the Sierra Nevada and Rocky Mountains Ranges.

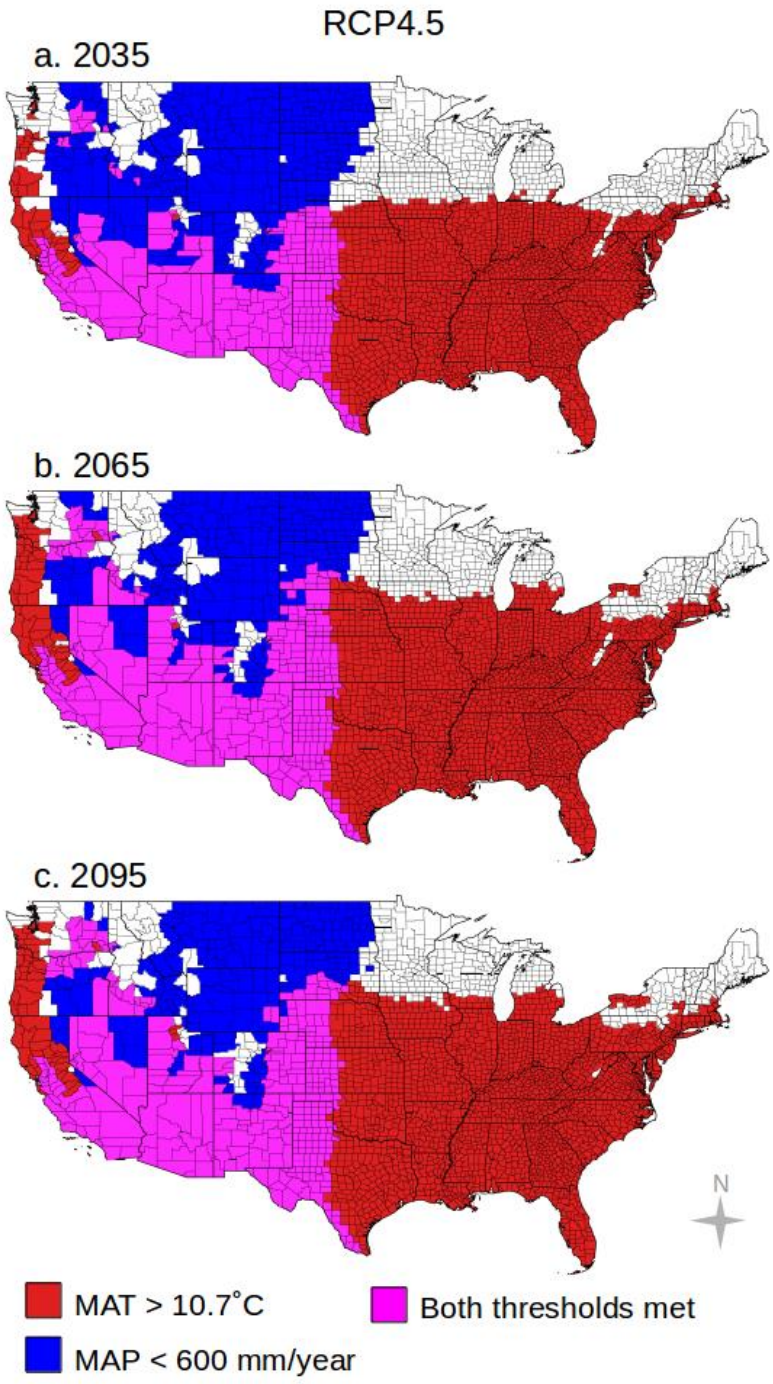

Figure A.4. There is strong model agreement throughout the majority of the area we estimate as endemic to Valley fever for the RCP4.5 climate scenario in years (a) 2035, (b) 2065, and (c) 2095. The model agreement shows a measure of uncertainty for the counties along the edge of the endemic area. Percent model agreement is calculated as the number of individual CMIP5 models that predict the county will have a climate that permits endemicity, divided by the total number of models (n = 30), as projected by the climate-constrained niche model.

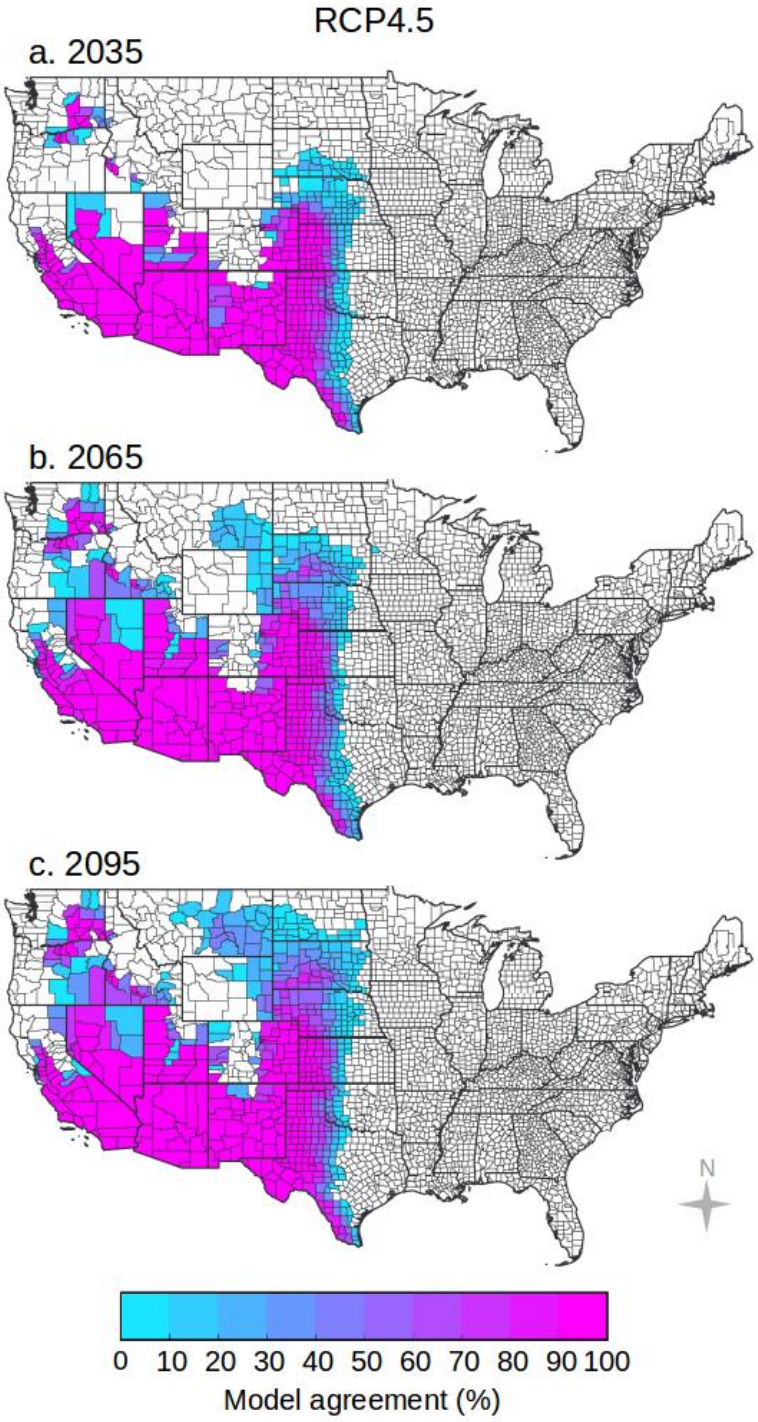

Figure A.5. We estimated an upper bound of future Valley fever incidence using a 90th percentile regression model for (a) our 2007 baseline period, (b) 2035, (c) 2065, and (d) 2095 for RCP4.5. Over time, our model predicted Valley fever incidence will increase throughout the extreme southwestern U.S. and the southern Great Plains. Incidence will also increase throughout the Central Valley of California and in the northwestern U.S.